RDU150382

SYNTHESIS AND CHARACTERIZATION OF NI-BASED CATALYSTS MODIFIED WITH RARE EARTH AND ALKALINE METAL OXIDES (CeO_2, La_2O_3, BaO) FOR METHANE CRACKING

(SINTESIS DAN PENCIRIAN MANGKIN BERASASKAN NI DIUBAHSUAI DENGAN OKSIDA LOGAM BUMI DAN ALKALI (CeO_2, La_2O_3, BaO) BAGI PERETAKAN METANA)

DR ASMIDA BINTI IDERIS

RESEARCH VOTE NO:
RDU150382

Faculty of Chemical and Processs Engineering Technology
Universiti Malaysia Pahang

2020

ACKNOWLEDGMENT

As the principle investigator of this project, I would like to sincerely thank Universiti Malaysia Pahang, mainly UMP Research & Innovation Department (PNI) for the opportunity in conducting research under the UMP internal grant scheme. This grant has been eventually served as a seed fund for an initial fundamental investigation in the particular area, thus has led to a successful application in FRGS research grant in the subsequent year.

I further my thanks to the management, administrative and technical personnel of Faculty of Chemical and Process Engineering Technology (FTKKP) previously known as FKKSA for the assistance in managing the grant at the faculty level.

I would also like to acknowledge my co-researchers, Assoc. Prof. Dr. Sumaiya Zainal Abidin and Dr. Mazni Ismail for the support provided during the research. The entire experimental work especially on the fixed bed reactor setup as well as gas outlet analysis would not be possible without the additional funding from the collaboration of this team.

Finally, my appreciation goes to our master and undergraduate students who have been working on the ground in ensuring the achievement of every milestone of the project possible.

ABSTRACT

Nickel (Ni) has been recognized as a low-cost and an efficient catalyst for hydrogen production from methane cracking. Nevertheless, methane cracking reaction is still hindered by accumulation of carbon on Ni catalyst, which is produced during the reaction. Modification of Ni catalyst with other substance known as promoter is essential to reduce the carbon deposition. Additionally, supported catalyst with relatively large surface area and highly catalyst dispersion for example is essential to develop carbon-resistance Ni-based catalysts.

In order to evaluate the effect of promoter, Ni metal has been modified with cerium (Ce), lanthanum (La) and barium (Ba) and a self-combustion process, glycine- nitrate process (GNP) has been employed for the catalyst preparation method. Effects of glycine-nitrate (G/N) ratio and calcination temperature have been investigated on Ni catalyst properties and morphology. Ni catalyst with modified La supported on an inert support, SiO_2 (Ni-La/SiO_2) was further chosen for catalytic activity in methane cracking. In situ self-combustion has been employed where the inert SiO_2 support is immersed into the fuel-nitrate solution where the solution is allowed to self-ignited. Effects of support sizes, support loading, La loading and reaction gas concentration have been evaluated on catalyst activity and carbon formation.

All Ni catalysts modified with Ce, La and Ba produced through GNP are very high in crystallinity. The reduced catalyst of Ni catalyst modified with Ce composed of Ni and CeO_2, the reduced Ni modified with La catalyst composed of separated phases of Ni and La_2O_3 while the reduced Ni catalyst modified with Ba composed of Ni and BaN_2O_6. The Ni-Ba catalyst however does not contain BaO as expected. G/N=1.0 ratio is the optimum G/N as it produced catalyst with large and more uniform macropores. Meanwhile 800°C was found to be the best calcination temperature for Ni metal catalysts modified with Ce, La and Ba.

From catalytic activity through methane cracking, Ni−La/SiO_2 supported with SiO_2 support with a lower particle size has a better methane conversion and H_2 yield than the shown by Ni-La/SiO_2 with a support of larger particle size. Catalyst dispersion calculated for Ni−La/SiO_2 supported with SiO_2 support with a lower particle size is higher than the one with a support of larger particle size, suggesting that catalyst supported on a support of high surface area has a better catalyst dispersion. Higher support loading also gave better catalyst dispersion. Nevertheless, massive amount of filament carbons is found on the surface of Ni−La/SiO_2 supported with SiO_2 support with a lower particle size catalyst suggesting that the catalyst is very active for catalytic activity. In Ni/SiO_2 without La, high initial methane conversion of 58% was achieved yet the conversion was drop gradually to 30% after 150 minutes of reaction time. As 5% of La was added into Ni catalyst, the methane conversion was stable at a lower ~40% throughout the experiment. Reaction gas composition CH_4: N_2= 1:2 have the highest methane conversion initially at ~75% and as the methane concentration decreased, the initial methane conversion decreased.

In conclusion, the work has successfully synthesized Ni modified with La catalyst supported on SiO_2 (Ni-La/SiO_2) catalyst using in situ glycine- nitrate process of high dispersion, thus resulted in a decent catalytic activity in methane cracking.

ABSTRAK

Nikel (Ni) telah diakui sebagai pemangkin kos rendah dan cekap untuk pengeluaran hidrogen dari keretakan metana. Walaupun begitu, proses peretakan metana masih terhalang oleh pengumpulan karbon pada pemangkin Ni. Pengubahsuaian pemangkin Ni dengan bahan lain yang dikenali sebagai promoter penting untuk mengurangkan pemendapan karbon. Pemangkin yang disokong dengan luas permukaan yang luas dan penyebaran pemangkin yang tinggi juga adalah mustahak untuk menghasilkan pemangkin berasaskan Ni yang tahan karbon.

Untuk menilai kesan promoter, logam Ni telah diubahsuai dengan cerium (Ce), lanthanum (La) dan barium (Ba) dan proses pembakaran sendiri iaitu proses glisin-nitrat (GNP) telah digunakan bagi penyediaan pemangkin. Kesan nisbah glisin-nitrat (G/N) dan suhu kalsinasi telah disiasat bagi sifat dan morfologi pemangkin Ni. Pemangkin Ni dengan La yang diubahsuai disokong pada sokongan lengai, SiO_2 (Ni-La/SiO_2) seterusnya dipilih bagi proses peretakan metana. Poses pembakaran sendiri in situ telah digunakan di mana sokongan SiO_2 lengai dimasukkan ke dalam larutan bahan bakar-nitrat di mana larutan tersebut dibiarkan menyala sendiri. Kesan saiz sokongan, kandungan sokongan, kandungan La dan kepekatan gas reaksi telah dinilai terhadap aktiviti pemangkinan dan pembentukan karbon.

Semua pemangkin Ni yang diubahsuai dengan Ce, La dan Ba yang dihasilkan melalui GNP mempunyai kristaliniti yang tinggi. Pemangkin katalis Ni yang diubahsuai dengan Ce yang terdiri daripada Ni dan CeO_2, pemangkin Ni yang diubahsuai dengan pemangkin La yang terdiri daripada fasa Ni dan La_2O_3 sementara pemangkin Ni yang diubahsuai dengan Ba terdiri daripada Ni dan BaN_2O_6. Pemangkin Ni-Ba bagaimanapun tidak mengandungi BaO seperti yang diharapkan. Nisbah G/N = 1.0 adalah G/N yang optimum kerana menghasilkan pemangkin dengan makropori besar dan seragam. Sementara itu 800°C didapati suhu kalsinasi yang paling optimum untuk pemangkin Ni yang diubahsuai dengan Ce, La dan Ba.

Dari aktiviti pemangkin melalui peretakan metana, Ni-La/SiO_2 yang disokong dengan sokongan SiO_2 dengan saiz partikel lebih rendah mempunyai penukaran metana dan hasil H_2 yang lebih baik daripada yang ditunjukkan oleh Ni-La/SiO2 dengan sokongan dengan saiz partikel yang lebih besar. Penyebaran pemangkin yang dikira untuk Ni-La/SiO_2 yang disokong dengan sokongan SiO_2 dengan saiz partikel lebih rendah lebih tinggi daripada yang dengan sokongan dengan saiz partikel yang lebih besar, menunjukkan bahawa pemangkin yang disokong pada sokongan berpermukaan tinggi mempunyai penyebaran pemangkin yang lebih baik. Kandungan sokongan yang lebih tinggi juga memberikan penyebaran pemangkin yang lebih baik. Walaupun begitu, sejumlah besar karbon filamen terdapat di permukaan Ni-La/SiO_2 yang disokong dengan sokongan SiO_2 dengan saiz partikel lebih rendah menunjukkan bahawa pemangkin sangat aktif untuk aktiviti pemangkin. Bagi Ni/SiO_2 tanpa La, penukaran metana awal yang tinggi sebanyak 58% telah dicapai namun penukaran berkurang secara beransur-ansur menjadi 30% setelah 150 minit. Setelah 5% La ditambahkan ke dalam pemangkin Ni, penukaran metana stabil pada ~ 40% sepanjang eksperimen. Komposisi gas CH_4: N_2 = 1: 2 mempunyai penukaran metana tertinggi pada ~ 75% dan pada kepekatan metana rendah, penukaran metana awal berkurang. Kesimpulannya, penyelidikan ini berjaya menghasilkan Ni yang diubahsuai dengan pemangkin La yang disokong pada pemangkin SiO2 (Ni-La/SiO_2) menggunakan proses glisin-nitrat in situ dengan penyebaran tinggi, sehingga menghasilkan aktiviti pemangkin yang baik bagi peretakan metana.

TABLE OF CONTENT

ACKNOWLEDGMENT ii
ABSTRACT iii
ABSTRAK iv
TABLE OF CONTENT v
LIST OF FIGURES vii
LIST OF TABLES viii
LIST OF ABREVIATIONS ix
CHAPTER 1 1
INTRODUCTION 1
1.1 General Problem Statement 1
1.2 Objectives and Scope of Research 1
CHAPTER 2 3
PAPER PUBLISHED IN MALAYSIAN JOURNAL OF CATALYSIS 3
ABSTRACT 3
1.0 INTRODUCTION 4
2.0 EXPERIMENTS 4
3.0 RESULTS AND DISCUSSION 5
4. CONCLUSION 9
ACKNOWLEDGEMENTS 9
REFERENCES 9
CHAPTER 3 11
PAPER PUBLISHED IN INDUSTRIAL & ENGINEERING CHEMISTRY RESEARCH 11
ABSTRACT 11
1.0 INTRODUCTION 12
2.0 EXPERIMENTAL METHODS 13
3.0 RESULTS AND DISCUSSIONS 15
4.0 CONCLUSIONS 24
ACKNOWLEDGMENT 24
REFERENCES 25

OVERALL CONCLUSIONS 29
APPENDIX 30
(URP TECHNICAL PAPER 1) 30
APPENDIX 36
(URP TECHNICAL PAPER 2) 36
APPENDIX 41
(URP TECHNICAL PAPER 3) 41
APPENDIX 47
(URP TECHNICAL PAPER 4) 47
APPENDIX 54
(URP TECHNICAL PAPER 5) 54
APPENDIX 63
(URP TECHNICAL PAPER 6) 63

LIST OF FIGURES

Figure 1 XRD patterns of a) Ni without La (calcined at 600°C); b) Ni modified with La (as-prepared); (c) Ni modified with La (calcined at 600°C); d) Ni modified with La (calcined 700°C); e) Ni modified La (calcined at 800°C); f) Ni modified with La (reduced at 700°C) 6
Figure 2 XRD patterns of a) Ni without Ce (calcined at 600°C); b) Ni modified with Ce (as-prepared); (c) Ni with modified Ce (calcined at 600°C); d) Ni modified with Ce (calcined 700°C); e) Ni modified with Ce (calcined at 800°C); f) Ni modified with Ce (reduced at 700°C) 7
Figure 3 SEM images of Ni catalysts modified with La (a – c) and Ce (d – f) at glycine-nitrate ratio (G/N) = 0.5, 1.0 and 1.5..... 8

LIST OF TABLES

Table 1 BET analysis of SiO_2 A and SiO_2 B..... 17

LIST OF ABREVIATIONS

(G/N) ratio	Glycine-nitrate ratio
BaO	Barium oxide
BSE	Back-scattered electron
CeO_2	Cerium oxide
EDX	Energy dispersive x-ray spectrometry
FESEM	Field emission scanning electron microscopy
FWHM	Full-width half maximum
GC	Gas chromatograph
GHSV	Gas space hour velocity
GNP	Glycine- nitrate process
in situ GNP	In situ glycine- nitrate process
La_2O_3	Lanthanum oxide
Ni	Nickel
SEM	Scanning electron microscopy
SiO_2	Silica
SOFC	Solid oxide fuel cell
TCD	Thermal conductivity detector
TGA	Thermos-gravimetric analysis
XRD	X-ray diffraction

CHAPTER 1

INTRODUCTION

1.1 General Problem Statement

Ni has excellent catalytic and electrochemical activities towards hydrocarbons cracking and fuel oxidation. Furthermore, the catalyst is ease of fabrication and is relatively inexpensive. Due to these desirable properties, Ni remains the preferable choice for catalyst in hydrogen production and for anode in solid oxide fuel cell (SOFC). The main drawback with Ni, however, is that it can also catalyze carbon formation. Ni particles may initiate the formation of carbon on their surfaces. Consequently, researchers have made great efforts to modify Ni catalyst to take advantage of it good properties while reducing the carbon and sintering problems. Most of these works have involved modification of Ni by alloying or impregnating the Ni with metals, noble materials or metal oxides.

Ni-supported catalysts produced using impregnation, co-precipitation and sol-gel have relatively low specific surface area or poor dispersion of Ni-particles. Under hydrocarbon atmosphere, low dispersed catalyst is more likely to form more carbon on catalyst surface. Hence, a highly dispersed Ni-based supported catalyst is essential to provide carbon-resistance catalysts, thus catalyst preparation method which produces as such catalyst morphology should be employed. In-situ glycine-nitrate combustion process is a recent catalyst synthesis process in which metal-supported catalyst is produced through a combination of impregnation and self-combustion approaches. A rapid high temperature reaction results in metal particles deposited onto the support. Highly dispersed metal particles as a result of a chemical reaction propagates through the support due to rapidly moving combustion wave. In-situ combustion synthesis is a cost effective method which display magnificent properties with respect to crystallite size and degree of reduction and metal dispersion.

1.2 Objectives and Scope of Research

The objectives of the entire project are:

(1) To synthesis and characterize Ni-based catalysts modified with La, Ce, and Ba using glycine-nitrate combustion process.

(2) To synthesize and characterize Ni-supported catalyst modified with selected promoter using in situ glycine-nitrate combustion process (in situ GNP).

(3) To investigate the catalytic performance and carbon formation of Ni-supported catalyst modified with selected promoter in methane cracking.

The scopes of the research are:

(1) Design of combustion chamber for glycine-nitrate combustion process

The combustion chamber was fabricated and utilized for glycine-nitrate combustion process.

(2) Synthesis of Ni catalysts modified with cerium (Ce), lanthanum (La) and barium (Ba) using glycine-nitrate combustion.

Ni catalysts modified with cerium (Ce), lanthanum (La) and barium (Ba) using a self-combustion process, glycine- nitrate process (GNP). The procedure has produced catalyst powders that are good in purity, crystalline and homogenous. Further, Ni catalysts modified with lanthanum (Ni-La) has been investigated for effects of glycine-nitrate (G/N) ratio (0.5, 1.0, 1.5) and calcination temperature (600, 700, 800 °C).

(3) Synthesis of Ni catalyst modified with lanthanum (La) supported on SiO_2 support using in-situ glycine-nitrate combustion

In situ self-combustion has been employed for preparation of Ni catalyst with modified La supported on an inert support, SiO_2 (Ni-La/SiO_2). In this process, the inert support is immersed into the fuel-nitrate solution where the solution is allowed to self-ignite throughout the porous media of the SiO_2 support. Effects of support sizes (44, 74μm), catalyst to support ratio (1:2, 1:5, 1:8), have been explored to improve the dispersion of catalyst on the support surface.

(4) Catalyst activity and carbon deposition study in methane cracking using fixed bed reactor

Effects support sizes, La loadings dan reaction gas concentration on catalytic performance on (Ni-La/SiO_2) have been explored in methane cracking in fixed reactor. The catalytic activity of the catalyst produced was analyzed for methane cracking at 550°C for 5 hr for methane conversion and hydrogen yield.

CHAPTER 2

PAPER PUBLISHED IN MALAYSIAN JOURNAL OF CATALYSIS

M.M. Tajuddin, M.H. Patulla, A. Ideris and M. Ismail (2017) Self-combustion synthesis of Ni catalysts modified with La and Ce using Glycine–Nitrate Process (GNP) Malaysian Journal of Catalysis 2 8-11*

ABSTRACT

Combustion synthesis has become an attractive method for preparing oxides and metallic materials for various applications including catalysts. One common combustion route is glycine–nitrate process (GNP). GNP involves a self-sustained reaction between metal nitrates (oxidizer) and glycine (fuel). The process is known to be rapid and simple, and generates catalyst powders that are high purity, crystalline and homogenous. In this work, Ni catalysts modified with La and Ce were synthesized using GNP. A precursor solution containing a stoichiometric mixture of metal nitrates was initially mixed with glycine at various glycine-nitrate ratios (G/N=0.5, 1.0, 1.5). The glycine-nitrate solution was then heated to yield a gel-like liquid. The gel was further heated until it self-ignited and produced an ash powder. The catalyst ash was calcined at different temperatures (600–800°C) and then reduced at 700°C. Catalyst characterization was performed using X-ray diffraction (XRD) and scanning electron microscopy (SEM). Once produced using GNP, the La element in Ni catalyst modified with La was presence in a form of LaNiO phase. After reduction, Ni catalyst modified with La contains only Ni and La2O3 phases. Meanwhile, Ce element in the Ni catalyst modified with Ce presence as CeO2 phase after the GNP combustion. The CeO2 phase remains after the reduction process and the reduced Ni catalyst modified with Ce composed of two separated phases; Ni and CeO2. Glycine-nitrate (G/N) ratio shows a significant effect on the morphology of the catalysts. At G/N=0.5, where the fuel composition is less than the stoichiometric ratio, the 'cottonwool-like' and highly porous structure were observed for both Ni catalysts modified La and Ce. At the fuel composition higher than the stoichiometric ratio (G/N= 1.5), both catalysts become dense in structure and contain less pores.

Keywords: glycine-nitrate process (GNP), glycine-nitrate (G/N) ratio, calcination, reduction, Ni modified with La, Ni modified with Ce

1.0 INTRODUCTION

Glycine–nitrate process (GNP) has been frequently employed for preparation of complex nanostructured metal oxides, aiming for fitted composition, phase, oxidation state and surface areas [1]. This method is preferred due to its simple process and effective in term of cost which permits high production rates [2, 3]. Moreover, GNP provides the desirable characteristics for most excellent catalyst such as fine crystalline powders, nanometer scale in particle size, highly chemical homogeneity, no impurities and narrow range of powder size distribution [4]. GNP involves a self-sustained combustion reaction between metal nitrates that act as oxidizers and fuel that acts as reducer. The fuel supplies energy required for the combustion and also acts as complexing agent.

Physical and chemical properties of the synthesized catalyst powders produced after the GNP are controlled mainly by the heat generated during the combustion that relied upon nature of the fuel and fuel-to-oxidant ratio. In GNP, volume of gas products generated during the rapid combustion dissipates heat and limits the temperature increase, thus decreases the chance for local sintering among catalyst particles and encouraging fine powder formation with high specific areas [5]. High crystallinity also can be achieved due to its short reaction time and moderate temperature [6]. Natures of the fuel and fuel to oxidizer ratio decide the maximum temperature reach during the process [7].

In present study, an attempt has been made to synthesize and characterize Ni catalysts modified with La and Ce using glycine–nitrate process (GNP). The effects of calcination, reduction and glycine-nitrate (G/N) ratio on the crystalline phase and morphology of Ni modified with La and Ni modified with Ce catalyst were examined. The combustion reactions between metal nitrate and glycine for synthesis of Ni modified with La and Ni modified with Ce catalysts using a GNP are given by Eq. 1 and Eq. 2, respectively. The lanthanum nickelate ($LaNiO_3$) produced in Eq. 1 can be further reduced into form its active form, Ni and La_2O_3 [8, 9].

$$Ni(NO_3)_2.6H_2O + La(NO_3)_3.6H_2O + mNH_2C_2O_2 + (2.25m - 6)\,O2 \rightarrow LaNiO_3 + (12 + 2.5m)\,H_2O + (2.5 + 0.5m)\,N_2 + 2mCO_2 \quad \text{(Eq. 1)}$$

$$Ni(NO_3)_2.6H_2O + 9\,Ce(NO_3)_3.6H_2O + 14NH_2C_2O_2 + 21.5\,O_2 \rightarrow 9\,CeO_2 + NiO + 95\,H_2O + 5.5\,N_2 + 28\,CO_2 \quad \text{(Eq. 2)}$$

2.0 EXPERIMENTS

2.1 Catalyst Preparation

Catalyst precursors were prepared by dissolving nickel (II) nitrate hexahydrate, $Ni(NO_3)_2{\cdot}6H_2O$ (Merck, USA) with cerium (III) nitrate hexahydrate, $Ce(NO_3)_3{\cdot}6H_2O$ (Merck, USA) or lanthanum (III) nitrate hexahydrate, $La(NO_3)_3{\cdot}6H_2O$ (Merck, USA) at a desired stoichiometric amount. Glycine (NH_2CH_2COOH) (Merck, USA) was added into the metal nitrate solution at the various glycine-nitrate (G/N) ratio (G/N=0.5, 1.0, 1.5). The glycine-nitrate solution was then mixed and heated overnight on a hot plate stirrer (IKA, Germany) at 90°C to form clear, homogeneous and viscous gel-like solutions. The gel was then placed in a ceramic bowl and further

heated to the temperatures of 180-250 °C until the gel was self-ignited, producing a catalyst ash. In order to remove the residual carbon and promote the crystallization, the catalyst ash was calcined at various sintering temperatures (600°C, 700°C and 800°C). Ni catalysts modified with La and Ce were then reduced under a flow of 10% H_2-N_2 mixture at 700°C for 2 hours.

2.2. Characterization

X-ray diffraction (XRD) analysis was performed using Miniflex II desktop powder diffractometer (Rigaku, Japan) to determine the crystalline structure of the catalyst prepared. Data sets were recorded in a step-scan mode in the 2θ ranged from 3° to 80° with intervals of 0.02 a counting time of 1 second per point. The morphology of Ni catalysts modified with La and Ce catalyst was characterized using TM3030 Plus tabletop scanning electron microscopy (SEM) (Hitachi, Japan).

3.0 RESULTS AND DISCUSSION

3.1 Phase analysis

Figure 1 shows the XRD patterns for Ni catalysts with and without La, synthesized using GNP. Figure 1a gives an XRD pattern for Ni catalyst without La after calcination at 600ºC. The patterns for Ni catalysts modified with La for as-prepared sample and when the catalysts were calcined at 600, 700 and 800°C are shown in Figures 1b – 1e. These patterns are compared with one for a reduced Ni modified with La catalyst (Figure 1f). The peaks belongs to NiO given by the planes (111), (200), (220), (311) and (222) at angles 37°, 43°, 63°, 76° and 79° were detected in Ni catalyst without La and Ni catalysts modified with La for as-prepared and calcined samples. These planes represent the cubic fluorite structure of NiO in the catalyst samples [10]. Ni catalyst without La is characterized by narrow and sharp peaks (Figure 1a). This is corresponding to the formation of large crystallite. The peaks for Ni catalyst with La were slightly broadened with the addition of La, suggesting that the modification of Ni catalyst with La might has slightly altered the average size of Ni crystallites.

In overall, as the calcination temperature increases, the crystallinity increases, exhibits by the increase of the sharpness of the peaks at higher temperatures (Figures 1c –1e). After the calcination process, La element in Ni catalysts modified with La became visible in a form of $LaNiO_3$. The peak of $LaNiO_3$ given by (100) plane at 33° became more obvious as the calcination temperature was increased from 600 to 800°C (Figures 1b – 1e). After the reduction process, the peak representing $LaNiO_3$ was entirely diminished while the peak belongs to La_2O_3 at (220) plane was detected at 77° (Figure 1f). Previous research by Zhu et al. [11] also found the same phenomena when the $LaNiO_3$ was replaced by La_2O_3 in a Ni-containing La catalyst after reduction process.

Meanwhile, in the same reduced sample, all the (111), (200), (220), (311) and (222) planes for NiO disappeared and the (111) and (200) planes for metallic Ni become visible (Figure 1f). This suggested that most of NiO phase in Ni catalysts modified with La have been reduced into metallic Ni after reduction process. Therefore, it can be concluded that the La element in Ni modified with La catalyst was initially presence in a form of $LaNiO_3$ phase before it was changed

into La_2O_3 after reduction. A reduced Ni catalyst modified with La composed of separated phases of Ni and La_2O_3.

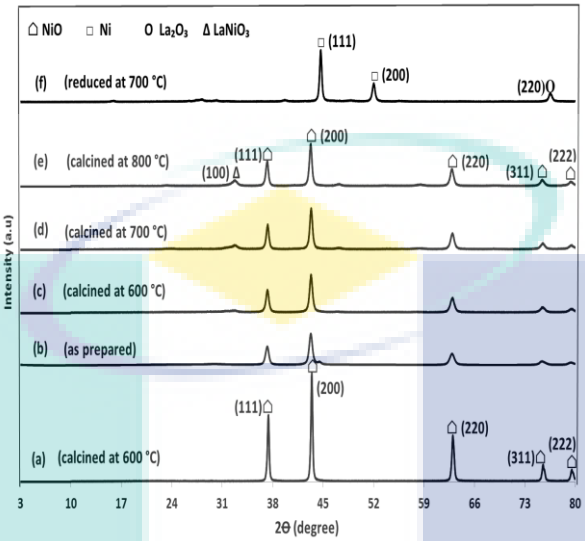

Figure 1 XRD patterns of a) Ni without La (calcined at 600°C); b) Ni modified with La (as-prepared); (c) Ni modified with La (calcined at 600°C); d) Ni modified with La (calcined 700°C); e) Ni modified La (calcined at 800°C); f) Ni modified with La (reduced at 700°C)

Figure 2 gives the XRD patterns for Ni catalysts with and without Ce. Figure 1a shows an XRD pattern for Ni catalyst without Ce after calcination at 600ºC. Meanwhile, Figures 2b – 2e show the patterns of Ni modified with Ce catalysts for as-prepared sample and after calcination at different temperatures. These patterns are compared with a reduced sample of Ni modified with Ce catalyst (Figure 2f). All patterns for as-prepared and calcined catalysts (including Ni catalyst without Ce) show the presence of (111), (200), (220), (311) and (222) planes for NiO at 37°, 43°, 63°, 76° and 79°, respectively. Similar to the patterns from Figure 1, the planes represent the cubic fluorite structure of NiO in the catalyst samples [10]. Like Ni catalysts modified with La, the peaks were slightly widened when the catalysts were added with Ce, suggesting that the modification of Ni catalyst with Ce has slightly reduced the average size of Ni crystallites.

In Figure 2b, the pattern for as-prepared Ni modified with Ce catalyst shows the presence of metallic Ni, demonstrated by the (111), (200) and (220) planes at 45°, 52° and 77°, respectively. The presence of metallic Ni in this as-prepared sample may be due to the localized reducing environment during the combustion process [12]. The calcination of the catalyst has resulted in the disappearance of these metallic Ni planes (Figures 2c– 2e). However, the peaks for metallic Ni ((111) plane at 45°) and ((200) at 52°) were reappeared and become obvious when the sample was reduced under a flow of H_2-N_2 mixture at 700°C (Figure 2f). During the reduction process, oxides available in NiO phase were removed from the catalyst. This is proven by the disappearance of the peaks belongs to NiO ((111), (200), (220), (311) and (222) NiO planes at 37°, 43°, 63°, 76° and 79° angles) in the reduced Ni modified with Ce catalyst (Figure 2f). The peaks belong to metallic Ni in Figure 2f become noticeable, suggesting that the NiO phase were reduced, resulting in most metallic Ni phase in the Ni modified with Ce catalyst.

The (111), (200), (220) and (311) of CeO_2 planes at 28°, 33°, 47° and 53°, respectively in the as-prepared and calcined Ni catalyst modified with Ce are belongs to the cubic fluorite structure of CeO_2 [13]. These planes were remained after reduction process. In addition, a new peak belongs to CeO_2 (220) at 77° was appeared after the reduction process (Figure 2f). The presence of CeO_2 peaks after reduction process was also reported by Bhavsar and Veser [14].This reveals that the CeO_2 phase in Ni modified catalyst was produced directly from the GNP. The CeO_2 remains after the reduction process and presence together with Ni in two separated phases (Ni and CeO_2) in the Ni modified Ce catalyst.

In order to evaluate the catalytic activity of the catalyst, the Ni crystallite sizes must be determined [15]. The crystallite sizes were calculated from the diffractograms according to the Scherrer equation [16]. The crystallite size for Ni catalyst without La or Ce when calcined at 600°C was35.2 nm. The Ni catalysts modified with La and Ce when calcined at the same temperature (600°C) provides the crystallite size of 18.9 and 31.2 nm, respectively. Hence, the crystallite sizes in Ni catalysts modified with La and Ce were smaller compared to the one for Ni without La and Ce. This may be happened due to the contraction of Ni lattice once the La^{3+} or Ce^{3+} ions were incorporated into the lattice of nickel during the synthesis process [17]. However, after the catalysts were reduced under a flow of H_2 for 2 hr, there was a slight increase in the Ni crystallite size when the crystallite size are 27.3 and 39.6 nm for Ni modified with La and Ce catalysts, respectively. One possible explanation of this phenomena is that the Ni particles might have formed clusters during catalyst reduction [18].

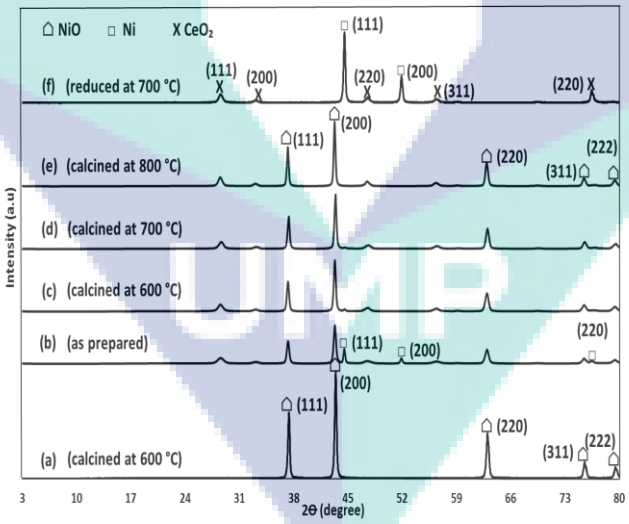

Figure 2 XRD patterns of a) Ni without Ce (calcined at 600°C); b) Ni modified with Ce (as-prepared); (c) Ni with modified Ce (calcined at 600°C); d) Ni modified with Ce (calcined 700°C); e) Ni modified with Ce (calcined at 800°C); f) Ni modified with Ce (reduced at 700°C)

3.2 Morphology analysis

SEM micrographs of Ni catalysts modified with La and Ce at various glycine-nitrate (G/N) ratios are shown in Figure 3. At G/N ratio of 0.5, Ni catalyst modified with La (Figure 3a) and Ni catalyst modified with Ce (Figure 3d) have 'cottonwool-like' structures. As the G/N ratio increased from 0.5 to 1.0, the catalysts formed a 'spongy-like' structure with random-size pores (Figures 3b and 3e). At G/N= 1.5, both catalysts become denser with much lesser pores on their surfaces (Figures 3c and 3f). Porous structure developed on catalysts produced from GNP is a result of large volume of gases generated from the combustion. Meanwhile, the pores size is directly related to the flame temperature and the nature of combustion [15]. The stoichiometric ratio of G/N for NiO, Ni modified with La and Ni-modified with Ce are G/N= 1.11, 1.33 and 1.44, respectively. Thus, the G/N= 0.5 is considered as fuel-lean, while G/N = 1.5 is a fuel-rich. The 'cottonwool-like' and highly porous structure observed for the catalysts at G/N=0.5 is due to the low flame temperature, which is associated with fuel-lean composition [15]. As the G/N ratio increases to G/N= 1.0, close to the stoichiometric ratio, the structure changed from 'cottonwool-like' to 'spongy-like' structure as the agglomeration increases due to higher flame temperature [15]. At G/N ratio above the stoichiometric ratio (G/N=1.5), the flame temperature decreases again with the increasing of fuel due to the incomplete combustion. This also led to the sintering of catalyst particles [19, 8]. Therefore, it can be observed that at fuel-rich composition (G/N=1.5), the catalyst become dense and the porosity was the least.

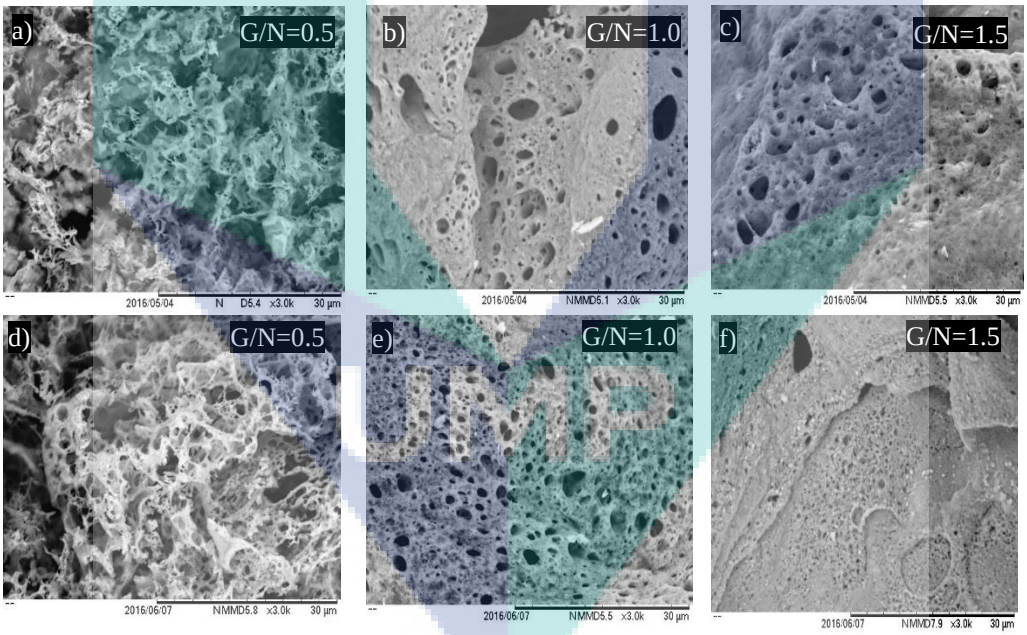

Figure 3 SEM images of Ni catalysts modified with La (a – c) and Ce (d – f) at glycine-nitrate ratio (G/N) = 0.5, 1.0 and 1.5.

4. CONCLUSION

Ni modified with La and Ni modified with Ce catalysts have been successfully synthesized using glycine-nitrate combustion process (GNP). XRD analysis shows that La element in Ni catalyst modified with La was initially existed as $LaNiO_3$ phase. After reduction under a flow of H_2, the $LaNiO_3$ was changed into La_2O_3 and the reduced Ni modified with La catalyst composed of separated phases of Ni and La_2O_3. Meanwhile, CeO_2 phase in Ni modified with Ce catalyst was produced directly from the glycine-nitrate combustion process. The CeO_2 remains after the reduction process. The reduced Ni modified with Ce catalyst composed of active Ni and CeO_2. The effect of glycine-nitrate (G/N) ratio on the morphology of the catalysts has been analyzed using SEM. When the G/N ratio employed is less than the stoichiometric ratio, the 'cottonwool-like' and highly porous structure were observed for both Ni catalysts modified La and Ce. At the fuel composition higher than the stoichiometric ratio, both Ni catalysts modified La and Ce catalysts become dense in structure and contain less pores.

ACKNOWLEDGEMENTS

This work was supported by Universiti Malaysia Pahang internal grant (RDU 150382).

REFERENCES

[1] Patil, K.C., Hegde, M.S., Tanu, R. and Aruna, S.T., (2008). Chemistry of Nanocrystalline Oxide Materials: Combustion Synthesis Properties and Applications, World Scientific, Singapore, 2008.

[2] He, T., He, Q., and Wang, N., (2005). Synthesis of nano-sized YSZ powders from glycine-nitrate process and optimization of their properties. *J. Alloys Comp*. 396, 309.

[3] Hwang, C. C., Wu, T. Y., Wan, J., and Tsai, J. S., (2004). Development of a novel combustion synthesis method for synthesizing of ceramic oxide powders. *Mater.Sci. Eng. B*, 111, 49.

[4] Yildiz, Ö., Soydan, A. M., Ata, A., Tunaboylu, B., Akin, D., and Ipcizade, E. F., (2013). Properties of ceria based novel anode nanopowders synthesized by glycine-nitrate process. *Acta Physica Polonica* A,123

[5] Purohit, R.D., Sharma, B.P., Pillai, K.T. and Tyagi, A.K. (2001). Ultrafine ceria powders via glycine-nitrate combustion. *Mater. Res. Bull.* 36 , 2711.

[6] Deshpande, K., Mukasyan, A. and Varma, A. (2003). Aqueous Combustion Synthesis of Strontium-Doped Lanthanum Chromite Ceramics. *J. Am. Ceram. Soc*., 86, 1149–1154.

[7] Ghose, R., Hwang, H.T. and Varma, A. (2013). Oxidative coupling of methane using catalysts synthesized by solution combustion method. *Applied Catalysis A: General*, 452, 147-154.

[8] Barros, B. S., Kulesza, J., Maria, Dulce. And Kienneman, Alain. (2015). Nickel-based catalyst precursor prepared via microwave-induced combustion method: Thermodynamics of synthesis and performance in dry reforming of CH_4. *Materials Research,* 18(4),732-739.

[9] Mokkelbost, T., Kaus, I., Grande, T. and Einarsrud, Mari-Ann. (2004). Combustion synthesis and characterization of nanocrystalline CeO_2-based powders. *Chem. Mater,* 16, 5489-5494.

[10] Pino, L., Vita, A., Cipitì, F., Laganà, M. and Recupero, V. (2011). Hydrogen production bymethane tri-reforming process over Ni-ceria catalysts: effect of La-doping,Appl. Catal. B 104,64–73.

[11] Zhu, Huaiyu,. Wang, Wei., Ran, Ran. And Shao, Zhaoping. (2013). A new nickel-ceria composite for direct-methane solid oxide fuel cells. International Journal of Hydrogen Energy 38, 3741-3749

[12] Prasad DH, Jung H-Y, Jung H-G, Kim B-K, Lee H-W, Lee J-H. Single step synthesis of nano-sized NiO–Ce0.75Zr0.25O2 composite powders by glycine nitrate process. vol. 62. 2008.

[13] Italiano C, Vita A, Fabiano C, Laganà M, Pino L. Bio-hydrogen production by oxidative steam reforming of biogas over nanocrystalline Ni/CeO2 catalysts. Int J Hydrogen Energy 2015;40:11823–30.

[14] Bhavsar, S. and Veser, G. (2013). Reducible Supports for Ni-based Oxygen Carriers in Chemical Looping Combustion. Energy & Fuels, 27, 2073-2084.

[15] Hadke S, Kalimila MT, Rathkanthiwar S, Gour S, Sonkusare R, Ballal A. Role of fuel and fuel-to-oxidizer ratio in combustion synthesis of nano-crystalline nickel oxide powders. Ceram Int 2015;41:14949–57.

[16] Cui, Y., Galvita, V., Rihko-Struckmann, L., Lorenz, H., Sundmacher, K. (2009). Steam reforming of glycerol: the experimental activity of La1_xCexNiO3 catalyst in comparison to the thermodynamic reaction equilibrium. Appl Catal B Environ ,90:29-37.

[17] Iriondo, A., Barrio, V. L., Cambra, J. F., Arias, P. L., Güemez, M. B., Navarro, R. M., Sánchez-Sánchez, M. C., and Fierro, J.L.G. (2008). Hydrogen production from glycerol over nickel catalyst supported on Al_2O_3 modified by Mg, Zr, Ce or La

[18] Yang, E., Kim, N. Y., Noh, Y., Lim, S. S., Jung, J., Lee, J. S., Hong, G. H. and Moon, D. J. (2015). Steam CO_2 reforming of methane over $La_{1-x}Ce_xNiO_3$ perovskite catalyst

[19] Nair, S. R., Purohit, R. D., Tyagi, A. K., Sinha, P. K. and Sharma, B. P. (2008). Role of glycine-to-nitrate ratio in influencing the powder characteristics of La(Ca) CrO3, Mater.Res.Bull.43,1573–1582.

CHAPTER 3

PAPER PUBLISHED IN INDUSTRIAL & ENGINEERING CHEMISTRY RESEARCH

Mohamad Muzakkir Tajuddin, Asmida Ideris, Mazni Ismail (2019) In Situ Glycine–Nitrate Combustion Synthesis of Ni–La/SiO_2 Catalyst for Methane Cracking, Ind. Eng. Chem. Res. 58, 2, 531–538

ABSTRACT

Ni–La catalyst supported on SiO_2 (Ni–La/SiO_2) synthesized using in situ glycine–nitrate combustion was analyzed for catalyst dispersion at various catalyst-to-support ratios and support surface areas. Catalytic activity of the catalyst was assessed for methane cracking. Catalyst with higher support loading had a better catalyst dispersion. The use of support with high surface area also improved catalyst dispersion. Ni–La/SiO_2 B synthesized using support with high surface area have a higher catalyst dispersion than that of Ni–La/SiO_2 A with support of low surface area. As a result, Ni–La/SiO_2 B had a better methane conversion (the maximum of ~60%) than that of Ni–La/SiO_2 A (~40%) and offered a higher H_2 yield. Moreover, Ni–La/SiO_2 B was found to be active for carbon formation. Nevertheless, the catalyst remained catalytically active for methane cracking without deactivation.

Keywords: *In situ glycine–nitrate combustion, Ni–La/SiO_2, catalyst dispersion, catalyst-to-support ratio, support surface area, methane cracking*

1.0 INTRODUCTION

Methane cracking is a moderate endothermic process for H_2 production as the energy required for every mole of H_2 is about 37.8 kJ/mol, lower than that needed for steam reforming, 63.3 kJ/mol.[1,2] Methane cracking involves the production of H_2 without carbon-containing gases (Eq. 1).[3] It is an alternative route for H_2 synthesis to eliminate the undesirable CO_2 generation from the conventional hydrocarbons processing which then simplifies the overall hydrogen production process[1]. Noncatalytic methane cracking requires high temperatures (>1200 °C) to achieve a considerable methane conversion due to high strength of C–H bond.[4] Transition metal catalysts are normally used to improve the dissociation of CH_4 molecules for a moderate-temperature methane cracking.[5] Among the transition metals, Ni-based catalyst has been broadly studied due to its high catalytic activity in methane cracking.[6] Although methane cracking favors high operating temperatures, the process is limited by Ni catalyst efficiency as the catalyst deactivates at high temperatures.[7]

$$CH_4 \rightarrow 2H_2 + C \qquad (1)$$

Silica, SiO_2 is the most effective support for metal-supported Ni-based catalyst for methane cracking as it gives the highest methane conversion compared with those of MgO, Al_2O_3, and ZrO_2.[8] Metal-supported catalysts derived from conventional catalyst preparation methods such as impregnation and coprecipitation have been reported to have low metal dispersion[9] and poor control of surface composition.[10] Mehrabadi et al.[9] reported that impregnation method rarely produces metal-supported catalyst of high dispersion. This is due to the absence of strong interaction between precursor and support, which then allows agglomeration of precursor during drying.[9,11] Additionally, the main disadvantage of impregnation and coprecipitation process is that both methods are unable to control the particel size and size distribution of metal catalyst formed.[12,13]

In situ glycine–nitrate combustion process is a catalyst synthesis process in which metal-supported catalyst is produced through a combination of impregnation and self-combustion approaches.[14] In situ combustion synthesis is a cost-effective method[15] and displays magnificent properties related to crystallite size, degree of reduction, and metal dispersion.[16–18] The combustion reaction occurs exothermically after the self-ignition of glycine–metal nitrates mixture in the presence of an inert support. The large amount of gaseous byproduct released during the combustion process brings a considerable expansion of the metal catalyst, and a rapid temperature drop after the combustion reaction results in both porous structure and high metal dispersion.[19] Highly dispersed metal particles are also produced as a result of a rapid moving combustion wave by the chemical reaction through the support.[20] Meanwhile, the high temperature of the reaction ensures the high purity product by the removal of low-boiling-point impurities.[21]

Catalyst dispersion can be defined as the fraction of the total number of metal atoms that are exposed on the surface.[11] Researchers have reported that catalyst dispersion of higher than 40% is considered as a decent catalyst dispersion and high catalyst dispersion has resulted in a high catalytic activity of metal-supported catalysts.[22,23] Urdiana et al.[24] found that catalysts with high dispersion of metal particles had a better methane conversion in methane cracking. The same trend was also observed in benzene hydrogenation reaction where the catalytic activity increased with

the increase of catalyst dispersion.[25] Various factors have been identified to have influence on catalyst dispersion in metal-supported catalysts which are properties of the support,[26] catalyst-to-support ratio,[27] catalyst preparation method,[28] and support surface area.[29] Researchers also have related the improvement of Ni dispersion with La introduction in Ni-based catalysts.[30,31,32] La content has been reported to enhance the catalytic activity of Ni–La_2O_3/SiO_2 and extended the stability of the catalyst during methane cracking and methane dry reforming.[33,34]

Previous works have reported that in situ glycine–nitrate combustion process produces catalyst with high dispersion.[19,20] In this work, Ni–La/SiO_2 has been successfully synthesized using in situ glycine–nitrate combustion process and catalyst dispersion of the catalyst has been explored. The effects of support surface area and catalyst-to-support ratio were evaluated towards catalyst dispersion and the catalytic performance of the produced Ni–La/SiO_2 was investigated in methane cracking process.

2.0 EXPERIMENTAL METHODS

2.1 Catalyst preparation

Ni–La/SiO_2 was synthesized via in situ glycine–nitrate combustion. Catalyst precursors of metal nitrates were prepared by dissolving nickel(II) nitrate hexahydrate, $Ni(NO_3)_2{\cdot}6H_2O$ (Merck, USA) and lanthanum(III) nitrate hexahydrate, $La(NO_3)_3{\cdot}6H_2O$ (Merck, USA) at a fixed Ni:La ratio of 0.95:0.05. Glycine (NH_2CH_2COOH, Merck, USA) was added into the precursor solution at a glycine-to-nitrate ratio (G/N) of 1.0. Two types of commercial SiO_2 support were used in this study; SiO_2 gel (Davisil Grade 633, particle size: 74 μm, designated as SiO_2 A) and SiO_2 amorphous fumed (particle size: 44 μm, designated as SiO_2 B). The support was added into the glycine–nitrate solution at various catalyst-to-support ratios (1:2, 1:5, and 1:8). The mixture of SiO_2–glycine–nitrate was heated overnight at 90 °C on a hot plate stirrer (IKA, Germany) to form a homogeneous, viscous, and gel-like slurry. The resulted slurry was then placed in a ceramic bowl and further heated until it was self-ignited and combusted, producing a metal-supported catalyst. The metal-supported catalyst was then calcined at a calcination temperature of 800 °C for 2 h and further sieved to produce a catalyst of a uniform particle size of 75 μm.

2.2 Support and catalyst characterizations

X-ray diffraction (XRD) analysis was performed on fresh metal-supported catalyst using a Miniflex II desktop powder diffractometer (Rigaku, Japan). Data sets were recorded in a step-scan mode for 2θ ranged from 3° to 80° with interval of 0.02°/s. The crystallite sizes of the catalyst were determined using Scherrer equation.[26] The morphology of fresh and spent catalysts were analyzed using field emission scanning electron microscopy (FESEM, Jeol JSM7800F, Japan). Thermogravimetric analysis was also conducted for the fresh and spent catalysts using a thermogravimetric analyzer (TGA, Mettler Toledo TGADSC1, Switzerland) under a flow of air. The weight loss of the catalysts was monitored within a temperature range of 30–1000 °C at 10 °C/min. Finally, specific surface areas of the two supports SiO_2 A and SiO_2 B were determined using a surface area analyzer (Micromeritics ASAP 2020, USA) using BET method.

2.3 Catalytic activity

Methane cracking activity was carried out in a fixed-bed quartz tube reactor system as shown in Figure 1. Initially, the catalyst was loaded onto the quartz wool inside the quartz tube reactor and in situ reduction was performed under a mixture of 10% H_2/N_2 at 700 °C for 2 h. The catalyst was then contacted to the reaction gas of 20% CH_4/N_2 at a total flow rate of 60 mL/min. Methane cracking was conducted at 500 °C for 6 h and the process was maintained at 45,000 mL/g·h of gas space hour velocity (GHSV). The product gas was collected throughout the experiment using gas bags and the composition of the product gas was determined by gas chromatograph (GC) equipped with thermal conductivity detector (TCD) (Agilent Technologies 6890 series, USA) using molecular sieve 13X column (Agilent, USA). Product gas composition was determined using an external standard method where volumetric flow rate of outlet gas was measured for each gas sample to consider the gas volume change due to the reaction. The catalytic performance of the catalyst was evaluated on the basis of methane conversion and hydrogen yield and the values were computed using Eqs. 2 and 3, respectively.[35,36]

Methane conversion, X_{CH_4}

$$X_{CH_4} = \frac{n_{CH_4}^{in} - n_{CH_4}^{out}}{n_{CH_4}^{in}} \times 100\% \qquad (2)$$

where

n_{CH4}^{in} = entering molar flow rate of CH_4 (mol/min), and

n_{CH4}^{out} = exiting molar flow rate of CH_4 (mol/min)

Hydrogen yield, Y_{H_2}

$$Y_{H_2} = \frac{Moles\ of\ H_2\ produced}{2 \times Moles\ of\ CH_4\ in\ feed} \times 100\% \qquad (3)$$

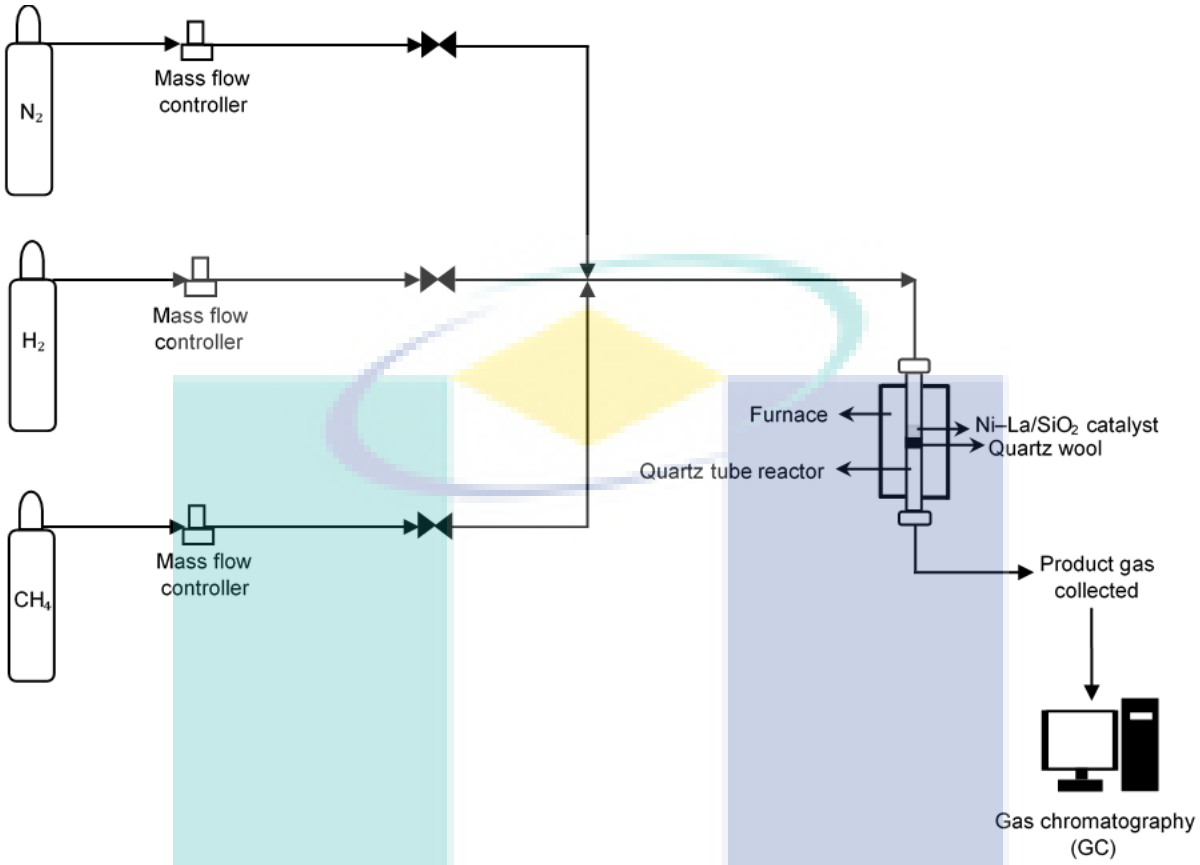

Figure 1. Fixed-bed quartz tube reactor system for methane cracking.

3.0 RESULTS AND DISCUSSIONS

3.1 Fresh catalyst

The XRD patterns for SiO_2 A, SiO_2 B, unreduced Ni–La catalyst, Ni–La catalyst, Ni–La catalyst supported on SiO_2 A (Ni–La/SiO_2 A), and Ni–La catalyst supported on SiO_2 B (Ni–La/SiO_2 B) are given in Figure 2. Figures 2a and 2b show the patterns of amorphous structure of SiO_2 for both SiO_2 A and SiO_2 B, given by a wide peak at 22.5°. Figure 2c demonstrates that the unreduced Ni–La catalyst freshly produced from the combustion synthesis had a crystalline structure. NiO phase detected at planes (111), (200), (220), (311), and (222) at the angles of 37°, 43°, 63°, 76°, and 79°, respectively, exhibited the cubic rock salt structure of NiO.[37] Meanwhile, the La element in the unreduced Ni–La catalyst existed in a form of $LaNiO_3$ phase as detected at the phase angle of 33°. After the reduction, the $LaNiO_3$ peak was entirely diminished and the peak of La_2O_3 plane (200) appeared at the phase angle of 77° (Figure 2d). The $LaNiO_3$ phase in the Ni–La catalyst formed as separated phases of Ni and La_2O_3 after the reduction process. The phenomenon where $LaNiO_3$ in the Ni–La catalyst was replaced by La_2O_3 after the reduction process was also found by other researcher.[38] Additionally, the NiO phase at planes (111), (200), (220), (311), and (222) also disappeared and replaced by metallic Ni as shown by Ni planes (111) and (200) (Figure 2d). The XRD patterns for reduced samples of Ni–La/SiO_2 A and Ni–La/SiO_2 B catalysts synthesized via

in situ glycine–nitrate combustion are shown in Figures 2e and 2f, respectively. Both catalysts were composed of an amorphous SiO_2, Ni metallic, and La_2O_3 phases. Compared with the pattern for the unsupported Ni–La catalyst (Figure 2d), the diffraction peaks for Ni phase at (111) and (200) planes in Ni–La/SiO_2 A and Ni–La/SiO_2 B became wider with the addition of supports. From Scherrer equation, the Ni crystallite size for Ni–La catalyst was 27.3 nm and decreased to 15.1 and 10.3 nm with the addition of support for Ni–La/SiO_2 A and Ni–La/SiO_2 B, respectively. This indicates that the introduction of SiO_2 support has reduced the crystallinity of Ni metal in Ni–La/SiO_2 catalysts, which also suggests that Ni metal catalyst has been highly dispersed over the surface of SiO_2 support in the Ni–La/SiO_2 catalysts.

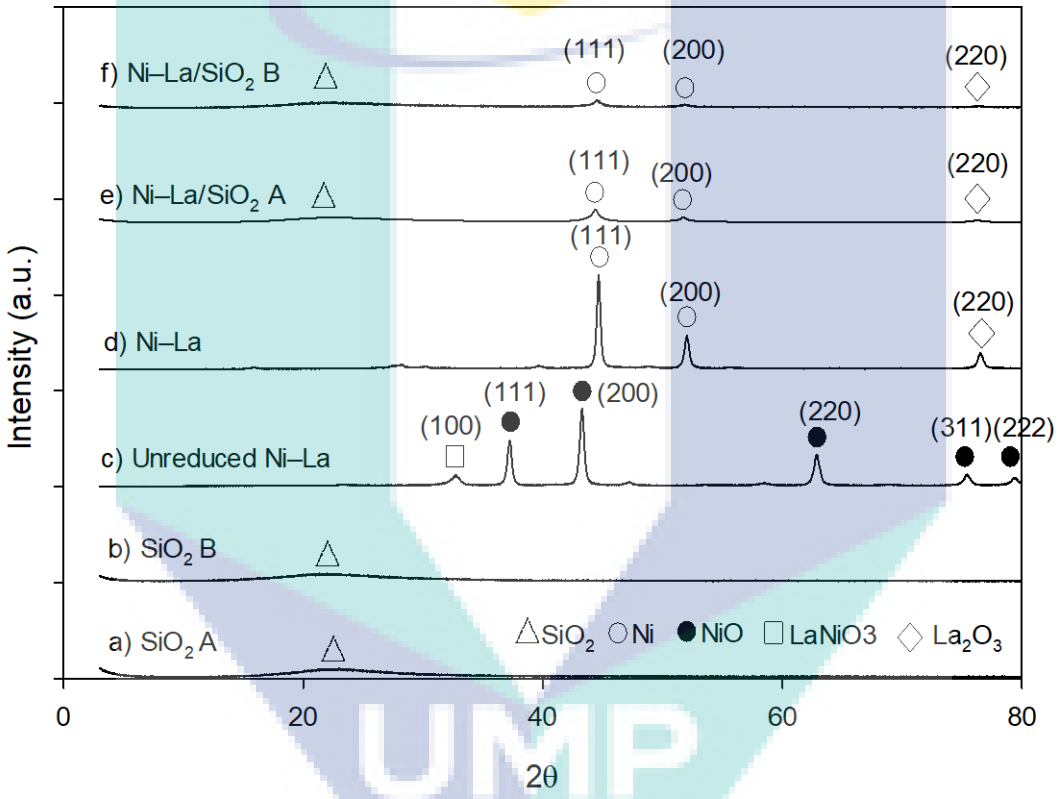

Figure 2. XRD patterns of (a) SiO_2 A, (b) SiO_2 B, (c) unreduced Ni–La catalyst, (d) Ni–La catalyst, (e) Ni–La/SiO_2 A, and (f) Ni–La/SiO_2 B. SiO_2 (△), NiO (●), Ni (○), La_2O_3 (◇), and $LaNiO_3$ (□).

The BET analysis conducted on both SiO_2 A and SiO_2 B shows that SiO_2 B had a higher surface area (477 m^2/g) than that of SiO_2 A (207 m^2/g) (Table 1). Figure 3 shows the FESEM images of Ni–La/SiO_2 A and Ni–La/SiO_2 B. The dense structure with a smooth surface belongs to the SiO_2 support while the porous-like structure on the surface of the support is the Ni–La catalyst. The porous-like structure is a unique feature for catalyst produced via glycine–nitrate combustion.[39] The Ni–La catalyst for Ni–La/SiO_2 B was distributed over the most area of the SiO_2 B surface (Figure 3b). Meanwhile for Ni–La/SiO_2 A, the Ni–La catalyst only disseminated on limited areas of the SiO_2 A surface (Figure 3a). This suggests that support with a high surface area would provide a better distribution of catalyst particles with a higher chance of better catalyst dispersion.

Table 1 BET analysis of SiO_2 A and SiO_2 B.

Support	Features	Surface area (m^2/g)
SiO_2 A	SiO_2 gel (Davisil Grade 633, average particle size: 74 μm)	207
SiO_2 B	SiO_2 amorphous fumed (average particle size: 44 μm)	477

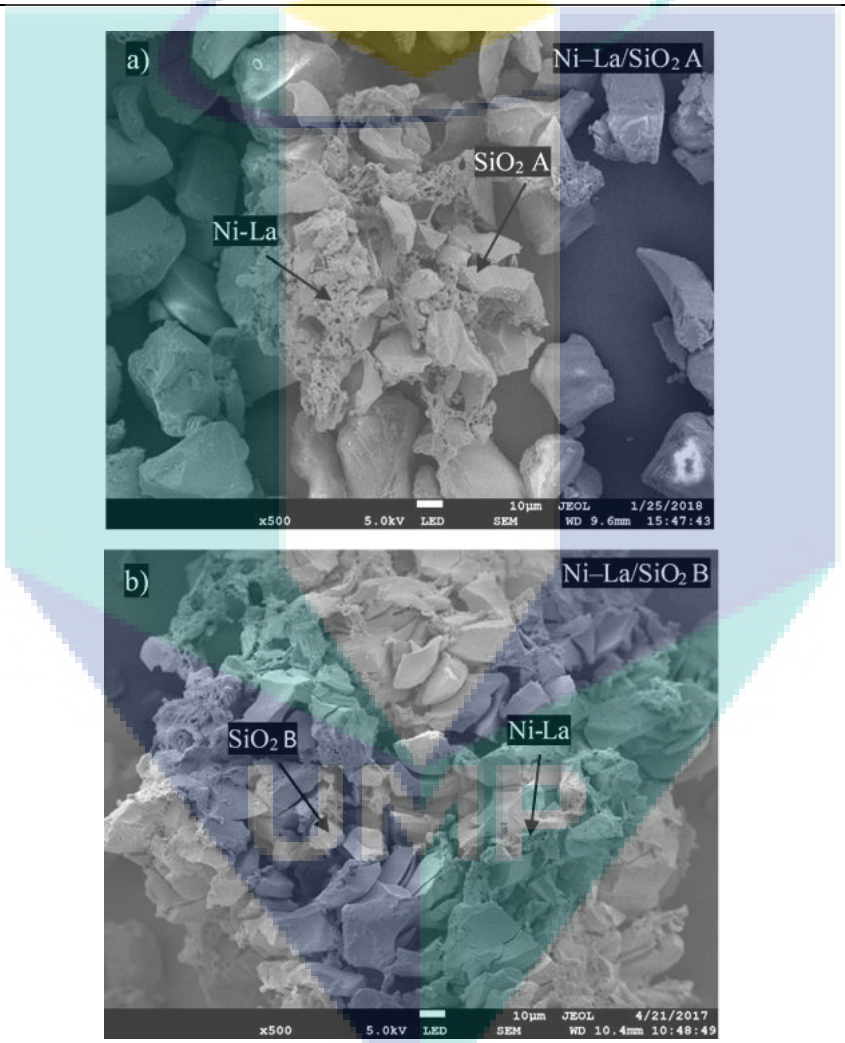

Figure 3. FESEM images of (a) Ni–La/SiO_2 A and (b) Ni–La/SiO_2 B.

3.2 Catalyst dispersion

From XRD analysis, the introduction of SiO_2 support has reduced the crystallinity the Ni–La catalyst, which indicates that high dispersion of Ni metal has been achieved over the surface of SiO_2 support. To further evaluate the dispersion of Ni–La/SiO_2 A and Ni–La/SiO_2 B catalysts, data

available from the XRD analysis was employed to calculate the catalyst dispersion.[40] The dominant peak for metallic Ni peak at 44.5° from the XRD patterns of reduced samples of Ni–La/SiO_2 catalyst was selected as a reference to determine the Ni metal dispersion on SiO_2 support. The dispersion of the catalysts was observed at various catalyst-to-support ratios (1:2, 1:5, and 1:8). The Ni crystallite size, d_{Ni} was determined using Scherrer equation as given by Eq. 4:

$$d_{Ni} = \frac{K\lambda}{B\cos\theta} \quad (4)$$

where K is a dimensionless shape factor (0.9), λ is the X-ray wavelength (0.15406 nm), and B is the full-width half maximum (FWHM) for the Ni peak chosen (at 44.5°) and θ is the angle at FWHM of the peak. The Ni crystallite size d_{Ni} was used to estimate the number of Ni particles N_1 (Eq. 5):

$$N_1 = \frac{m_{Ni}}{\frac{2}{3}\pi(\frac{d_{Ni}}{2})^3\rho_{Ni}} \quad (5)$$

where ρ_{Ni} is the density of Ni (8.902×10^6 g/m^3) and m_{Ni} is the Ni atomic mass (58.69).
The Ni crystallite size d_{Ni} and estimated number of Ni particles N_1 were further used to calculate the overall surface area of Ni particles, S using Eq. 6:

$$S = 2\pi(\frac{d_{Ni}}{2})^2 N_1 \quad (6)$$

Finally, the Ni catalyst dispersion D was calculated using Eq. 7:

$$D = \frac{Sk}{m_{Ni}N_A} \quad (7)$$

where k is Ni atom density (1.529×10^{19} m^{-2}) and N_A is the Avogadro number (6.02×10^{23} mol^{-1}).

The calculated catalyst dispersions for Ni–La/SiO_2 A and Ni–La/SiO_2 B at various catalyst-to-support ratios are shown in Figure 4. For Ni–La/SiO_2 A, higher support loading gave better dispersion when the dispersion increased from 20.4% to 55.8% as the catalyst-to-support ratio was increased from 1:2 to 1:8. A similar finding was also reported in a previous work when the catalyst dispersion increased with the increase of support loading.[25] However, the trend for Ni–La/SiO_2 B on varying the support loading was not obvious. The catalyst dispersion for Ni–La/SiO_2 B remained high at low and high support loadings. Nevertheless, the values obtained were relatively higher than those for Ni–La/SiO_2 A at any catalyst-to-support ratio. This is consistent with the FESEM images in Figure 3 suggesting that catalyst supported on a support of high surface area would have a better catalyst dispersion. Yang et al.[40] calculated the Ni dispersion for Ni/MgO catalysts synthesized using impregnation. The Ni catalyst dispersions were between 14% and 19% which are much lower than those obtained for Ni–La/SiO_2 B prepared via in situ glycine–nitrate combustion in this work (55%–68%).

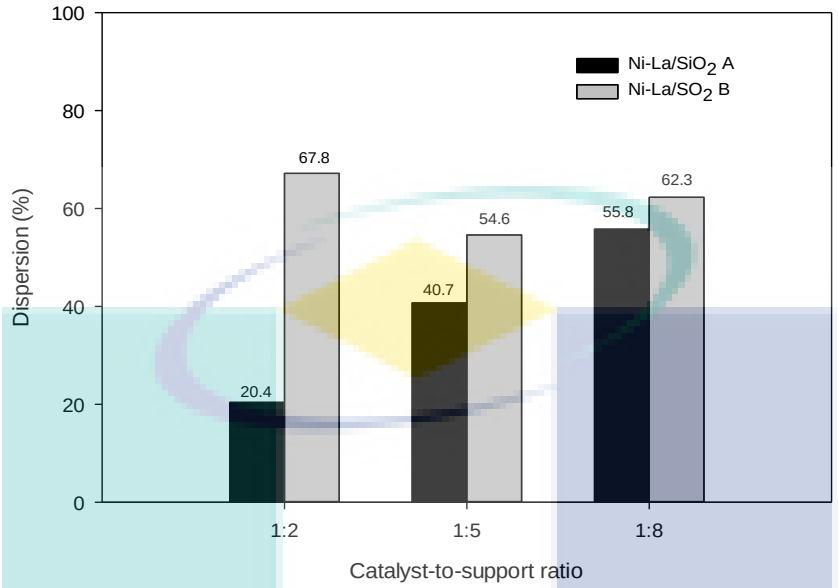

Figure 4. Calculated catalyst dispersions for Ni–La/SiO_2 A and Ni–La/SiO_2 B at various catalyst-to-support ratios.

3.3 Catalytic activity

The catalytic performances of the Ni–La/SiO_2 catalysts were evaluated in methane cracking at 500 °C. The methane conversions for Ni–La/SiO_2 A and Ni–La/SiO_2 B are shown in Figure 5. A support loading at catalyst-to-support ratio of 1:8 was applied for these catalysts. The methane conversions for Ni–La/SiO_2 A were within the range of 20%–40%. Ni–La/SiO_2 B on the other hand exhibited a higher methane conversion (maximum of ~60%) during the first 120 min before it decreased to ~30% and maintained until the end of the reaction. Support with high surface area is expected to provide a high number of catalytic active sites for metal-supported catalyst.[41] High support loading has also been reported to give high methane conversion.[42] Therefore, the combination of high support surface area and high support loading would result in a high catalyst dispersion for Ni–La/SiO_2 B with a catalyst-to-support ratio of 1:8, thus giving a high catalytic activity. Nevertheless, the catalyst is also expected to be active for carbon deposition. High catalytic activity will induce more dissociation of C–H on the Ni surface, thus encouraging more carbon to deposit on the catalyst active sites.[43] Carbon accumulation on catalyst surface could be the reason for the significant decrease of methane conversion of Ni–La/SiO_2 B after 2 h of its operation.

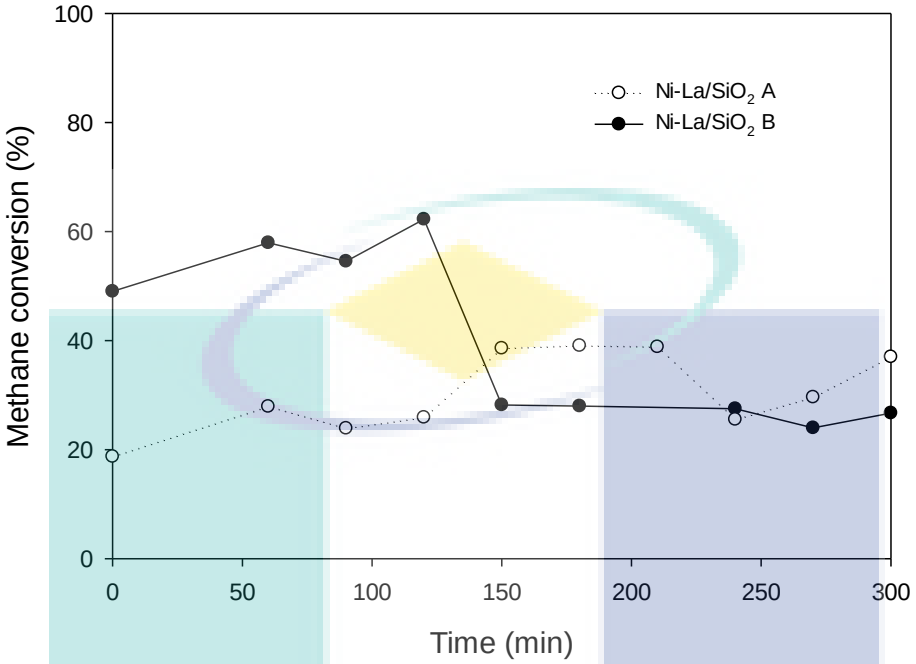

Figure 5. Methane conversions for Ni–La/SiO_2 A and Ni–La/SiO_2 B at a catalyst-to-support ratio of 1:8.

Hydrogen yields for Ni–La/SiO_2 A and Ni–La/SiO_2 B are shown in Figure 6. Ni–La/SiO_2 A only managed to produce less than 3% hydrogen yield and the amount depleted to zero after 90 min of the reaction time. A better hydrogen yield was produced by Ni–La/SiO_2 B when the catalyst gave an approximately 10% of hydrogen yield at the beginning of the reaction before the value decreased and became constant at ~4%. Ni–La/SiO_2 B continuously produced H_2 until the reaction was terminated at 300 min. This explains that Ni–La/SiO_2 B with high support surface area and high support loading provided more active sites for the hydrogen production to continuously take place during the cracking reaction.[41,44]

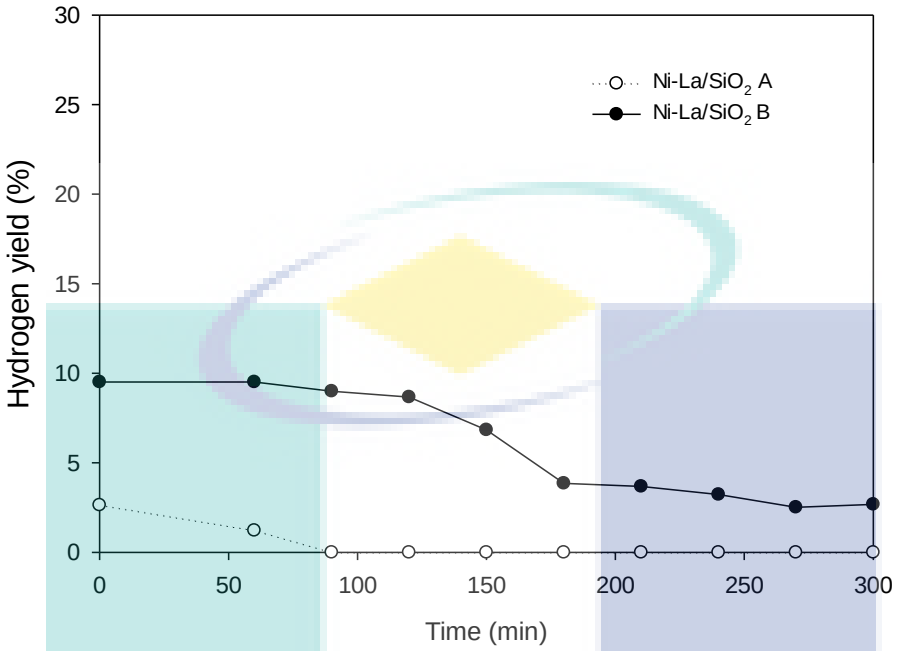

Figure 6. Hydrogen yields for Ni–La/SiO_2 A and Ni–La/SiO_2 B at a catalyst-to-support ratio of 1:8.

3.4 Characterization of spent catalysts

Figure 7 shows the FESEM images for spent Ni–La/SiO_2 A and Ni–La/SiO_2 B catalysts after methane cracking. Ni–La/SiO_2 A comprises two distinctive structures, which are spherical- and fiber-like structures (Figure 7a). An EDX analysis (result is not shown here) verified that the spherical-like structure was due to the Ni particles while the fibers were identified as filament carbons. The filament carbons were distributed within the Ni particles on the surface of Ni–La/SiO_2 A. It is believed that the spherical Ni particles available on the catalyst surface were the result of the Ni particles detachment from the bulk of Ni due to the activity of the filament carbons.[45] The detachment of the Ni particles explains the very low H_2 yield by Ni–La/SiO_2 A during the methane cracking process (Figure 6). Meanwhile, a massive amount of filament carbons was found on the surface of Ni–La/SiO_2 B (Figure 7b). The entire surface of Ni–La/SiO_2 B was covered with the filament carbons suggesting that the catalyst had been active for catalytic activity. Nevertheless, the detachment of the Ni particles was not observed on the spent Ni–La/SiO_2 B, thus giving a better H_2 yield compared with that of Ni–La/SiO_2 A (Figure 6). High catalyst dispersion is associated with a strong metal-support interaction in metal-support catalyst.[46] With high catalyst dispersion, strong metal-support interaction restrains the movement of Ni particles on SiO_2 surface, which is believed occurred within Ni–La/SiO_2 B catalyst. Meanwhile, a weak metal-support interaction could be the reason the detachment of Ni metal particles in Ni–La/SiO_2 A.[47] Additionally, the growth mechanism of filament carbons is also influenced by metal-support interaction.[48] In Ni–La/SiO_2 B where it is expected to have a strong metal-support interaction, Ni particles remain at the support and the filament carbons grow from the bulk surface of Ni catalyst. Meanwhile, in a catalyst with a weaker metal-support interaction (Ni–La/SiO_2 A), Ni particles are detached from the support due to the growth of carbon and located at the tip of filaments.

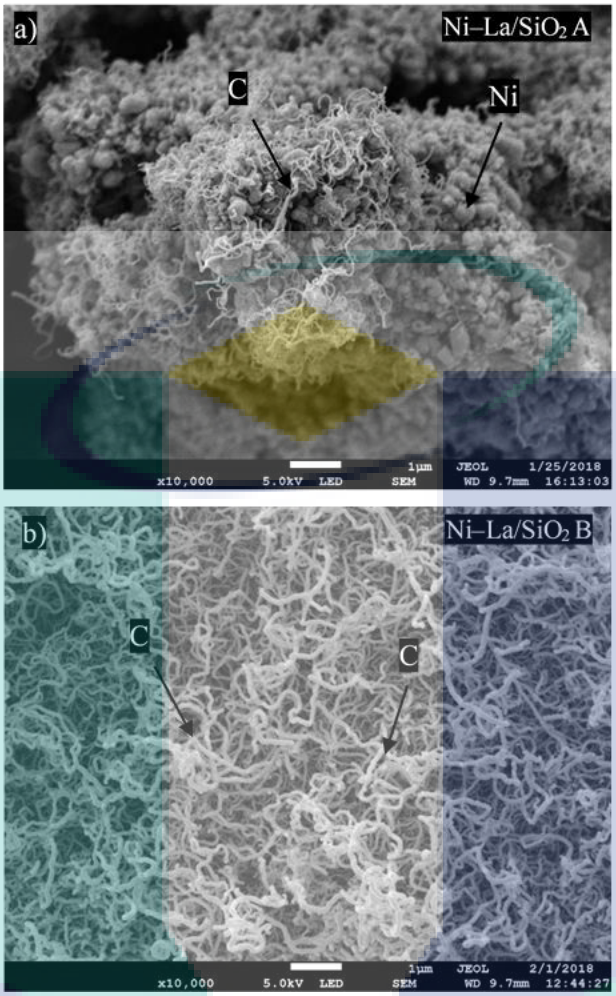

Figure 7. FESEM images of spent (a) Ni–La/SiO_2 A and (b) Ni–La/SiO_2 B.

3.5 Types of carbon

The spent Ni–La/SiO_2 A and Ni–La/SiO_2 B were analyzed using XRD to evaluate the types of carbon deposited and the XRD patterns are shown in Figure 8. A Ni metallic phase was detected for both Ni–La/SiO_2 A and Ni–La/SiO_2 B at the phase angles of 44.5° and 52°, respectively. The crystallinity of the spent Ni–La/SiO_2 B was higher than that of the spent Ni–La/SiO_2 A, given by the sharper peak of Ni phase for the spent Ni–La/SiO_2 B (Figure 8a). This also suggests that Ni–La/SiO_2 B catalyst suffered from sintering on the over the reaction.[49] Meanwhile, the peaks of Ni for the spent Ni–La/SiO_2 A in Figure 8b were remained in a broad form as a fresh catalyst in Figure 2e. No peak for La phase was detected on the spent catalysts. An obvious and high intensity peak at the angle of 26° for the spent Ni–La/SiO_2 B in Figure 8a was attributed to graphitic carbon.[50] A similar graphitic carbon peak appeared at the shoulder of the Ni peak at 44.5°. No graphitic carbon was detected on the surface of Ni–La/SiO_2 A although carbon was found deposited on the catalyst surface (Figure 7a). The Ni particles detachment from Ni bulk in Ni–La/SiO_2 A catalyst may have disrupted the formation of carbons on the surface of the catalyst. Meanwhile, the presence of graphitic carbon species on the spent Ni–La/SiO_2 B catalyst is corresponding to the accumulation of filament carbons on the surface of the catalyst as shown previously in Figure 7b. Graphitic

carbon is formed on the catalyst surface due to the constant exposure of the carbon over high temperature and prolonged reaction time.[51] This demonstrates that Ni–La/SiO_2 B with high support surface area was catalytically active for carbon deposition yet kept producing H_2 without catalyst deactivation for 6 h of methane cracking.

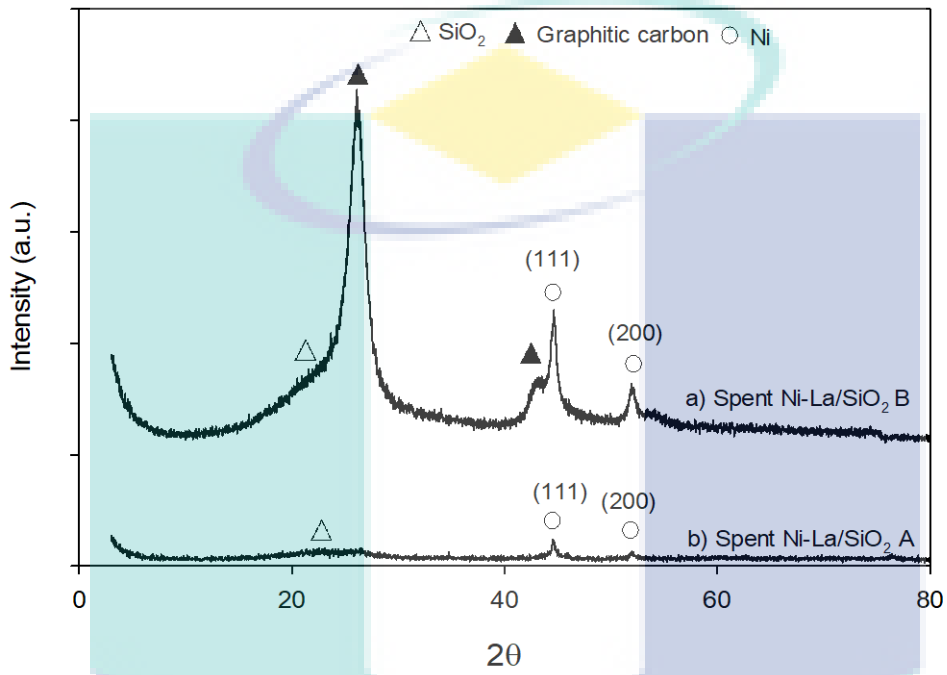

Figure 8. XRD patterns for (a) spent Ni–La/SiO_2 A and (b) spent Ni–La/SiO_2 B after methane cracking.

The TGA profiles for the fresh and spent Ni–La/SiO_2 A and Ni–La/SiO_2 B performed are shown in Figure 9. The weight loss for the spent Ni–La/SiO_2 A was within the range of 600–700 °C while the weight loss for the spent Ni–La/SiO_2 B occurred within the range of 500–850 °C. The weight loss within these temperature ranges is associated to the decomposition of carbon on the surface of catalyst.[52,53] From this analysis, it can be concluded that the carbon formed on the surface of Ni–La/SiO_2 B catalyst was more difficult to be removed compared with that deposited on the surface of Ni–La/SiO_2 A. This is consistent with the results from previous XRD analysis (Figure 8) where the carbon formed on Ni–La/SiO_2 B was a graphitic carbon. Additionally, the weight loss for the spent Ni–La/SiO_2 B was higher (~80%) than the weight loss for the spent Ni–La/SiO_2 A (~20%), which is related to the amount of carbon deposited on each catalyst. This shows that Ni–La/SiO_2 B was not only active for the H_2 production but also for the carbon deposition, allowing more carbon to be deposited on its surface.

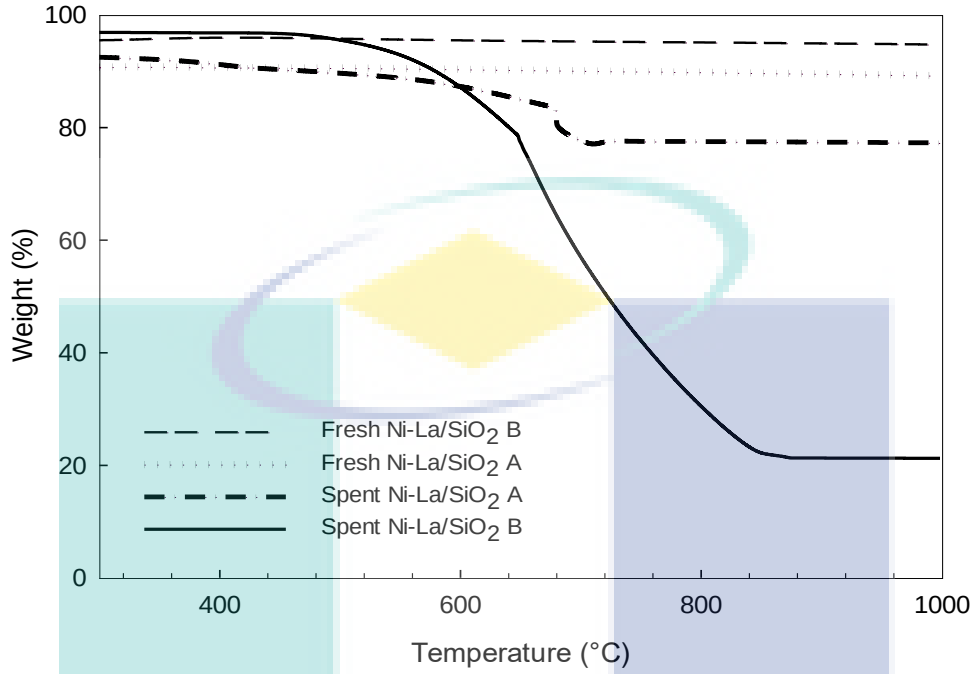

Figure 9. TGA profiles of the fresh and spent Ni–La/SiO_2 A and Ni–La/SiO_2.

4.0 CONCLUSIONS

Catalyst dispersion of Ni–La/SiO_2 catalyst produced via in situ glycine–nitrate combustion process has been successfully evaluated. Ni–La/SiO_2 catalyst with higher support loading had a better catalyst dispersion when the dispersion increased as the catalyst-to-support ratio increased. Support surface area also influenced catalyst dispersion. Ni–La/SiO_2 B catalyst with high support surface area had a higher catalyst dispersion compared with Ni–La/SiO_2 A with low support surface area, thus giving a higher catalytic activity. During methane cracking, Ni–La/SiO_2 B showed the maximum methane conversion of ~60%, better than the conversion shown by Ni–La/SiO_2 A at ~40%. A similar trend was also observed for the H_2 production when Ni–La/SiO_2 B gave a higher H_2 yield compared with that yield given by Ni–La/SiO_2 A. Moreover, the catalyst was also active for carbon formation. A large amount of carbons was deposited on the surface of Ni–La/SiO_2 B that was identified as graphitic carbon. Nonetheless, Ni–La/SiO_2 B remained catalytically active throughout the 6 h of methane cracking and continuously produced H_2 without catalyst deactivation.

ACKNOWLEDGMENT

Authors would like to acknowledge the funding received for this wok from Universiti Malaysia Pahang Internal Grant (RDU150382).

REFERENCES

(1) Muradov, N. Hydrogen via Methane Decomposition : An Application for Decarbonization of Fossil Fuels. *Int. J. Hydrogen Energy* **2001**, *26*, 1165–1175.

(2) Muradov, N.; Smith, F.; Huang, C.; T-Raissi, A. Autothermal Catalytic Pyrolysis of Methane as a New Route to Hydrogen Production with Reduced CO_2 emissions. *Catal. Today* **2006**, *116* (3), 281–288.

(3) Rodat, S.; Abanades, S. .; Flamant, G. Co-Production of Hydrogen and Carbon Black from Solar Thermal Methane Splitting in a Tubular Reactor Prototype. *Sol. Energy* **2011**, *85*, 645–652.

(4) García-Sancho,C., Guil-López, R., Sebastián-López, A., Navarro, R. M., Fierro, J. L. G. Hydrogen Production by Methane Decomposition: A Comparative Study of Supported and Bulk Ex-Hydrotalcite Mixed Oxide Catalysts with Ni, Mg and Al. *Int. J. Hydrogen Energy* **2018**, 1–15.

(5) Li, Y.; Li, D.; Wang, G. Methane Decomposition to CO_x-Free Hydrogen and Nano-Carbon Material on Group 8–10 Base Metal Catalysts : A Review. *Catal. Today* **2011**, *162* (1), 1–48.

(6) Amin, A. M.; Croiset, E.; Epling, W. Review of Methane Catalytic Cracking for Hydrogen Production. *Int. J. Hydrogen Energy* **2010**, *36* (4), 2904–2935.

(7) Torres, D.; Pinilla, J. L.; Suelves, I. Screening of Ni-Cu Bimetallic Catalysts for Hydrogen and Carbon Nanofilaments Production via Catalytic Decomposition of Methane. *Appl. Catal. A Gen.* **2018**, *559*, 10–19.

(8) Ermakova, M. A.; Ermakov, D. Y.; Kuvshinov, G. G. Effective catalysts for direct cracking of methane to produce hydrogen and filamentous carbon: Part I. Nickel catalysts. *Appl. Catal. A: General.* **2000**, 201**,** 61-70.

(9) Mehrabadi, B. A. T.; Eskandari, S.; Khan, U.; White, R. D.; Regalbuto, J. R. *A Review of Preparation Methods for Supported Metal Catalysts*, 1st ed.; Elsevier Inc., 2017.

(10) Diao, W. Preparation and Characterization Of Pt-Ru Bimetallic Catalysts Using Electroless Deposition Methods And Mechanistic Study Of Re And Cs Promoters For Ag-Based, High Selectivity Ethylene Oxide Catalysts (Doctoral dissertation). 2015. Retrieved from http://scholarcommons.sc.edu/etd/3232

(11) Tengco, J. M. M. Synthesis of Well Dispersed Supported Metal Catalysts by Strong Electrostatic Adsorption and Electroless Deposition. (Doctoral dissertation). 2016 Retrieved from http://scholarcommons.sc.edu/etd/3540

(12) Liu,Y.; Chao, C., Enhanced electrochemical performance of nano-sized $LiFePO_4$/C synthesized by an ultrasonic-assisted co-precipitation method *Electrochim. Acta*. **2010,** *55* (16), 4694-4699

(13) Galhenage, R. P.; Xie, K.; Diao, W.; Tengco, J.M.M.; Seuser G.S.; Monnier, J. R; Chen, D. A. Platinum-Ruthenium Bimetallic Clusters on Graphite: A Comparison of Vapor Deposition and Electroless Deposition Methods. *Phys. Chem. Chem. Phys.* **2015**, *17* (42), 28354–28363.

(14) Cross, A.; Roslyakov, S.; Manukyan, K. V; Rouvimov, S.; Rogachev, A. S.; Kovalev, D.; Wolf, E. E.; Mukasyan, A. S. In Situ Preparation of Highly Stable Ni-Based Supported Catalysts by Solution Combustion Synthesis. *J. Phys. Chem.* **2014**, *118* (45), 26191–26198.

(15) Kang, W.; Varma, A. Hydrogen Generation from Hydrous Hydrazine over Ni/CeO_2 Catalysts Prepared by Solution Combustion Synthesis Hydrous Hydrazine Is a Promising

Hydrogen Carrier for Fuel Cell Vehicles Owing to Its High. *"Appl. Catal. B, Environ.* **2017**.
(16) Phienluphon, R.; Shi, L.; Sun, J.; Niu, W.; Lu, P.; Zhu, P.; Vitidsant, T.; Yoneyama, Y.; Chen, Q.; Tsubaki, N. Ruthenium Promoted Cobalt Catalysts Prepared by an Autocombustion Method Directly Used for Fischer–Tropsch Synthesis without Further Reduction. *Catal. Sci. Technol.* **2014**, *4* (9), 3099.
(17) Shi, L.; Jin, Y.; Xing, C.; Zeng, C.; Kawabata, T.; Imai, K.; Matsuda, K.; Tan, Y.; Tsubaki, N. Studies on Surface Impregnation Combustion Method to Prepare Supported Co/SiO_2 catalysts and Its Application for Fischer-Tropsch Synthesis. *Appl. Catal. A Gen.* **2012**, *435–436*, 217–224.
(18) Shi, L.; Tao, K.; Kawabata, T.; Jun, Z. X.; Shimamura, T. Surface Impregnation Combustion Method to Prepare Nanostructured Metallic Catalysts without Further Reduction: As-Burnt Co/SiO_2 Catalysts for Fischer–Tropsch Synthesis. *ASC Catal.* **2011**, *1*, 1225–1233.
(19) Varma, A.; Mukasyan, A. S.; Rogachev, A. S.; Manukyan, K. V. Solution Combustion Synthesis of Nanoscale Materials. *Chem. Rev.* **2016**, *116* (23), 14493–14586.
(20) Ail, S. S.; Benedetti, V.; Baratieri, M.; Dasappa, S. Fuel-Rich Combustion Synthesized Co/Al2O3 Catalysts for Wax and Liquid Fuel Production via Fischer–Tropsch Reaction. *Ind. Eng. Chem. Res.* **2018**, *57* (11), 3833–3843.
(21) Mukasyan, A. S.; Epstein, P.; Dinka, P. Solution Combustion Synthesis of Nanomaterials. *Proc. Combust. Inst.* **2007**, *31 II*, 1789–1795.
(22) Parapat, R. Y.; Saputra, O. H. I.; Ang, A. P.; Schwarze, M. Support Effect in the Preparation of Supported Metal Catalysts via Microemulsion. *RSC Adv.* **2014**, *4*, 50955–50963.
(23) Thyssen, V. V.; Assaf, E. M. Ni/La_2O_3-SiO_2 Catalysts Applied to Glycerol Steam Reforming Reaction: Effect of the Preparation Method and Reaction Temperature. *J. Braz. Chem. Soc.* **2014**, *25* (12), 2455–2465.
(24) Urdiana, G.; Valdez, R.; Lastra, G.; Valenzuela, M.; Olivas, A. Production of Hydrogen and Carbon Nanomaterials Using Transition Metal Catalysts through Methane Decomposition. *Mater. Lett.* **2018**, *217*, 9–12.
(25) Boudjahem, A. G.; Bouderbala, W.; Soltani, A. Relationship between Metal Dispersion, Hydrogen Desorption, and Activity for Benzene Hydrogenation over Pd/SiO_2 Catalysts. *Synth. React. Inorganic, Met. Nano-Metal Chem.* **2013**, *43* (10), 1397–1401.
(26) Liu, Y.; Sheng, W.; Hou, Z.; Zhang, Y. Homogeneous and Highly Dispersed Ni–Ru on a Silica Support as an Effective CO Methanation Catalyst. *RSC Adv.* **2018**, *8* (4), 2123–2131.
(27) Setiabudi, H. D.; Chong, C. C.; Abed, S. M.; Teh, L. P.; Chin, S. Y. Comparative Study of Ni-Ce Loading Method: Beneficial Effect of Ultrasonic-Assisted Impregnation Method in CO_2 reforming of CH_4 over Ni-Ce/SBA-15. *J. Environ. Chem. Eng.* **2018**, *6* (1), 745–753.
(28) Pegios, N.; Bliznuk, V.; Prünte, S.; Schneider, J. M.; Palkovits, R.; Simeonov, K. Comparative Study on La-Promoted Ni/γ-Al_2O_3 for Methane Dry Reforming – Spray Drying for Enhanced Nickel Dispersion and Strong Metal–support Interactions. *RSC Adv.* **2018**, *8* (2), 606–618.
(29) Suttiponparnit, K.; Jiang, J.; Sahu, M.; Suvachittanont, S.; Charinpanitkul, T.; Biswas, P. Role of Surface Area, Primary Particle Size, and Crystal Phase on Titanium Dioxide Nanoparticle Dispersion Properties. *Nanoscale Res. Lett.* **2011**, *6* (1), 1–8.
(30) Gao, J.; Hou, Z.; Guo, J.; Zhu, Y.; Zheng, X. Catalytic Conversion Of Methane and CO_2 to Synthesis Gas Over a La_2O_3-Modified SiO_2 Supported Ni Catalyst in Fluidized-Bed Reactor. *Catal. Today*. **2008**, *131* (1–4), 278–284.

(31) Roh, H. S.; Jun, K. W. Carbon Dioxide Reforming of Methane Over Ni Catalysts Supported On Al_2O_3 Modified with La_2O_3, MgO, and CaO. *Catal. Surv. Asia*, **2008**, *12* (4), 239–252.
(32) Anjaneyulu, C.; Kumar, V.V.; Bhargava, S.K.; Venugopal, A. Characteristics of La-modified Ni-Al_2O_3 and Ni-SiO_2 Catalysts For CO_x-Free Hydrogen Production By Catalytic Decomposition Of Methane. *J. Energy Chem.* **2013**, *22* (6) 853–860.
(33) Wang, H.; Wang, W.; Yang, Y.; Peng, S. Effects of La_2O_3, Cu and Fe Addition On the Catalytic Performance of Ni-SiO_2 Catalysts for Methane Decomposition. *J. Plasma Fusion Res*. **2013**, *10*, 42–48.
(34) Chen, C.; Wang, X.; Zhang, L.; Zou, X.; Ding, W.; Lu, X. Synthesis of Mesoporous Ni–La_2O_3/SiO_2 by Ploy(Ethylene Glycol)-Assisted Sol-Gel Route as Highly Efficient Catalysts For Dry Reforming of Methane With a H_2/CO Ratio of Unity. *Catal. Commun.* **2017**, 94, 38–41.
(35) Sengupta, S.; Ray, K.; Deo, G. Effects of Modifying Ni / Al_2O_3 Catalyst with Cobalt on the Reforming of CH_4 with CO_2 and Cracking of CH_4 Reactions. *Int. J. Hydrogen Energy* **2014**, *39* (22), 11462–11472.
(36) Ibrahim, A. A.; Fakeeha, A. H.; Al-fatesh, A. S.; Abasaeed, A. E.; Khan, W. U. Methane Decomposition over Iron Catalyst for Hydrogen Production. *Int. J. Hydrogen Energy* **2014**, *40* (24), 7593–7600.
(37) Han, D.Y.; Yang, H.Y.; Shen, C.B.; Zhou, X.; Wang, F.H. Synthesis and size control of NiO nanoparticles by water-in-oil microemulsion. *Powder Technol.* **2004**, 147,113-116.
(38) Zhu, H.; Wang, W.; Ran, R.; Shao, Z. A New Nickel-Ceria Composite for Direct-Methane Solid Oxide Fuel Cells. *Int. J. Hydrogen Energy* **2013**, *38* (9), 3741–3749.
(39) Tajuddin, M. M., Patulla, M. H., Ismail, M. Self-Combustion Synthesis of Ni Catalyst Modified with LA and Ce Using Glycine–Nitrate Process (GNP). *MJCat* **2017**, *2* (3), 8–11.
(40) Yang, X.; Wang, Y.; Wang, Y. Significantly Improved Catalytic Performance of Ni-Based MgO Catalyst in Steam Reforming of Phenol by Inducing Mesostructure. *Catalyst* **2015**, *5*, 1721–1736.
(41) Wi, R.; Imran, M.; Lee, K. G.; Hong Yoon, S.; Gyoo Cho, B.; Hyun Kim, D. Effect of Support Size on the Catalytic Activity of Metal-Oxide-Doped Silica Particles in the Glycolysis of Polyethylene Terephthalate. *J. Nanosci. Nanotechnol.* **2011**, *11*(c), 6544–6549.
(42) Setiabudi, H. D.; Lim, K. H.; Ainirazali, N.; Chin, S. Y. CO_2 Reforming of CH_4 over Ni/SBA-15 : Influence of Ni Loading on the Metal-Support Interaction and Catalytic Activity. *Jounal Mater. Environ. Sci.* **2017**, *8* (2), 573–581.
(43) Venugopal, A.; Naveen Kumar, S.; Ashok, J.; Hari Prasad, D.; Durga Kumari, V.; Prasad, K. B. S.; Subrahmanyam, M. Hydrogen Production by Catalytic Decomposition of Methane over Ni/SiO_2. *Int. J. Hydrogen Energy* **2007**, *32* (12), 1782–1788.
(44) Gutta, N. Design and Development of Ni Based Catalyst for CO_x Free H_2 Production by Catalytic Decomposition of Methane, RMIT University, 2017.
(45) Frusteri, F.; Italiano, G.; Espro, C.; Cannila, C.; Bonura, G. H_2 Production by Methane Decomposition: Catalytic and Technological Aspects. *Int. J. Hydrogen Energy* **2012**, *37* (21), 16367–16374.
(46) Yang, M.; Wu, H.; Wu, H.; Huang, C.; Weng, W.; Chen, M.; Wan, H. Preparation and Characterization of a Highly Dispersed And Stable Ni Catalyst With A Microporous Nanosilica Support. *RSC Adv.* **2016**, *6*, 81237–81244.
(47) Li, Y.; Li. D.; Wang, G. Methane Decomposition to COx-free Hydrogen and Nano-Carbon

Material On Group 8 – 10 Base Metal Catalysts: A review. *Catal. Today* **2011**, *162* (1),1–48.
(48) Lamouroux, E.; Philippe Serp, P.; Kalck, P. Catalytic Routes Towards Single Wall Carbon Nanotubes. *Catal. Rev.* **2007**, *49* (3), 341-405.
(49) Cai, W.; Ye, L.; Zhang, L.; Ren, Y.; Yue, B.; Chen, X.; He, H. Highly Dispersed Nickel-Containing Mesoporous Silica with Superior Stability in Carbon Dioxide Reforming of Methane: The Effect of Anchoring. *Materials (Basel).* **2014**, *7* (3), 2340–2355.
(50) Awadallah, A. E.; El-desouki, D. S.; Aboul-Gheit, N. A. K.; Ibrahim, A. H.; Aboul-gheit, A. K. Effect of Crystalline Structure and Pore Geometry of Silica Based Supported Materials on the Catalytic Behavior of Metallic Nickel Particles during Methane Decomposition to CO_x-Free Hydrogen and Carbon Nanomaterials. *Int. J. Hydrogen Energy* **2016**, *41* (38), 16890–16902.
(51) Ayillath Kutteri, D.; Wang, I.-W.; Samanta, A.; Li, L.; Hu, J. Methane Decomposition to Tip and Base Grown Carbon Nanotubes and CO_x-Free H_2 over Mono- and Bimetallic 3D Transition Metal Catalysts. *Catal. Sci. Technol.* **2018**, *8* (3), 858–869.
(52) Al-swai, B. M.; Osman, N. B.; Abdullah, B. Catalytic Performance of Ni/MgO Catalyst in Methane Dry Reforming. In *AIP Conference Proceedings* **2017**, Vol. 1891.
(53) Donphai, W.; Witoon, T.; Faungnawakij, K.; Chareonpanich, M. Carbon-Structure Affecting Catalytic Carbon Dioxide Reforming of Methane Reaction over Ni-Carbon Composites. *J. CO_2 Util.* **2016**, *16*, 245–256.

OVERALL CONCLUSIONS

In summary, Ni catalysts been modified with cerium (Ce), lanthanum (La) and barium (Ba) has been successfully synthesized using a self-combustion process, glycine- nitrate process (GNP). In all catalysts produced are high in crystallinity and crystallinity of the catalyst has increased with the increased of calcination temperature. 800°C was found to be the best calcination temperature for Ni metal catalysts modified with Ce, La and Ba. The Ni catalyst modified with Ce composed of Ni and CeO_2, the Ni modified with La catalyst composed of separated phases of Ni and La_2O_3 while the Ni catalyst modified with Ba composed of Ni and BaN_2O_6. Ni catalyst with modified La supported on an inert support, SiO_2 (Ni-La/SiO_2) was further chosen for catalytic activity in methane cracking. The catalyst was successfully produced using in situ glycine- nitrate process (in situ GNP). Ni−La/SiO_2 supported with SiO_2 support with a lower particle size has a better conversion than the shown by Ni-La/SiO_2 with a support of larger particle size. Initial H_2 yield for Ni−La/SiO_2 supported with SiO_2 support with a lower particle size was higher compared that for by Ni-La/SiO_2 with a support of larger particle size. Nevertheless, massive amount of filament carbons is found on the surface of Ni−La/SiO_2 supported with SiO_2 support with a lower particle size catalyst suggesting that the catalyst is very active for catalytic activity. Catalyst dispersion for Ni−La/SiO_2 supported with SiO_2 support with a lower particle size is higher than the one with a support of larger particle size, suggesting that catalyst supported on a support of high surface area has a better catalyst dispersion. Higher support loading also gave better catalyst dispersion. In overall, all three objectives of the project have been complied and the work has successfully produced Ni catalyst modified with La supported with SiO_2 with a decent stability and catalytic activity for methane cracking process.

APPENDIX

(URP TECHNICAL PAPER 1)

SELF-COMBUSTION SYNTHESIS OF LANTHANUM-MODIFIED NICKEL CATALYST FOR HYDROGEN PRODUCTION

Muhammad Hasbullah Patulla and Asmida Ideris
Faculty of Chemical & Natural Resources Engineering,
Universiti Malaysia Pahang, 26300 Gambang, Pahang, MALAYSIA.
Tel: +6019-5284361, Fax: +6095492889

ABSTRACT
The cost of catalyst production is significantly influenced by the synthesis route. One of the cheapest synthesis methods is through glycine-nitrate combustion process (GNP). In this work, glycine-nitrate combustion process was used to produce Ni catalyst modified with lanthanum. In the process, a precursor was prepared using a stoichiometric mixture of nickel nitrate and lanthanum nitrate. The precursor was then mixed with glycine which acts as a fuel. The nitrate-glycine solution was heated to evaporate the excess water and formed a viscous gel. The gel was further heated using an electronic stove until it self-ignited and produced an ash powder. The effects of calcination temperature and glycine-to- nitrate (G/N) ratio on the catalyst produced were investigated. The catalyst characterization was performed using X-Ray Diffraction (XRD) and Scanning Electron Microscopy (SEM) coupled with Energy-dispersive X-Ray Spectroscopy (EDX). XRD results shows that the calcination temperature of 800°C gave more crystalline structure compared to that at 700°C and 600°C. Meanwhile, the morphology structure of the catalyst can be controlled by the G/N ratio as proved by the SEM characterization. The catalysts show a foamy agglomerated structure with macropores, originating from the rapid evolution of gases during the combustion process.

Key-words: Glycine nitrate combustion process, Lanthanum-modified Nickel catalyst, calcination temperature, G/N ratio.

INTRODUCTION
Catalyst is usually defined as a substance that increases the rate of chemical reaction but not being consumed in the process (Lawrie, 2011). It is used to accelerate the rate of reaction toward chemical equilibrium and as a result it can improve the process economics. The principal catalytic components, for example nickel is normally mixed with other components, usually by co-precipitation or impregnation from solution.
Self-combustion has become an attractive and very popular synthetic method for preparation of catalyst powder (Shi et al., 2006). This method offers several distinct advantages. Firstly, the homogeneous mixtures of several components at molecular or atomic levels can be achieved in solution, and thus the ultra-fine powders can be obtained. The process is also time saving, cost effective, and produces catalyst powder with high purity (Aruna & Mukasyan, 2008). One of the most popular self-combustion methods is glycine nitrate combustion process (GNP). It uses amino glycine as a fuel and metal nitrates of the targeted composition as an oxidant for combustion process. Glycine serves in a dual role in the GNP process. In the precursor solution, it prevents selective precipitation in the glycine complexes of metal cations, and it also oxidizes the nitrate anions.
Physical properties of the synthesized catalyst powders are directly influenced by the process constituents. The average particle size decreases and the specific surface area increases with increasing glycine amount in the starting composition. The glycine-to-nitrate (G/N) ratio is known to have an effect on the flame temperature, combustion rate and product morphology of the catalyst produced (Guo et al., 2010). Calcination is a thermal treatment process which takes place at temperatures below the melting point to bring about thermal decomposition, phase transition or removal of volatile fractions of the catalyst. Calcination temperature significantly affects the texture property and the phase composition of catalysts (Ding et al., 2015). In this work, the effects of two variables; glycine-to-nitrate (G/N) ratio and calcinations temperature on the crystalline structure and morphology of the lanthanum-modified nickel catalyst were examined.

MATERIALS AND METHODS

Catalyst preparation

Nickel (II) nitrate ($Ni(NO_3)_2).6H_2O$) and lanthanum nitrate ($La(NO_3)_3).6H_2O$) were purchased from Merck (Darmstadt, Germany). Glycine ($C_2H_5NO_2$) was obtained from Sigma Aldrich (St. Louis, MO). A precursor solution was prepared by dissolving the nickel nitrate and lanthanum nitrate in the deionized water. The precursor of nitrates solution contains Ni^{2+} and La^{3+} concentrations in a ratio of La : Ni = 0.05 : 0.95. Glycine was then slowly added into the nitrate solution and the glycine-nitrate solution was heated at 90°C under a constant stirring using a hot plate stirrer (Sharma et al., 2014). With the evaporation of water, the glycine-nitrate solution was converted to a viscous gel. The gel was then further heated until it is self-ignited, yielding a foamy and voluminous catalyst ash.

Catalyst Characterization

X-ray diffraction analysis was performed using D8 Advance, Bruker-AXS, with Cu-Kα (0.15406 nm) radiation (30 kV, 15 mA) to determine the crystalline structure of the catalyst prepared. Data sets were recorded in a step-scan mode in the 2θ ranged from 10° to 80° with intervals of 0.02 a counting time of 1 second per point. The morphology of the catalyst powder and the elemental distribution of the catalysts were characterized using scanning electron microscopy (SEM) coupled by energy dispersive X-ray spectroscopy (EDXS) at 15 keV.

RESULTS AND DISCUSSION

Figure 1 shows the SEM image of the lanthanum-modified Ni catalyst with glycine-to-nitrate (G/N) ratio = 1.5:1 and calcined at 600°C. The presence of nickel (Ni) and lanthanum (La) can be distinguished by difference of the colour shown in the image. As the intensity of the back-scattered electron (BSE) signal of the SEM is proportional to the atomic number, the dark spots on the Ni catalyst surface are proposed to be the La element of the catalyst. The lighter in color of the surface was belonging to Ni.

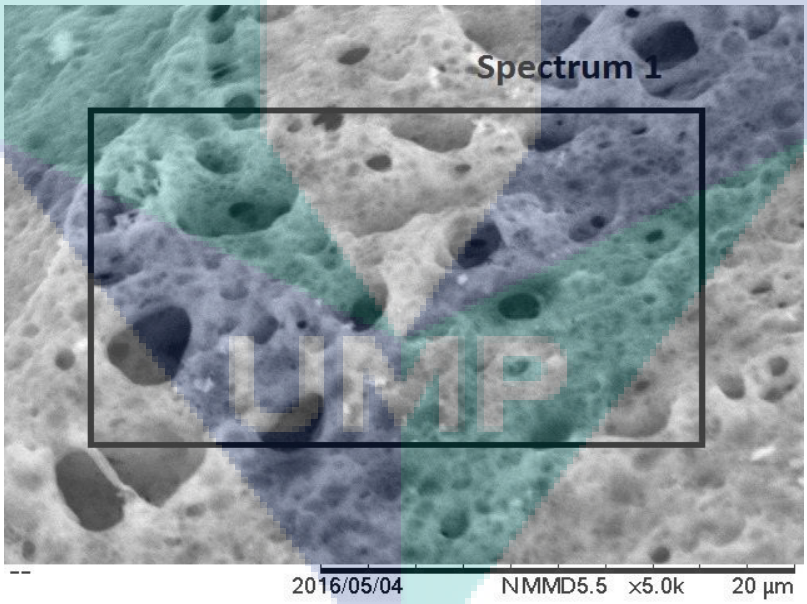

Figure 1: SEM-EDX micrographs of lanthanum-modified Ni catalyst (G/N= 1.5:1, calcined at 600°C).

EDX analysis was employed to confirm the existence of lanthanum in the catalyst. The analysis was performed on the mapped area of the catalyst surface shown previously in Figure 1. The EDX spectrum of the catalyst shows the presence of carbon (C), oxygen (O), nickel (Ni) and lanthanum (La) elements (Figure 2).

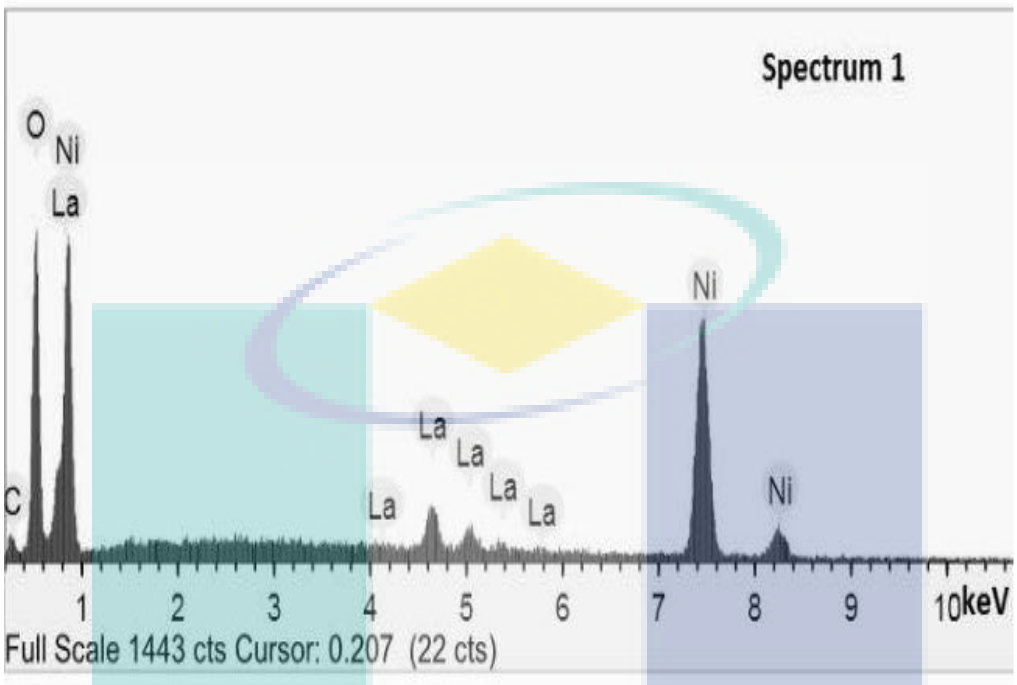

Figure 2: Compositions of elements in the $La_{0.05}Ni_{0.95}$ catalyst (G:N= 1.5:1).

Effect of Glycine-to-Nitrate (G/N) Ratio

The effect of glycine-to-nitrate (G/N) ratio on the morphology the catalyst prepared is shown by the SEM micrographs in Figure 3. All catalysts prepared demonstrate a spongy nature, originating from the rapid evolution of gases during the combustion process. It is clearly shown that the catalysts exhibit larger pores as the G/N decreases. The catalyst with G/N= 0.5 ratio displays a foam-like open-pore structure with non-uniform macropores (Figure 3(a)). The catalyst with large and more uniform macropores are resulted from the usage of G/N=1.0 (Figure 3(b)). Meanwhile, the G/N= 1.5 produce catalyst with small pores with the presence of dense surfaces. Glycine acts as a fuel during the glycine-nitrate combustion process. This process is a rapid self-sustaining process. Thus, increasing the amount of glycine would lead to an increase in the rate of combustion of the metal nitrates and cause the reaction to combust faster, drying out the nitrates and producing smaller primary particles (Thomas et al., 2011). These particles can be aggregated quickly, thus producing more dense structure as shown in Figure 3(c). This suggests that the morphology of the catalyst can be controlled by varying the G/N ratio in the catalyst preparation.

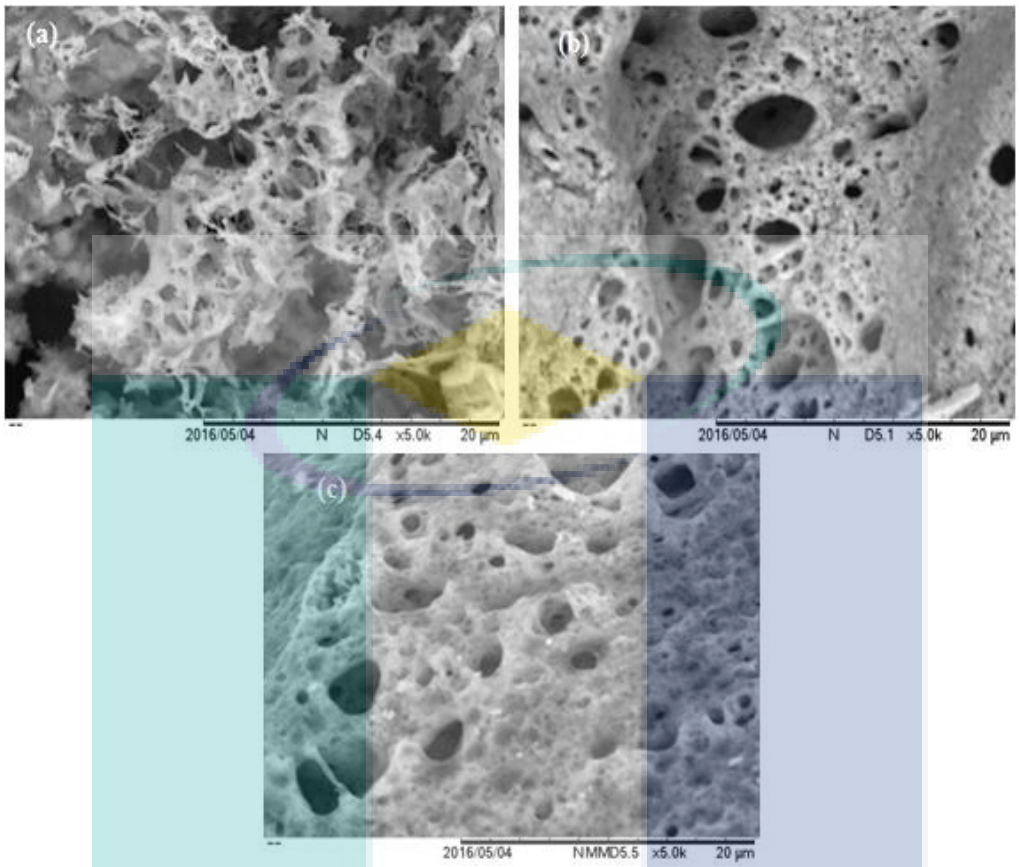

Figure 3: SEM micrographs of the lanthanum-modified Ni catalyst prepared with a) G/N ratio =0.5, b) G/N ratio =1.0, c) G/N ratio =1.5 at 5000x magnification.

Effect of Calcination Temperature

The XRD patterns of lanthanum-modified Ni catalysts calcined at different temperatures of 600°C, 700°C and 800°C for 2 hours are shown in Figures 4(a-c). As the calcinations temperature increases, the XRD patterns show higher and sharp peaks, presenting the catalyst with high crystalline in phase. The calcination temperature of 800°C gave more crystalline structure compared to that at 700 and 600°C. The typical diffractions for NiO phase are at 37.2°, 43.2°, 62.6°, 75.3° and 79.2° (Yan et al., 2014) at observed in all patterns. The characteristic hexagonal phase of La_2O_3 given by a small peak at 57.8° in was observed in La-Ni catalyst calcined at 700°C Figure 4(b) and 800°C Figure 4(c). Most likely, La^{3+} which is a considerably large ion and hence difficult to diffuse into the support's vacant sites. Consequently, it exists as La_2O_3 with high metal dispersion within the solid matrix. The finely-dispersed La_2O_3 practically ensures lesser carbon deposition, improves catalyst sintering and an increase in surface area (Jerkiewickz et al., 2007). Meanwhile, the reflection peaks at 32.8° and 47.1° in all XRD patterns could be assigned to La_2NiO_4 (Pérez-coll et. al, 2009). This suggests that the small amout of NiO and La_2O_3 might have reacted with each other to form a secondary phase (La_2NiO_4). The results are compared with the XRD pattern for Ni catalyst alone calcined at 600°C (Figure 4(d)).

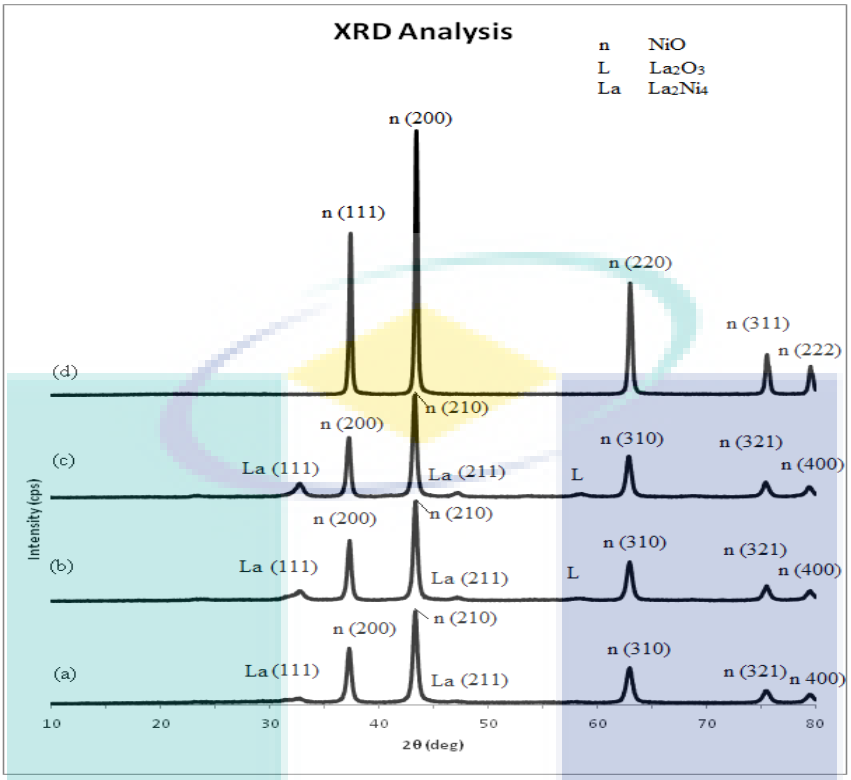

Figure 4: XRD patterns of lanthanum-modified Ni catalyst (a) calcined at 600°C; (b) calcined at 700°C; (c) calcined at 800°C and (d) Ni catalyst powder alone calcined at 600°C.

CONCLUSION

This study successfully employed the GNP method to obtain porous, homogeneous, stoichiometric Ni-modified with lanthanum catalyst powders. The glycine-nitrate ratio affected the morphology of the $La_{0.05}Ni_{0.95}$ particles. The combustion processes and physicochemical properties of catalysts are greatly influenced by the glycine amount. The particle size of catalysts shows volcano variation trends, increase of particle size and crystallinity with the increase in the glycine amount. Increasing the amount of glycine would lead to an increase in the rate of combustion of the metal nitrates and cause the reaction to combust faster and hotter, drying out the nitrates and producing smaller primary particles. These particles can aggregate quickly, because they are close together and sticky, leading to the formation of the more porous structures. The calcination and of the catalyst have a great influence on its activity and stability. As the calcination temperature is higher, the catalyst reducibility diminishes due to the formation of La_2Ni_4 which has stronger interaction with the support of La. Consequently, the catalyst calcined at 800°C has the most suitable structural features (the greatest metal surface with the best dispersion). The calcination at 800°C produces a larger amount of highly dispersed Ni oxides, which are more resistant to sintering. These better structural features lead to a higher catalyst activity and a more steady hydrogen production because of the catalyst ability to avoid both coke formation on its surface (small and well dispersed nickel crystallites) and metal sintering.

REFERENCES

Aruna, S. T., & Mukasyan, A. S. (2008). Combustion synthesis and nanomaterials. *Current Opinion in Solid State and Materials Science*, *12*(3-4), 44–50.

Ding, C., Liu, W., Wang, J., Liu, P., Zhang, K., Gao, X., … Ma, X. (2015). One step synthesis of mesoporous NiO–Al2O3 catalyst for partial oxidation of methane to syngas: The role of calcination temperature. *Fuel*, *162*, 148–154.

Guo, X., Mao, D., Lu, G., Wang, S., & Wu, G. (2010). Glycine–nitrate combustion synthesis of CuO–ZnO–ZrO2 catalysts for methanol synthesis from CO2 hydrogenation. *Journal of Catalysis*, *271*(2), 178–185.

Jerkiewickz, G., Moreira, E., & Lucre, A. F. (2007). Nickel catalysts promoted with cerium and lanthanum to reduce carbon formation in partial oxidation of methane reactions, *333*, 90–95.

Lawrie L., (2011), Fundamental and Applied Catalysis, Chapter 3, In *Handbook of Industrial Catalysts* (pp,78-95), New York: Springer

Pérez-coll, D., Aguadero, A., Escudero, M. J., & Daza, L. (2009). Effect of DC current polarization on the electrochemical behaviour of La 2 NiO 4 + ı, *192*, 2–13.

Shi, M., Liu, N., Xu, Y., Yuan, Y., Majewski, P., & Aldinger, F. (2006). Synthesis and characterization of Sr- and Mg-doped LaGaO3 by using glycine–nitrate combustion method. *Journal of Alloys and Compounds*, *425*(1-2), 348–352.

Sharma, A., Rani, A., Singh, A., Modi, O. P., & Gupta, G. K. (2014). Synthesis of alumina powder by the urea–glycine–nitrate combustion process: a mixed fuel approach to nanoscale metal oxides. *Applied Nanoscience*, *4*(3), 315–323.

Thomas, E., Lee, D. H., Yoon, M. Y., Ehrman, S. ., & Hwang, H. J. (2011). Synthesis and sintering behavior of La0.8Sr0.2CrO3 by a glycine nitrate process. *Ceramics International*, *37*(7), 2269–2274.

Yan, C.-F., Chen, H., Hu, R.-R., Huang, S., Luo, W., Guo, C.,Li, W. (2014). Synthesis of mesoporous Co–Ce oxides catalysts by glycine-nitrate combustion approach for CO preferential oxidation reaction in excess H2. *International Journal of Hydrogen Energy*, *39*(32), 18695—18701.

APPENDIX

(URP TECHNICAL PAPER 2)

SELF-COMBUSTION SYNTHESIS OF CERIA-MODIFIED NI CATALYST FOR HYDROGEN PRODUCTION

Nur Suhana Aisha Isa and Asmida Ideris
Faculty of Chemical & Natural Resources Engineering,
Universiti Malaysia Pahang, 26300 Gambang, Pahang, MALAYSIA.
Tel: +60108875905

ABSTRACT

Hydrogen is commonly produced through steam reforming, partial oxidation and methane cracking. One main problem associated with hydrogen production through these processes is carbon deposition. Produced as a by-product in hydrogen production, carbon will deposit on the catalyst and deteriorates the catalyst activity. One way to reduce carbon deposition is by modifying the catalyst used for the hydrogen production. In this work, Ni-based catalyst will be modified by ceria (CeO_2). The addition of ceria is expected to inhibit carbon deposition. Glycine-nitrate self-combustion process (GNP) is chosen for catalyst preparation in this work since it is simple and less expensive, and produces catalyst with high purity. The catalyst produced from GNP will be characterized with thermo-gravimetric analysis (TGA). Based on TGA results, Ni catalyst modified with CeO_2 at G/N= 0.5 has achieved its complete formation and perfectly crystallized at T≈ 800°C. At G/N= 1.0 and G/N= 1.5, the catalysts have reach their complete and crystallization at T≈ 500°C. This suggested that the higher the G/N ratio used, the lower the crystallization temperature of the catalyst. High G/N ratio also has led to a higher increment of catalyst weight when the catalyst formation went to a completion.
Keywords: nickel catalyst modified with ceria, glycine-nitrate process, thermo-gravimetric analysis (TGA), glycine-nitrate (G/N) ratio

1. Introduction

Nickel-based catalyst is an excellent catalyst for hydrogen production due to its promising catalytic performance in terms of conversion and selectivity (Istadi et al., 2011) and less expensive (Belhadi at al., 2011). Although the catalyst is a favorable for hydrocarbon processing, Ni alone is very prone to carbon deposition. In order to take advantages of Ni good properties, the modification of Ni catalyst with other substance known as carbon inhibitor is essential to reduce the carbon deposition.

There are many substances that can be added into Ni to improve the carbon tolerant of the Ni catalyst namely as metals, noble materials and metal oxides. Known metals used are gold (Au), silver, tin, cooper, cobalt, molybdenum, iron, gadolinium and boron (Hongjing et al., 2013). Nickel modified with Au catalyst, for example has been reported to be active for steam reforming and has the ability as a carbon-tolerant reforming catalyst (Hongjing et al., 2013). Platinum, palladium and rhodium are amongst noble metals added in Ni catalyst. It has been found that the addition of Pt and Pd to Ni/Al_2O_3 has shown a remarkable effect on the resistance to deactivation by Ni oxidation and exhibits high resistance to coke formation (Tomishige, 2007).

Metal oxides also have the ability as carbon tolerant materials. One example of the metal oxides is ceria (CeO_2). Ni catalyst highly dispersed with ceria has shown to have a high resistance towards carbon deposition (Zhuang et al., 1991). Ceria is an effective support catalyst for oxidation of hydrocarbon (Fu et al., 2003). Ceria is able to shift easily between reduced and oxidized state ($Ce^{3+} \Leftrightarrow Ce^{4+}$) and accommodate variable levels of bulk and surface oxygen vacancies thus improving catalytic performances (Jun et al., 2007). As stated by Hongpeng et al (2007), carbon formation was significantly reduced and the interaction of carbon and nickel is weaker with the presence of ceria. Metallic catalysts promoted with cerium are interesting due to cerium properties that can influence the mechanic and thermal resistance of support, metallic dispersion, catalytic performance, and carbon reduction on the surface catalyst (Centeno et al., 2002).

In this study, ceria-modified catalyst will be prepared by one type of self-combustion method, glycine-nitrate combustion process (GNP). GNP is a redox-type reaction which provides heat energy to the system without needing any extra external energy. Glycine (NH_2CH_2COOH) will act as fuel to carry out the combustion process while the

nitrate solution acts as an oxidizer. Combustion technique has the ability to produce ultra-fine powders amongst with other available wet chemical processes (Ferreira et al., 1992; Kingsley et al., 1990). Furthermore, it produces catalyst with to high purity and has an incredible efficiency. In this work, Ni catalyst will be modified with ceria and the modified catalyst will be synthesized using GNP. This research aims to evaluate the effect of glycine-nitrate ratio (G/N) used in preparation of nickel modified with ceria catalyst using thermo-gravimetric analysis (TGA).

2. Experimental

2.1. Catalyst preparation process

Ceria-modified nickel catalyst was synthesized using GNP with solution precursor acts as the oxidizer and glycine as the fuel. The precursor is a solution containing cerium nitrate hexahydrate ($Ce(NO_3)_3 \cdot 6H_2O$) and nickel nitrate hexahydrate ($Ni(NO_3)_2 \cdot 6H_2O$) (Ni-0.90, CeO_2-0.10) in a deionized water. Glycine (NH_2CH_2COOH) is added into the precursor and stirrer to produce a glycine-nitrate solution. The glycine nitrate solution was then heated using a hot plate at 90°C and stirred for overnight until a of viscous gel of glycine-nitrate solution was formed. The gel was then transferred into a ceramic container and further heated at higher temperature (180°C) until the gel solution self-ignited. The combustion of the gel resulted in catalyst powder and large amount of released of gases. The catalysts powders were then further characterized in a thermo-gravimetric analysis (TGA).

2.2. Characterization process

The catalysts prepared were characterized in a thermal-gravimetric analysis to analyze the thermal stability of catalysts prepared. It is a technique where the substance is heated or cooled to record the mass loss during heating or cooling process. TGA analysis is commonly described by the percentage of weight (%) and temperature difference curves. Weight loss (%) curve is presented in a graph of mass versus temperature while temperature difference curve is plotted based on temperature difference versus temperature. The condition of TGA analysis used in this work is according to Patil et al. (2014) and shown in Table 1 below.

Table 2: Parameters for TGA analysis (Patil et al., 2014)

Parameter	
Initial temperature	20°C
Final temperature	800°C
Heating rate	10°C/min
Gases used	N_2, Air

3. Result and discussion

3.1. Effect of different glycine-nitrate (G/N) ratios

Figure 1 shows the results from TGA analysis for Ni modified with CeO_2 catalysts prepared at different G/N ratios. All graphs for different G/N ratios studied showed a same trend in which the percentage of weight is increased with the increased of temperature in air environment. Patil et al. (2014) has suggested that some of the unreacted glycine and nitrate in catalyst powder left after the combustion might have reacted each other in air environment producing additional amount catalyst powder. It also suggested that the catalyst achieved their complete formation and perfectly crystallized at the highest endothermic peak (Patil et al., 2014). Thus, Ni catalyst modified with CeO_2 at G/N= 0.5 has achieved its complete formation and perfectly crystallized at T≈ 800°C (Figure 1a). At higher G/N ratios (G/N= 1.0 and G/N= 1.5), the catalysts managed to reach their complete and crystallization at a lower temperature which is at T≈ 500°C (Figures 1b and 1c). Thus, it is suggested that the higher the G/N ratio, the lower the crystallization temperature. This clearly showed that the glycine-nitrate ratio has a significant effect on the crystallization temperature of the catalyst produced using GNP. Additionally, Wattanasiriwech et al. (2012) stated that the increase of G/N ratio

resulted in a combustion with a greater amount of residue ash content. In this work, it is also evidence that high G/N ratio has led to a higher increment of catalyst weight (up to 112%) compared to low G/N ratio (up to 103%) when the catalyst formation went to a completion.

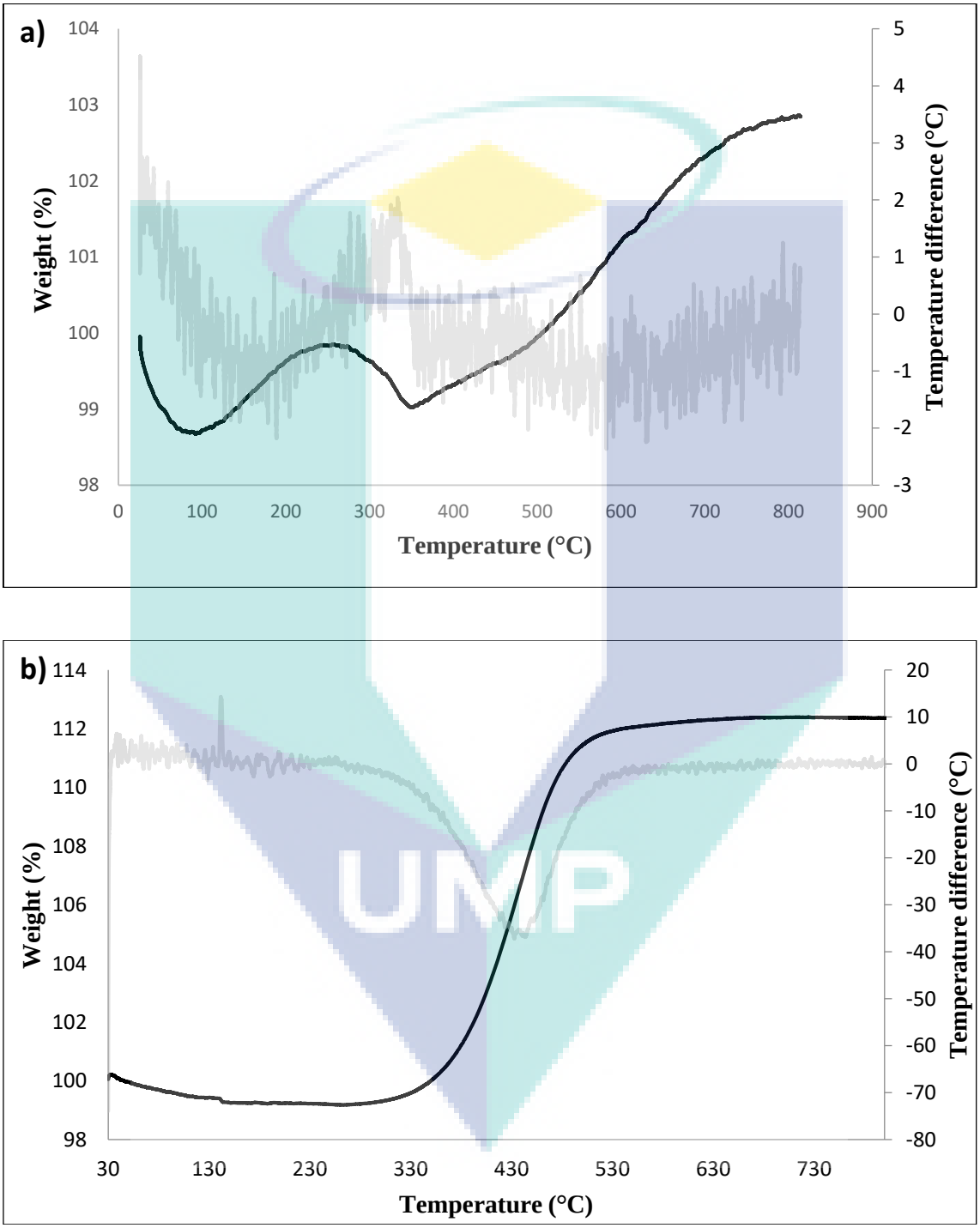

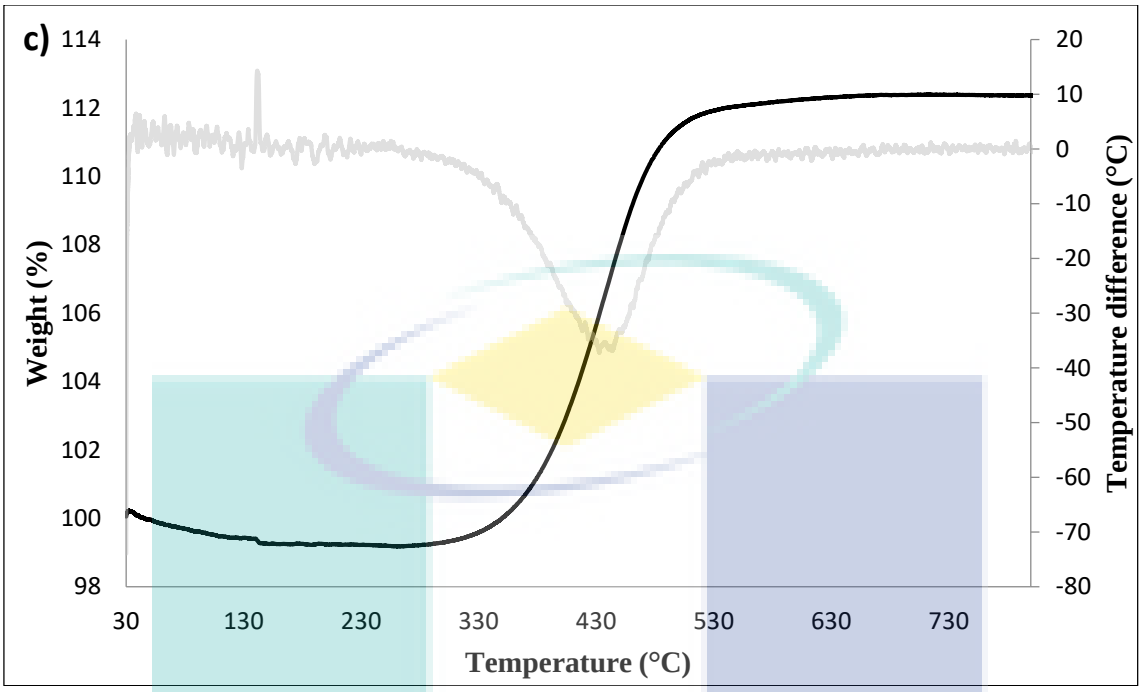

Figure 1: TGA results for Ni catalysts modified with ceria at a) G/N= 0.5; b) G/N= 1.0; and c) G/N=1.5

4.0 Conclusion

Nickel catalyst-modified with ceria has been successfully synthesized using glycine nitrate process (GNP). The effect of three different glycine-nitrate (G/N) ratios which are G/N=0.5, G/N=1.0 and G/N=1.5 has been investigated and the prepared catalysts were characterized using thermal-gravimetric analysis (TGA). Based on TGA results, Ni catalyst modified with CeO_2 at G/N= 0.5 has achieved its complete formation and perfectly crystallized at T≈ 800°C. At G/N= 1.0 and G/N= 1.5, the catalysts have reach their complete and crystallization at T≈ 500°C. Thus, the glycine-nitrate ratio has a significant effect on the crystallization temperature of the catalyst produced, where the higher the G/N ratio used, the lower the crystallization temperature of the catalyst. This work also shows that high G/N ratio has led to a higher increment of catalyst weight (up to 112%) compared to low G/N ratio (up to 103%) when the catalyst formation went to a completion.

References

1. Belhadi A., Trari M., Rabia C., and Cherifi O., Methane steam refroming on supported nickel based catalyst: effect of oxide ZrO_2, La_2O_3 and nickel composition. *Open Journal of Physical Chemistry. 2013; 3:89-96. http://dx.doi.org/10.4236/ojpc.2013.32011*.
2. Centeno M.A., Paulis M., Montes M., Odriozola J. A., Apply. Catal. A 234, 65 – 78, 2002.
3. Ferreira, VM, Azough F, Baptista, JL, Freer R. DiC12: Magnesium titanate microwave dielectric ceramics. Ferrolectrics, 133:127-132 1992.
4. Hongjing W., Valeria L. P., Giuseppe P., Fabrizio P., Anna M. V., and Leonarda F. L., Ni-Based Catalysts for Low Temperature Methane Steam Reforming: Recent Results on Ni-Au and Comparison with Other Bi-Metallic Systems, Catalysts, 2013.
5. Hongpeng H. and Josephine M. H., Carbon deposition on Ni/YSZ composites exposed to humidified methane, applied Catalysis, 284-292, 2007.
6. Istadi I., Anggoro D. D., Amin N. A. S., and Ling D. H. W., Catalyst Deactivation Simulation Through Carbon Deposition in Carbon Dioxide Reforming over $Ni/CaO-Al_2O_3$ Catalyst, Buletin of chemical reaction engineering & catalyst, 2011.
7. Jun K. W., Roh H. S., Chary K. V. R., Structure and Catalytic Properties of Ceria-based Nickel Catalysts for CO_2 Reforming of Methane, Catal Surv Asia, 97-113, 2007.

8. Kingsley JJ, Suresh K, Patil KC. Combustion synthesis of fine-particle metal aluminates. J Mater Sci, 25:1305-1312, 1990.
9. Patil B., Basu S., Synthesis and characterization of PdO-NiO-SDC nano-powder by glycine-nitrate combustion synthesis for anode of IT-SOFC, Energy Procedia 54, 669-679, 2014.
10. Tomishige, K. Oxidative steam reforming of methane over Ni catalysts modified with noble metals. J. Jpn. Pet. Inst. 50, 287–298, 2007.
11. Wattanasiriwech D., Wattanasiriwech S., Effects of fuel contents and surface modification on the sol-gel combustion $Ce_{0.9}Gd_{0.1}O_{1.95}$ nanopowder, Energy Procedia 34, 524-533, 2013.
12. Zhuang Q., Qin Y., and Chang L., Promoting effect of cerium oxide in supported nickel catalyst for hydrocarbon steam-reforming, applied catalysis, 1991.

APPENDIX

(URP TECHNICAL PAPER 3)

SELF-COMBUSTION SYNTHESIS OF BARIUM-MODIFIED NICKEL FOR HYDROGEN PRODUCTION

Mudakarran Murugaiah and Asmida Ideris
Faculty of Chemical & Natural Resources Engineering,
Universiti Malaysia Pahang, 26300 Gambang, Pahang, MALAYSIA

ABSTRACT
Nickel-based catalyst modified with barium (Ba) has been synthesized using a self-combustion technique, glycine-nitrate combustion process (GNP). GNP is selected in this study because the process is simple, less expensive and produces high purity catalyst. The addition of barium in Ni catalyst is expected to improve the tolerance of the catalyst towards carbon deposition. In this work, a solution mixture of nickel and barium nitrates was mixed with glycine and heated overnight to produce glycine-nitrate solution in gel form. The glycine-nitrate gel was further heated until the gel was combusted itself, producing a catalyst powder. In this work, factors such as glycine-nitrate (G/N) ratio and calcination temperature have been investigated. SEM micrographs show that glycine-to-nitrate (G/N) ratio has a significant effect on the morphology of Ni catalyst modified with barium. The catalyst synthesized with G/N= 0.5 ratio has a foamy structure and spongy in nature with micropores. The morphologies for the catalysts produced with G/N= 1.0 and G/N= 1.5 on the other hand were similar with dense surfaces and larger pores on the surface. The catalysts exhibit more pores as the G/N decreases and become denser as the G/N is increased higher than G/N= 1.0. From XRD analysis, peaks belongs to $BaCO_3$ phase were detected in Ni catalysts modified with barium calcined at 600 and 700°C. The $BaCO_3$ peaks however disappeared and new peaks belongs to BaN_2O_6 phase were appeared as the calcination temperature increased to 800°C. Thus, barium-containing compound in Ni catalyst modified with barium calcined at 800°C existed as BaN_2O_6 phase.

Key-words: Glycine-nitrate combustion process (GNP); nickel catalyst modified with barium; glycine-nitrate (G/N) ratio; calcination temperature.

INTRODUCTION
Catalyst is a substance that starts or speeds up a chemical reaction while undergoing no permanent change itself. Catalyst stability is one of the most important challenges in the development of new catalyst. Catalyst modification is one of the method used to reduce carbon deposition in the catalyst. Ni, the main catalyst for hydrogen production can be modified with carbon inhibitor (V.R. Choudhary et al., 1997).
Kobayashi et al. observed that the presence of Ba species in catalysts has increased the conversion of CO, NOx and hydrocarbons. Moreover, they suggested that the addition of barium has enhanced the basicity of catalysts. In addition, that barium can help to suppress the sintering of the catalysts (L. Liotta et al., 2003). The mobility of atoms could be reduced by barium, which suppresses the formation of larger particles at high-temperatures (Yidan Cao et al., 2015).
Self-combustion synthesis method has gained a lot of attentions for catalyst preparation due to its rapid process and economical. Self-combustion synthesis method comprised of oxidizer-fuel solution which will be self-ignited, converting the solution into a solid product. Self-combustion method is an energy efficient process that has been used for synthesis of powder (Xu, Nanping et al., 2008). Glycine nitrate process (GNP) is one of the most popular self-combustion method used for preparation of catalyst powders (Kumar, A et al., 2015). GNP is simple, rapid, inexpensive and a self-sustaining combustion synthesis technique. The process allows for preparation of compositionally homogeneous powders with high purity and high surface area.
The combustion process and physico-chemical properties of catalysts produced are greatly influenced by glycine amount. The glycine-to-nitrate (G/N) ratio is known to have effect on catalyst surface area and combustion duration. An increase in the glycine amount may lead to a marked decrease in the surface area and the amount of glycine changes the duration of combustion. In addition, the intensity of combustion and particle size of catalysts are highly affected by the amount of glycine used in the combustion (Guo et al., 2010). Calcination temperature also greatly determines the properties and catalytic performance of the catalyst. Calcination temperature has a significant effect on the catalyst

physico-chemical properties, such as crystallite size, surface area, catalyst reducibility, metal-support complex and acidity-basicity of the catalyst surface (Sanjay Katheria et al., 2016).

In this work, Ni catalyst modified with Ba is synthesized using GNP. The effects of glycine-to-nitrate (G/N) ratio and calcination temperature on the crystalline structure and morphology on Ni catalyst modified with barium were examined. The modified catalysts were characterized using x-ray diffraction (XRD) and scanning electronic microscopy (SEM) coupled with energy-dispersive x-ray spectroscopy (EDX).

MATERIALS AND METHODS

Catalyst preparation

Glycine-nitrate process (GNP) consists of two main steps. The first part is the preparation of precursor solution where an aqueous solution of nickel and barium nitrates was produced as a catalyst precursor. The precursor of nitrates solution contains Ni^{2+} and Ba^{2+} concentrations in a ratio of Ba:Ni = 0.05:0.95. Glycine was then added into the homogeneous solution of nickel nitrates at various glycine-to-nitrate (G/N) ratios (G/N=0.5, G/N=1.0, G/N=1.5). The glycine-nitrate solution was heated at 90°C under a constant stirring using a hot plate until the water evaporates and the glycine-nitrate solution converted to a gel form. The second part is the self-combustion of the precursor solution. The gel was heated at 180°C until it self-ignited and produced catalyst powder. Catalyst powders were further calcined for 2 hrs at various calcination temperatures (600, 700, 800°C).

Catalyst Characterization

X-ray diffraction analysis was performed using D8 Advance, Bruker-AXS, with Cu-Kα (0.15406 nm) radiation (30 kV, 15 mA) to determine the crystalline structure of the catalyst prepared. Data sets were recorded in a step-scan mode in the 2θ ranged from 10° to 80° with intervals of 0.02 a counting time of 1 second per point. The morphology of the catalyst powder and the elemental distribution of the catalysts were characterized using a desktop scanning electron microscopy (SEM) coupled by energy dispersive X-ray spectroscopy (EDXS) at 15 keV.

RESULTS AND DISCUSSION

Figure 1 shows the SEM image and EDX spectrum of the Ni catalyst modified with barium at (G/N)= 1.5 and calcined at 600°C. The catalysts were characterized using EDX to confirm the existence of barium in the catalyst. EDX detects the characteristic X-rays that are emitted from the first few micrometers beneath the specimen's surface after inner shell ionization by the primary electrons. The analysis was performed on the mapped area of the catalyst surface shown in Figure 1a. The EDX spectrum shows the presence of carbon (C), oxygen (O), nickel (Ni), aluminium (Al) and barium (Ba) elements in the catalyst prepared (Figure 1b).

a)

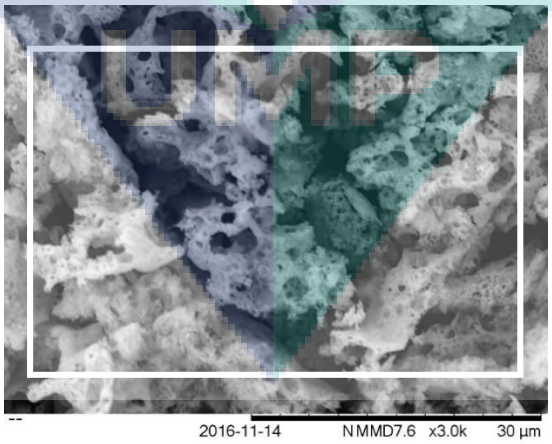

b)

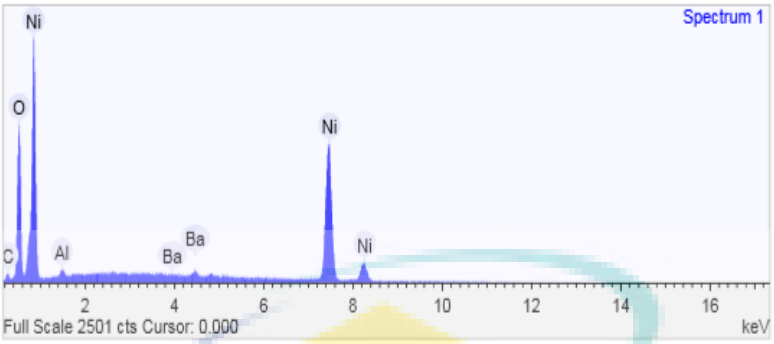

Figure 1: a) SEM image and b) EDX spectrum of the Ni catalyst modified with barium at (G/N)= 1.5 and calcined at 600°C.

Effect of Glycine-to-Nitrate (G/N) Ratio

The morphological characteristics of the produced powders were inspected by SEM analysis in Figure 2. The morphology of Ni catalyst modified with barium produced were inspected using SEM and the micrographs are shown in Figure 2. It is proven that glycine-to-nitrate (G/N) ratio has a pronounce effect on the morphology of the catalyst. Due to the vigorous nature of the combustion synthesis reaction and the evolution of large amount of gas phase products, this method produces a unique surface morphology on all catalysts. The gas evolved during the combustion synthesis reaction, form channels in the resulting solid product and hence the product is porous in nature (Kumar et al., 2015). All the catalysts exhibited highly porous microstructure, but with different morphology. Catalyst with G/N= 0.5 ratio has a foamy structure and spongy in nature with micropores (Figure 2(a)). The G/N= 1.0 on the other hence produces catalyst with dense surfaces and larger pores on the surface (Figure 2(a)). The morphology for the catalyst with G/N= 1.5 was also similar with one produced using G/N= 1.0 (Figure 2(ac)). SEM images show that the catalysts exhibit more pores as the G/N decreases. The morphology of Ni catalyst modified with barium become denser as the G/N employed is higher than G/N= 1.0.

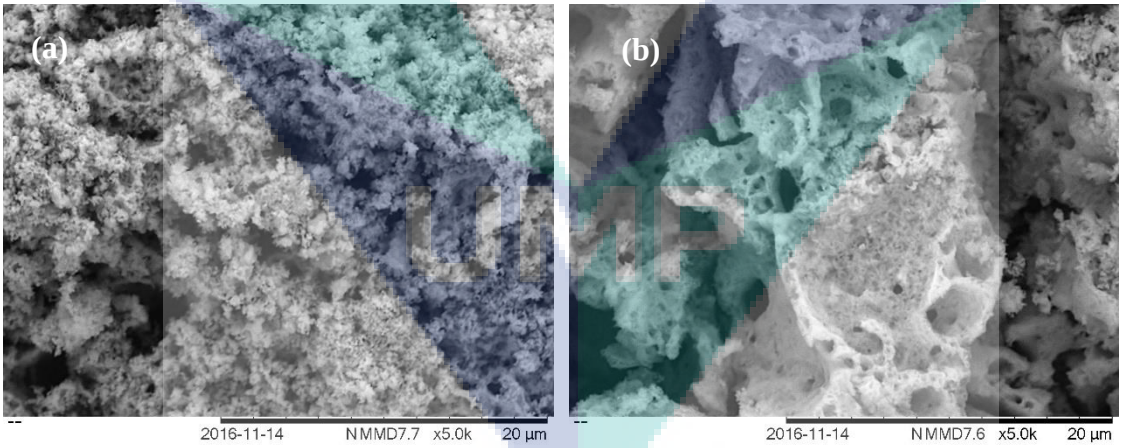

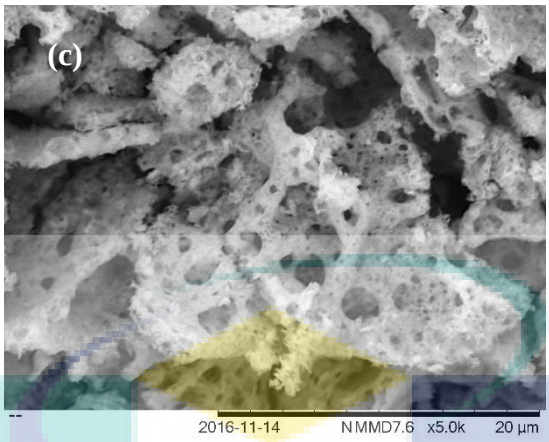

Figure 2: SEM micrographs of Ni catalysts modified with barium prepared with a) G/N ratio =0.5, b) G/N ratio =1.0, c) G/N ratio =1.5 at 5000x magnification.

Effect of Calcination Temperature

Figure 3 shows the XRD patterns of Ni catalysts modified with barium calcined at different temperatures (600°C, 700°C and 800°C) for 2 hours. The diffractions for NiO phase at 37.2°, 43.2°, 62.6°, 75.3° and 79.2° were observed in all catalysts including one for an uncalcined sample (Yan et al., 2014). The peaks belongs to $BaCO_3$ phase were detected at 24.2°, 34.2°and 46.8° in Ni catalysts modified with barium calcined at 600 and 700°C (Figures 3a and 3b) (Jin-Shu et al., 2013). The peaks however were diminished when the calcination temperature was increased to 800°C (Figure 3c). At the same time, new peaks belongs to BaN_2O_6 phase were appeared in the catalyst calcined at 800°C (Figure 3c) (Abdul Qadeer Malik et al., 2014). Therefore, barium-containing compound in Ni catalysts modified with barium calcined at 800°C existed as BaN_2O_6 phase. The BaN_2O_6 peaks detected at 21.93°, 38.5° and 59.15° were observed in catalysts calcined at 800°C as well as uncalcined catalyst (Figures 3c and 3d). The XRD patterns show that the peaks become higher and sharper as the calcinations temperature increases. This suggested that the crystallinity of the catalyst has increased with the increased of calcination temperature.

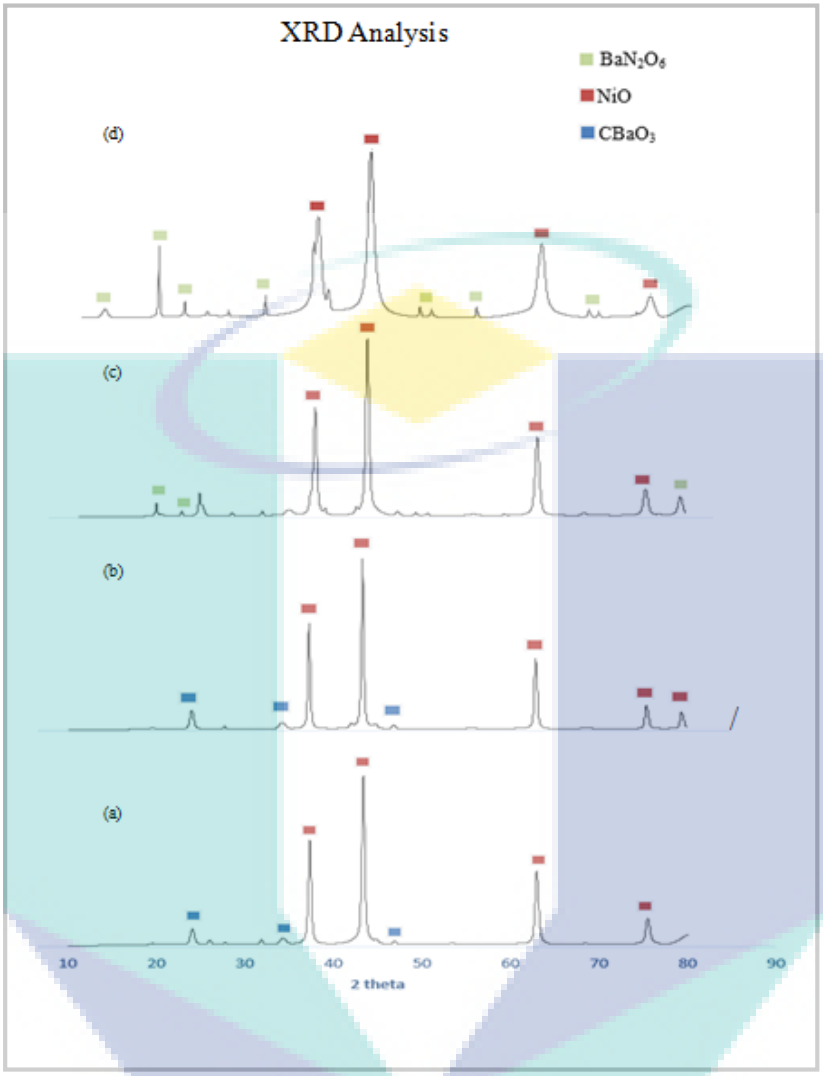

Figure 3: XRD patterns of barium-modified Ni catalyst (a) calcined at 600°C; (b) calcined at 700°C; (c) calcined at 800°C and (d) uncalcined

CONCLUSION

Ni catalysts modified with barium have been successfully synthesized using the glycine nitrate process (GNP). Three different glycine-nitrate (G/N) ratios (G/N=0.5, G/N=1.0, G/N=1.5) were employed and the catalysts produced were calcined at 600, 700 and 800°C for 2 hours. Glycine-to-nitrate (G/N) ratio has an important effect on the morphology of the catalyst produced. SEM images show that the catalysts exhibit more pores as the G/N decreases. The morphology of Ni catalyst modified with barium become denser as the G/N employed is higher than G/N= 1.0. From XRD analysis, peaks belongs to $BaCO_3$ phase were detected in Ni catalysts modified with barium calcined at 600 and 700°C. As the catalyst was calcined at a higher temperature (800°C), barium-containing compound in the Ni catalyst modified with barium existed as BaN_2O_6 phase.

REFERENCES

1. Yidan Caoa, Rui Rana, Xiaodong Wua, Duan Weng , 2015. A new insight into the effects of barium addition on Pd-only catalysts: Pd-support interface and CO + NO reaction pathway. Applied Catalysis A: General 501 (2015) 17–26

2. WANG Kai-Feng, LIU Wei, WANG Jin-Shu , 2013. Influence of Aluminates Composition on Ba-W Cathode Characteristics. Journal of Inorganic Materials » Vol. 28 » Issue (12): 1354-1358
3. Ryu Soo-Sung , 2012. Synthesis of Nanocrystalline BaTiO3 Powder by the Combination of High Energy Ball Milling of BaCO3-TiO2 Mixture and Solid-State Reaction. Vol.19 No.4 of Korean Powder Metallurgy Institute in Journal pp.310-316
4. Zaheer-ud-din Babar , Abdul Qadeer Malik , 2014. Synthesis of micro porous barium nitrate with improved ignition reliability as a reliable pyrotechnic oxidant. Journal of Saudi Chemical Society (2014) 18, 707–711
5. V.R. Choudhary, V.H. Rane, A.M. Rajput , 1997. Beneficial effects of cobalt addition to Ni-catalysts for oxidative conversion of methane to syngas. Applied Catalysis A: General 162. 235-238
6. Kumar, A. , Cross, A. , Manukyan, K. , Bhosale, R. R. , Van Den Broeke, L. J P , Miller, J. T. , Mukasyan, A. S. , Wolf, E. E. , 2015. Combustion synthesis of copper-nickel catalysts for hydrogen production from ethanol. Elsevier B.V. 46-54
7. S. Hajarpour , A. Honarbakhsh Raouf , Kh. Gheisari , 2014. Structural evolution and magnetic properties of nanocrystalline magnesium–zinc soft ferrites synthesized by glycine–nitrate combustion process. Journal of Magnetism and Magnetic Materials 363. 21–25
8. Wenling Chu , Weishen Yang and Liwu Lin , 2001.Selective oxidation of methane to syngas over NiO/barium hexaaluminate. Catalysis Letters Vol. 74. No. 3–4

APPENDIX

(URP TECHNICAL PAPER 4)

PREPARATION OF NI CATALYST SUPPORTED ON LANTHANA USING IN-SITU SELF-COMBUSTION PROCESS

Rais Fakhruddin Roslan and Asmida Ideris
Faculty of Chemical & Natural Resources Engineering,
Universiti Malaysia Pahang, 26300 Gambang, Pahang, MALAYSIA.
Tel: +60139427709

ABSTRACT

The production of hydrogen by methane cracking becomes a popular route due to its low cost and clean fuel production. However, carbon deposition formed from the process deactivates the catalyst used in methane cracking because of the low dispersion catalyst morphology. Hence, the objectives of this research are to synthesis Ni-supported La_2O_3 catalyst using in-situ self-combustion process and to study the effects of synthesis parameters on its morphology and properties. The parameters involved in in-situ self-combustion have been varied to obtain morphology of the metal-supported catalyst with high Ni dispersion. The parameters involved are glycine-nitrate (G/N) ratio of 0.5 to 1.5, Ni to support ratio of 1:3 to 1:8, and calcination temperature of 600 to 800°C. The morphology and microstructure of the catalyst produced have been analyzed using scanning electron microscopy (SEM) and X-ray diffraction (XRD). From XRD analysis, the NiO/La_2O_3 catalyst produced from in-situ self-combustion is associated to the crystalline phases of NiO, La_2O_3, $LaNiO_3$ and La_2NiO_4. Ni to support ratio employed during the catalyst preparation strongly influenced the formation of La-containing phases in the NiO/La_2O_3 catalyst. SEM micrographs show that NiO catalyst is found to be porous in structure and distributed evenly on the surface of La_2O_3 support. There is no significant different of the morphology of the catalyst at the variation of glycine-nitrate ratio. Nevertheless, NiO/La_2O_3 catalyst prepared using glycine-nitrate (G/N) ratio of 1.5:1 have large pore size on its surface, which is may attributed to large volume of gas releases at high glycine-nitrate (G/N) ratio. Finally, the crystalline structure of NiO/La_2O_3 catalyst produced from in-situ self-combustion is highly dependent on the calcination temperature of the catalyst.

Keywords: Ni-supported La_2O_3 catalyst, In-situ self-combustion process, Glycine-nitrate ratio, Ni to support ratio, Calcination temperature

INTRODUCTION

Hydrogen (H_2) productions have become a well-known source of renewable clean energy and one of the common process routes for H_2 production is methane cracking. Metallic catalyst is commonly employed for the decomposition of adsorbed methane into H_2. Nickel (Ni) is the main catalyst for methane cracking due to its low cost and has higher catalytic activity (Gong, et al., 2014). Nevertheless, Ni catalyst during methane cracking suffers from rapid catalyst deactivation due to carbon deposition (Guizani, et al., 2016). Catalyst improvement is essential to minimize carbon deposition and this can be done through catalyst preparation.

One of preferable method in catalyst preparation is in-situ self-combustion method. Self-combustion method involves the reaction between oxidizing solution containing the desired metal salts (nitrates are generally preferred because of their oxidizing property and high solubility in water) and an organic fuel which acts as a reducing agent (Lucilha et al., 2014). In-situ self-combustion involves incorporating inert support in the reaction media for preparation of metal-supported catalyst and it is expected to produce catalyst with high surface area and improved active phase dispersion (Cross et al., 2014). Metal supported catalyst with high Ni dispersion is essential as it can reduce carbon deposition and increase Ni catalytic activity (Zhao et al., 2016).

In this study, lanthanum oxide, La_2O_3 will be used as a catalyst support for the in-situ self-combustion technique of Ni catalyst. Some researchers claim that La_2O_3 can help reducing the deactivation of the catalyst by preventing the sintering of the Ni metallic phase and the deposition of carbon on its surface (Thyssen & Assaf, 2014). Glycine will be used as a medium in the catalyst preparation as it can be serve as a suitable fuel for the synthesis of nanocrystalline metal oxides (Miranda et al., 2015)

The purpose of this research is to synthesis Ni-supported La_2O_3 catalyst using in-situ self-combustion process. Several parameters have been varied to observe their effects on catalyst properties and morphology. The parameters varied during the catalyst preparation using in-situ self-combustion are glycine-nitrate (G/N) ratio (G/N= 0.5, 1.0 and 1.5), Ni to support ratio (1:3, 1:5 and 1:8) and calcination temperature (600°C, 700°C and 800°C). The effects of the parameters on the catalyst morphology and properties have been characterized using scanning electron microscopy (SEM), and X-ray diffraction (XRD).

EXPERIMENTAL

Materials

Nickel (II) nitrate hexahydrate, ($Ni(NO_3)_2{\cdot}6H_2O$), glycine ($C_2H_5NO_2$), and lanthanum oxide (La_2O_3) were all the chemicals used in catalyst preparation and be purchased from Sigma-Aldrich Co (Malaysia).

Catalyst preparation

Nickel (II) nitrate hexahydrate, ($Ni(NO_3)_2{\cdot}6H_2O$), and glycine ($C_2H_5NO_2$) have been dissolved in 250 mL deionized water to form a reaction media. Support material (lanthanum oxide, La_2O_3) has been added into the reaction media and stirred overnight at 90°C to form a viscous gel-like support-reaction media. The gel then was placed in a ceramic dish and further heated to the temperatures of 180 °C until the gel is self-ignited, producing a metal-supported catalyst ash. In order to remove residual carbon and improve catalyst crystallinity, the catalyst ash has been calcined at various calcination temperatures (600°C, 700°C and 800°C). Glycine-nitrate (G/N) ratio will be varied at G/N= 0.5, 1.0 and 1.5 while Ni to support ratio of 1:3, 1:5 and 1:8 have been varied. The Ni-supported La_2O_3 produced from in-situ self-combustion was further characterized using scanning electron microscopy (SEM) and X-ray diffraction (XRD) analysis.

Catalyst characterisation

X-ray diffraction (XRD) has been employed to study the crystalline phase of the catalyst. XRD analysis of catalyst has been carried out using a diffractometer with the scanning step and range of 2θ from 0° and 80° with interval of 0.02° a counting time of 1 second per point. Scanning electron microscopy equipped with energy dispersive X-Ray (SEM-EDX) has been used to study the surface morphology of the synthesized catalyst. SEM analysis allows for images of the sample surface to be taken with high resolution while elemental component the catalysts surfaces was analysed using EDX.

RESULT AND DISCUSSION

Effect of Ni to Support Ratio

Figure 1 presents the XRD patterns of NiO catalyst supported on lanthana (NiO/La_2O_3) after calcination process at 800°C. The Ni to support ratio during the in-situ self-combustion process was varied at three different ratios; 1:3, 1:5 and 1:8. The XRD analysis for Ni supported catalysts is compared with the XRD patterns for NiO catalyst and La_2O_3 support alone. Referring to the patterns for NiO and La_2O_3, the NiO/La_2O_3 catalyst can be associated to the crystalline phases of NiO, La_2O_3, $LaNiO_3$ and $LaNiO_3$. This reveals that the NiO/La_2O_3 catalyst produced from in-situ self-combustion is crystalline.

The presence of diffraction peaks at 15.7°, 28°, 39.5° and 48.8° in the XRD patterns for all NiO/La_2O_3 catalysts suggests that the catalysts with Ni to support ratio of 1:3, 1:5 and 1:8 contain the crystallites of La_2O_3 (Figures 1a-c). However, the peaks for La_2O_3 for NiO/La_2O_3 catalyst at Ni to support ratio of 1:3 is not too obvious, suggesting that the amount of La_2O_3 phase at this Ni to support ratio is small and below the XRD detection limit (Figure 1a) (Fayaz, et al., 2017). Meanwhile, the presence of NiO phase given by the phase angle of 43.5° is found in the catalyst with both Ni to support ratios of 1:3 and 1:5 (Figures 1a and 1b). No obvious peak of NiO is observed at Ni to support ratios of 1:8 (Figure 1c). This suggests that the presence of both NiO and La_2O_3 in the NiO/La_2O_3 catalyst can only available at Ni to support ratios of 1:3 and 1:5. Therefore, it is concluded that the crystal structure of NiO/La_2O_3 catalysts is closely related to their Ni to support ratios used during the catalyst preparation.

$LaNiO_3$ can be seen developed at peak 31° in with both Ni to support ratios of 1:3 and 1:5 (Figures 1a and 1b). The formation of this LaNiO3 phase in can be related due the self-combustion reaction. It is reported that the existence of $LaNiO_3$ in catalyst may help solving the carbon deposition problem (Silva, et al., 2013; Nie, et al., 2017). The other peaks shown in the Figures 1a and 1b for catalysts prepared using Ni to support ratios of 1:3 and 1:5 are belongs to La_2NiO_4 phase, which the crystalline peaks appeared at 25.9° and 34.3° (Lee & Kim, 2015). The formation of this LaNiO3 is due to the same reason, a reaction during self-combustion reaction. Barros et al (2015) suggests that the formation of La_2NiO_4 and $LaNiO_3$ during self-combustion reaction is due to the limited availability of oxygen from the reactants. However, at Ni to support ratios of 1:8, neither clear peak of La_2NiO_4 nor $LaNiO_3$ are observed (Figure 1c). Hence, the formation of La-containing phases in NiO/La_2O_3 catalyst produced from in-situ self-combustion is strongly dependent on the Ni to support ratios employed during the catalyst preparation

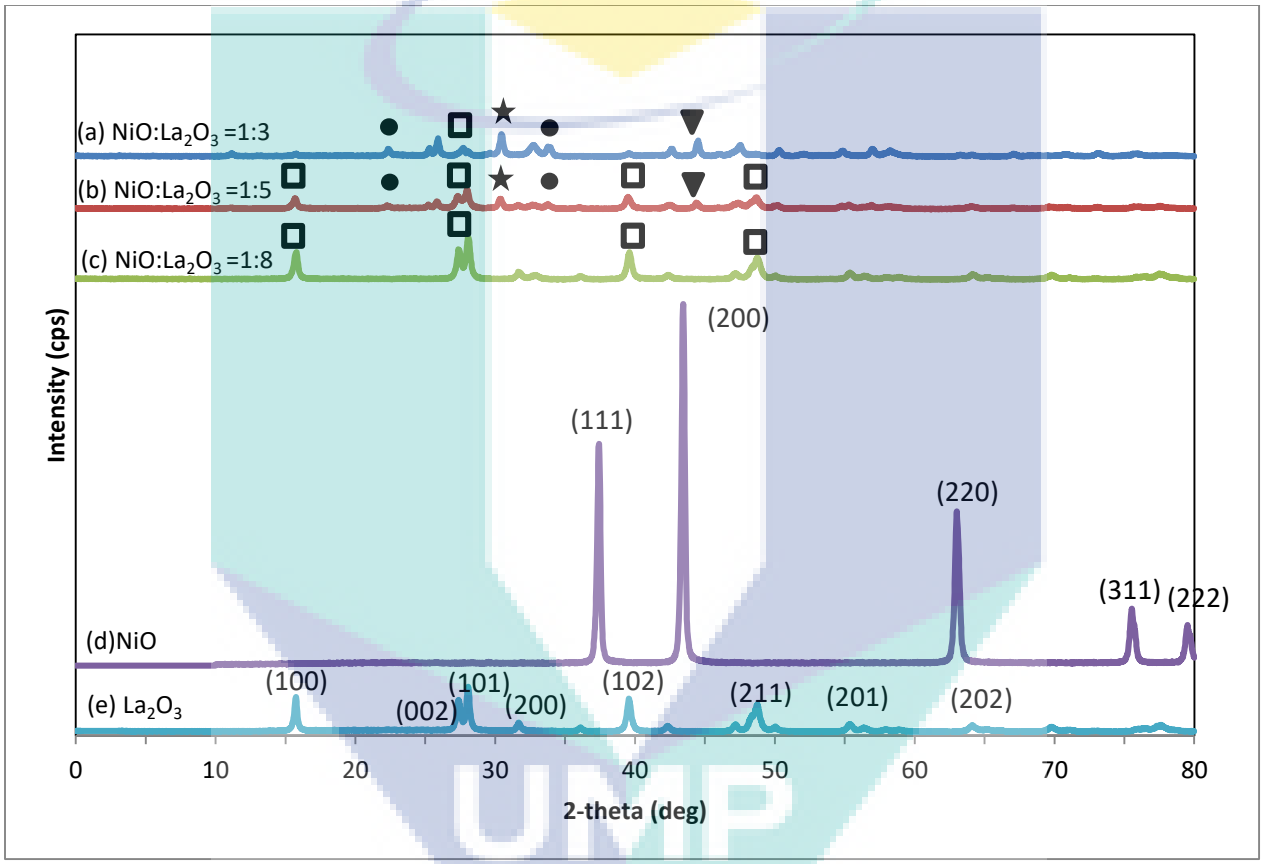

Figure 1: XRD patterns of NiO supported La_2O_3 (NiO/ La_2O_3) catalyst at Ni to support ratio of a) 1:3 b) 1:5 c) 1:8. The patterns are compared with the XRD patterns for d) NiO catalyst and e) La_2O_3 support. Symbols: La_2O_3 (□); NiO (▼); La_2NiO_4 (●); LaNiO3 (★)

Effect of Glycine-Nitrate (G/N) Ratio

The SEM-EDX micrographs of NiO supported La_2O_3 (NiO/La_2O_3) catalysts with glycine-nitrate (G/N) ratio of 0.5:1, 1:1 and 1.5:1 is given in Figure 2. NiO/La_2O_3 catalyst in Figures 2a-c displays the surface of La_2O_3 support and it is composed of agglomerated NiO catalyst grains with random shapes. NiO catalyst is found to porous in structure and distributed evenly on the surface of La_2O_3 support. Except for NiO/La_2O_3 catalyst prepared with glycine-nitrate (G/N) ratio of 1.5:1 (Figure 2c), there is no significant different of the morphology of the catalyst at the variation of glycine-nitrate ratio between 0.5:1 and 1:1 (Figures 2a-b). Catalyst prepared using glycine-nitrate (G/N) ratio of 1.5:1 seems to have larger pore size compared to the other two. This shows points that high glycine to nitrate ratio will contribute to large pore size in the catalyst structure, which is also found by Goula, et al. (2016) and Hadke, et al., (2015) in previous work. This could be due to the fact that at high glycine to nitrate ratio large volume of gas is released and thus creates larger pore size on the catalyst surface (Liu, et al,. 2017; Wei, et al., 2012).

EDX analysis has been conducted on the NiO supported La_2O_3 catalyst synthesized at different glycine-nitrate (G/N) ratio and the compositions are tabulated in Table 1. There is a slight increase of Ni elements on the catalyst surface at high glycine-nitrate (G/N) ratio. This is different from the finding by Ishizaki et al. (2016), Singh et al. (2017), and Torrente-Murciano (2016) where the Ni atoms should have been decreased with G/N ratio increases.

Table 1: EDX analysis of elemental components of NiO supported La_2O_3 prepared at G/N ratio = 0.5:1, 1:1, and 1.5:1

Elements	Atomic percent, %		
	G/N ratio = 0.5:1	G/N ratio = 1:1	G/N ratio = 1.5:1
Ni	1.4	1.3	3.7
La	20.3	19.9	17.4

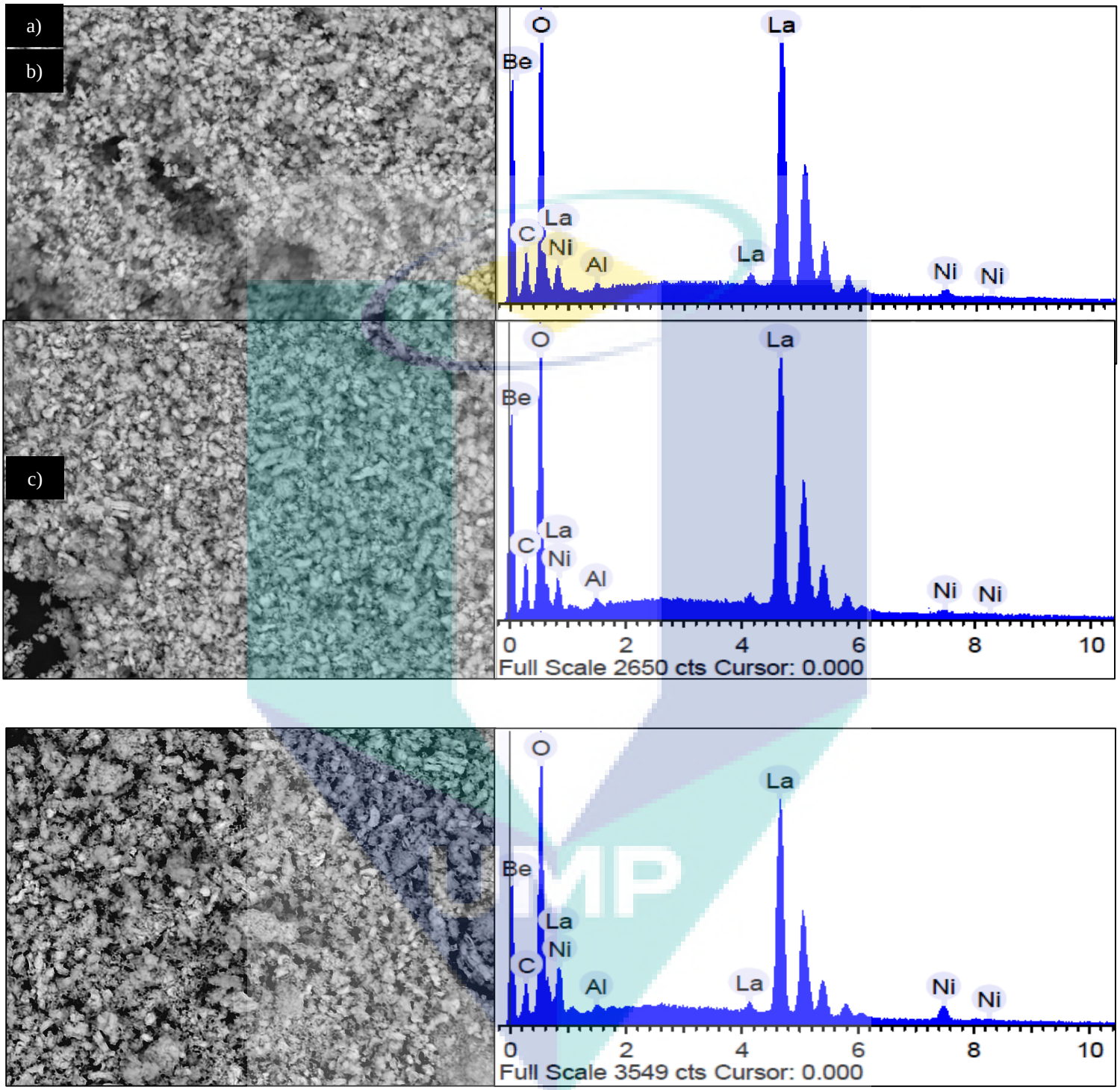

Figure 2: SEM-EDX micrographs of NiO-supported La_2O_3 (NiO/La_2O_3) catalysts with glycine- nitrate (G/N) ratio of a) 0.5:1, b) 1:1 and c) 1.5:1

Effect of Calcination Temperature

The effect of calcination temperature on the NiO and La_2O_3 phases of is observed and Figure 3 presents the XRD patterns of NiO/La_2O_3 catalyst at different calcination temperatures (600, 700 and 800°C). Both Ni to support ratio and glycine-nitrate (G/N) ratio are maintained at $NiO:La_2O_3$=1:5 and G/N ratio=1:1, respectively.

The diffraction peaks at 15.7°, 28°, 39.5° and 48.8° belongs to the crystallites of La_2O_3. NiO/La_2O_3 catalyst with the calcination temperature of 800°C shows the occurrence of all La_2O_3 peaks (Figure 3a). Meanwhile NiO/La_2O_3 catalyst calcined at 600°C and 700°C only contains small peak of 28° for the La_2O_3 phase (Figures 3b and c). This suggest that the calcination temperature of below 800°C in insufficient for formation of La_2O_3 crystalline phase as calcination temperature had a direct influence on their properties (Karthikeyan, et al., 2015). The presence of NiO crystalline phase ($2\theta = 43.5°$) is observed in all NiO/La_2O_3 catalysts calcined at 600°C, 700°C and 800°C. This suggests that the formation of NiO crystalline phase is possible at calcination temperature below 800°C.

NiO/La_2O_3 catalyst calcined at 700°C (Figure 3b) tend to have sharper peak for $LaNiO_3$ (peak=32°) and La_2NiO_4 (peak =25.9° and 34.3°). This result indicates that $LaNiO_3$ and La_2NiO_4 phases formed at 700°C are more crystalline, allowing the catalyst to form perovskite-type oxide precursor (Santos, et al., 2012). Therefore, it is concluded that the crystalline structure of NiO/La_2O_3 catalyst produced from in-situ self-combustion is highly dependent on the calcination temperature of the catalyst.

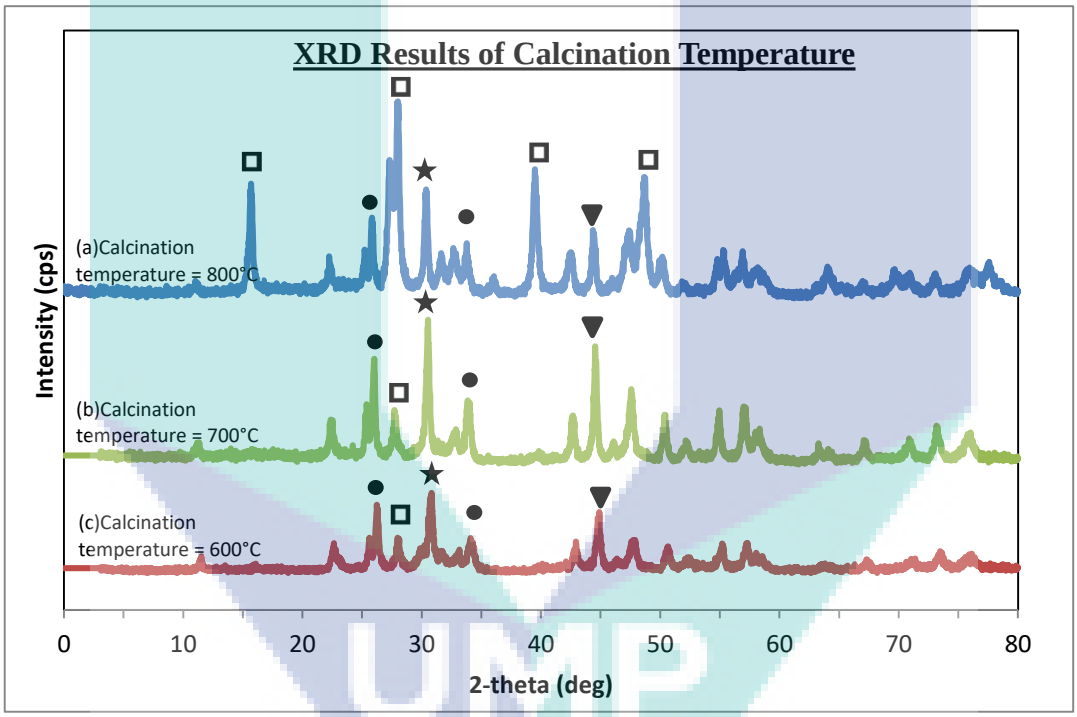

Figure 3: XRD patterns of NiO supported La_2O_3 (NiO/ La_2O_3) catalyst at calcination temperature of a) 800°C, b) 700°C and c) 600°C. Symbols: La_2O_3 (□); NiO (▼); La_2NiO_4 (●); LaNiO3 (★)

CONCLUSION

The synthesis and characterization of Ni/La_2O_3 catalyst using various variables for in-situ self-combustion are described in this work. Ni to support ratio, glycine-nitrate ratio, and calcination temperature have been investigated and the properties and morphology of Ni/La_2O_3 produced were evaluated using XRD and SEM-EDX. From XRD analysis, the NiO/La_2O_3 catalyst produced from in-situ self-combustion is associated to the crystalline phases of NiO, La_2O_3, $LaNiO_3$ and $LaNiO_3$. Ni to support ratio employed during the catalyst preparation strongly influenced the formation of La-containing phases in the NiO/La_2O_3 catalyst. SEM micrographs show that NiO catalyst is found to be porous in structure and distributed evenly on the surface of La_2O_3 support. There is no significant different of the morphology of the catalyst at the variation of glycine-nitrate ratios. NiO/La_2O_3 catalyst prepared using glycine-nitrate (G/N) ratio of 1.5:1 have large pore size on its surface, which is may attributed to large volume of gas releases at high glycine-nitrate (G/N) ratio. From XRD results, it is found that the crystalline structure of NiO/La_2O_3 catalyst produced from in-situ self-combustion is highly dependent on the calcination temperature of the catalyst.

REFERENCES

Barros, B., Kulesza, J., Melo, D., & Kienneman, A. (2015). Nickel-based Catalyst Precursor Prepared Via Microwave-induced Combustion Method: Thermodynamics of Synthesis and Performance in Dry Reforming of CH4. *Materials Research 18(4)*, 732-739.

Cross, A., Roslyakov, S., Manukyan, K., Rouvimov, S., Rogachev, A., Kovalev, D., . . . Mukasyan, A. (2014). In Situ Preparation of Highly Stable Ni-Based Supported Catalysts by Solution Combustion Synthesis. *J. Phys. Chem. C, 118 (45)*, 26191–26198.

Fayaz, F., Bahari, M., Nguyen-Phu, H., Nguyen-Huy, C., Abdullah, B., & Vo, D. (2017). Syngas Production via Ethanol Dry Reforming: Effect of Promoter Type on Al2O3-supported Co Catalysts. *CEST 2017*.

Gong, M., Zhou, W., Tsai, M., Zhou, J., Guan, M., Lin, M., . . . Dai, H. (2014). Nanoscale nickel oxide/nickel heterostructures for active hydrogen evolution electrocatalysis. *Nature Communication*.

Goula, M., Charisiou, N., Siakavelas, G., Tzounis, L., Tsiaoussis, I., Panagiotopoulou, P., . . . Yentekakis, I. (2016). Syngas production via the biogas dry reforming reaction over Ni supported on zirconia modified with CeO2 or La2O3 catalysts. *i n t e r n a t i o n a l journal of hydrogen energy xxx*, 1-17.

Guizani, C., Sanz, F., & Salvador, S. (2016). The nature of the deposited carbon at methane cracking over a nickel loaded wood-char. *C. R. Chimie 19*, 423-432.

Hadke, S., Kalimila, M., Rathkanthiwar, S., Gour, S., Sonkusare, R., & Ballal, A. (2015). Role of fuel and fuel-to-oxidizer ratio in combustion synthesis of nano-crystalline nickel oxide powders. *Ceramics International 41*, 14949–14957.

Ishizaki, T., Yatsugi, K., & Akedo, K. (2016). Effect of Particle Size on the Magnetic Properties of Ni Nanoparticles Synthesized with Trioctylphosphine as the Capping Agent. *Nanomaterials 6*, 172.

Karthikeyan, S., Dhayal Ra, A., Albert Irudayaraj, A., & Magimai Antoni Raj, D. (2015). Effect of temperature on the properties of La2O3 nanostructures. *Materials Today: Proceedings 2*, 1021 – 1025.

Lee, Y., & Kim, H. (2015). Electrochemical performance of La2NiO4+δ cathode for intermediate-temperature solid oxide fuel cells. *Ceramics International 41*, 5984-5991.

Liu, J., Wang, D., Dong, P., Zhao, J., Meng, Q., Zhang, Y., & Li, X. (2017). Effect of Glycine-to-nitrate Ratio on Solution Combustion Synthesis of ZnFe2O4 as Anode Materials for Lithium Ion Batteries. *Int. J. Electrochem. Sci., 12*, 3741 – 3755.

Lucilha, A., Afonso, R., Silva, P., Lepre, L., Ando, R., & Antonia, L. (2014). ZnO Prepared by Solution Combustion Synthesis: Characterization and Application as Photoanode. *J. Braz. Chem. Soc.Vol. 25, No. 6*, 1091-1100.

Miranda, E., Carvajal, J., & Baena, O. (2015). Effect of the Fuels Glycine, Urea and Citric Acid on Synthesis of the Ceramic Pigment ZnCr2O4 by Solution Combustion. *Materials Research*, 1038-1043.

Nie, L., Wang, J., & Tan, Q. (2017). In-situ preparation of macro/mesoporous NiO/LaNiO3 pervoskite composite with enhanced methane combustion performance. *Catalysis Communications 97*, 1-4.

Santos, J., Souza, M., Ruiz, J., Melo, D., Mesquita, M., & Pedrosa, A. (2012). Synthesis of LaNiO3 perovskite by the modified proteic gel method and study of catalytic properties in the syngas production. *J. Braz. Chem. Soc. 23*.

Silva, A., Costa, L., Mattos, L., & Noronha, F. (2013). The study of the performance of Ni-based catalysts obtained from LaNiO3 perovskite-type oxides synthesized by the combustion method for the production of hydrogen by reforming of ethanol. *Catalysis Today 213*, 25-32.

Singh, S., & Singh, D. (2017). Synthesis of LaFeO3 nanopowders by glycine–nitrate process without using any solvent: effect of temperature. *Monatsh Chem 148*, 879–886.

Thyssen, V., & Assaf, E. (2014). Ni/La2O3-SiO2 Catalysts Applied to Glycerol Steam Reforming Reaction: Effect of the Preparation Method and Reaction Temperature. *J. Braz. Chem. Soc.Vol. 25, No. 12*, 2455-2465.

Torrente-Murciano, L. (2016). The importance of particle-support interaction on particle size determination by gas chemisorption. *J Nanopart Res*, 18-87.

Wei, X., Hua, Z., Yong, L., & Lin, L. (2012). Effect of catalyst confinement and pore size on Fischer-Tropsch synthesis over cobalt supported on carbon nanotubes. *SCIENCE CHINA Chemistry 55*, 1811–1818.

Zhao, K., Wang, W., & Li, Z. (2016). Highly efficient Ni/ZrO2 catalysts prepared via combustion method for CO2 methanation. *Journal of CO2 Utilization 16*, 236–244.

APPENDIX

(URP TECHNICAL PAPER 5)

IN-SITU PREPARATION OF NI-BASED CATALYST SUPPORTED ON SILICA USING SELF-COMBUSTION PROCESS

Jane Tong Huixia and Asmida Ideris
Faculty of Chemical & Natural Resources Engineering,
Universiti Malaysia Pahang, 26300 Gambang, Pahang, MALAYSIA.
Tel: +60164558820

ABSTRACT

Ni-based catalyst is an active catalyst used for methane cracking reaction. However, Ni catalyst is affected by carbon deposition on Ni particles, resulting in poor stability and low catalytic activity during methane cracking. One strategy for catalyst stability through carbon minimization is by improving the morphology of the catalyst. In this study, in-situ self-combustion synthesis has been to produce Ni-supported silica catalyst with highly dispersed structure. This morphology is expected to have low carbon deposition and thus have a prolonged catalyst lifespan during methane cracking. The objectives of this research are to synthesis Ni-La/SiO_2 using in-situ self-combustion process and to investigate the effects of synthesis parameters towards the properties and the morphology of the catalyst produced. In-situ self-combustion was performed by incorporating inert silica support in the glycine-nitrate reaction media and heated until the solution is self-combusted to produce Ni-supported catalyst ash. The variation in glycine-to-nitrate (G/N) ratio (G/N= 0.5, 1, 1.5), Ni-La catalyst to support ratios (1:3, 1:5 and 1:8) and addition of lanthanum promoter (3%, 5% and 7) were investigated. The properties and morphology of the synthesized Ni-La/SiO_2 catalyst were characterized using XRD, SEM and TGA. The SEM results show that varying the glycine to nitrate (G/N) ratios do not show significant difference in the morphology of catalyst. However, TGA analysis show the catalyst weight loss decreases with high glycine-to-nitrate (G/N) ratio. From XRD analysis, the optimum conditions for the Ni-La/SiO_2 are glycine-to-nitrate (G/N) ratio of 1:1 and Ni-La catalyst to support ratio of 1:5. Besides, La loadings of 5 wt% was found to be the optimum promoter for Ni-La/SiO_2. On the other hand, the crystallite size of Ni-La/SiO_2 is decreased with the increase of Ni-La to support ratio, which is a desirable factor in order to reduce carbon formation. Therefore, glycine-to-nitrate (G/N) ratios, Ni-La to support ratio and lanthanum loading affect the crystallinity as well as the presence of NiO, SiO2 and lanthanum in Ni-La/SiO2 catalyst. Finally, it can be concluded that in-situ self-combustion method has a potential to produce a pure Ni-La/SiO_2 catalyst with porous structure and high crystallinity.

1. Introduction

Metallic catalysts have been reported to lower activation energy, thus reduce the reaction temperature required for H_2 production. Nickel (Ni) is an active catalyst for methane cracking. However, catalyst deactivation occurs during methane cracking due to deposition of carbonaceous species on Ni catalyst (Amin et al., 2011). To improve the efficiency of Ni catalyst, porous supports such as carbon, alumina or silica can be incorporated to the metal catalyst to improve the dispersion of catalyst active phase and strengthen the thermal stability of the catalyst (Cross et al., 2014).

Various approaches have been reported for synthesis of Ni-supported catalysts such as incipient wetness impregnation, co-precipitation and sol-gel methods (Cross et al., 2014). One concern associated with these techniques is the requirement of high temperature heat treatment for the catalyst to achieve the desired phase composition and crystalline structure required (Mukasyan & Dinka, 2006). Another issue is related to morphology of the catalyst where metal-supported catalyst produced has relatively low Ni dispersion (Du et al., 2017). Thus, it is important to develop a synthetic route that leads to low cost production and producing catalyst with high dispersion structure. In this study, in-situ self-combustion synthesis has been employed to produce Ni-supported catalyst as the process has been reported to produce catalyst with high specific surface area and high metal dispersion (Mukasyan & Dinka, 2006).

In-situ self-combustion is an incorporation of inert support to self-combustion process to produce metal-supported catalysts. In-situ self-combustion is a very promising and cost-effective catalyst synthesis route, an alternative to traditional processes for catalyst preparation systems. In-situ self-combustion method has been proposed in the recent years due to the speediness of the reaction and relatively low cost. Besides, in-situ self-combustion is a preparation method also allows the catalyst produced to be high porosity and high degree of purity. Additionally, one important feature of self-combustion process is that it generates heat energy that enough to generate crystalline materials in single self-sustained step (Cross et al., 2014). Therefore, synthesizing metal-supported catalyst through in-situ self-combustion involves a relatively simple procedure.

In this work, Ni-supported silica catalysts (Ni-La/SiO_2) has been synthesized using in-situ self-combustion technique. The effects of glycine-nitrate (G/N) ratio, Ni to support ratio and addition of lanthanum as a promoter on the catalyst structure and morphology have been investigated. The catalysts produced were characterized using X-ray diffraction (XRD), scanning electron microscopy (SEM) and thermal gravimetric analyzer (TGA).

2. Experimental

2.1. Materials and Catalyst Preparation

Ni-La catalysts supported on SiO_2 were synthesized using in-situ self-combustion method. Nickel nitrate hexahydrate ($Ni(NO_3)_2.6H_2O$), glycine ($C_2H_5NO_2$), lanthanum nitrate hexahydrate, $La(NO_3)_3 \cdot 6H_2O$ and silica (SiO_2) were used as raw materials. Initially, nickel nitrate hexahydrate and glycine were dissolved in deionized water to form a reaction media solution. Porous solid silica (SiO_2) was added to the reaction media solution. The support-reaction media was stirred and heated overnight at 90ºC until it forms a gel solution. The gel solution was then heated at 180ºC until the solution was self-ignited and combusted to produce an ash catalyst powder. The ash powder was then calcined at 700ºC. In this work, effects of glycine-to-nitrate (G/N) ratio, Ni-La to support ratio and addition of promoter (La) on the structure and morphology of Ni supported silica catalyst have been investigated. The glycine-to-nitrate (G/N) ratios used in this study were G/N =0.5:1, 1:1 and 1.5:1. The Ni-La to SiO_2 support ratios were 1:3, 1:5 and 1:8. The loadings employed for the promoter which is lanthanum were at 3%, 5% and 10%.

2.2. Catalyst Characterization

The physical properties and morphology of the synthesized Ni-La/SiO_2 catalyst were characterized using X-ray diffraction (XRD), scanning electron microscopy (SEM) and thermal gravimetric analyzer (TGA). X-ray diffraction (XRD) was used to determine the composition and the crystalline properties of the synthesized catalysts. The surface morphology of catalyst on the silica support was characterized using scanning electron microscopy equipped with EDX (SEM-EDX). Finally, thermal gravimetric analyzer (TGA) was used to determine the weight loss of the prepared catalyst as a function of temperature.

3. Result and discussion

3.1 Catalyst Characterization

Figure 1 shows the SEM images of Ni-La/SiO_2 catalyst after calcination at 800°C. SEM-EDX mapping is performed on the surface of the bulk catalyst and given by Figure 1a. The presences of Ni, La, Si and O elements confirm the formation of Ni-La/SiO_2 catalyst from the in-situ self-combustion process. Two points were selected from the bulk sample to compare the elements presence at on the catalyst surface. EDX spectra confirms that the dark region is for lighter elements (Si and O) and the bright region is for heavier element (Ni). The dense structure and dark region on the catalyst surface is belongs to SiO_2 support, as indicates by SEM-EDX in Figure 1b. Meanwhile, a bright region of the catalyst is the Ni-La which is porous in structure as shown by the SEM-EDX in Figure 1c. Figure 1b has higher atomic percentage of Si (21%) compared to the atomic percentage of Ni which is 6%. Figure 1c, on the other hand has larger amount of Ni which 43% than that of Si which is 0.7%. The Ni-La catalyst is found to be deposited and dispersed well on the surface of SiO_2 support.

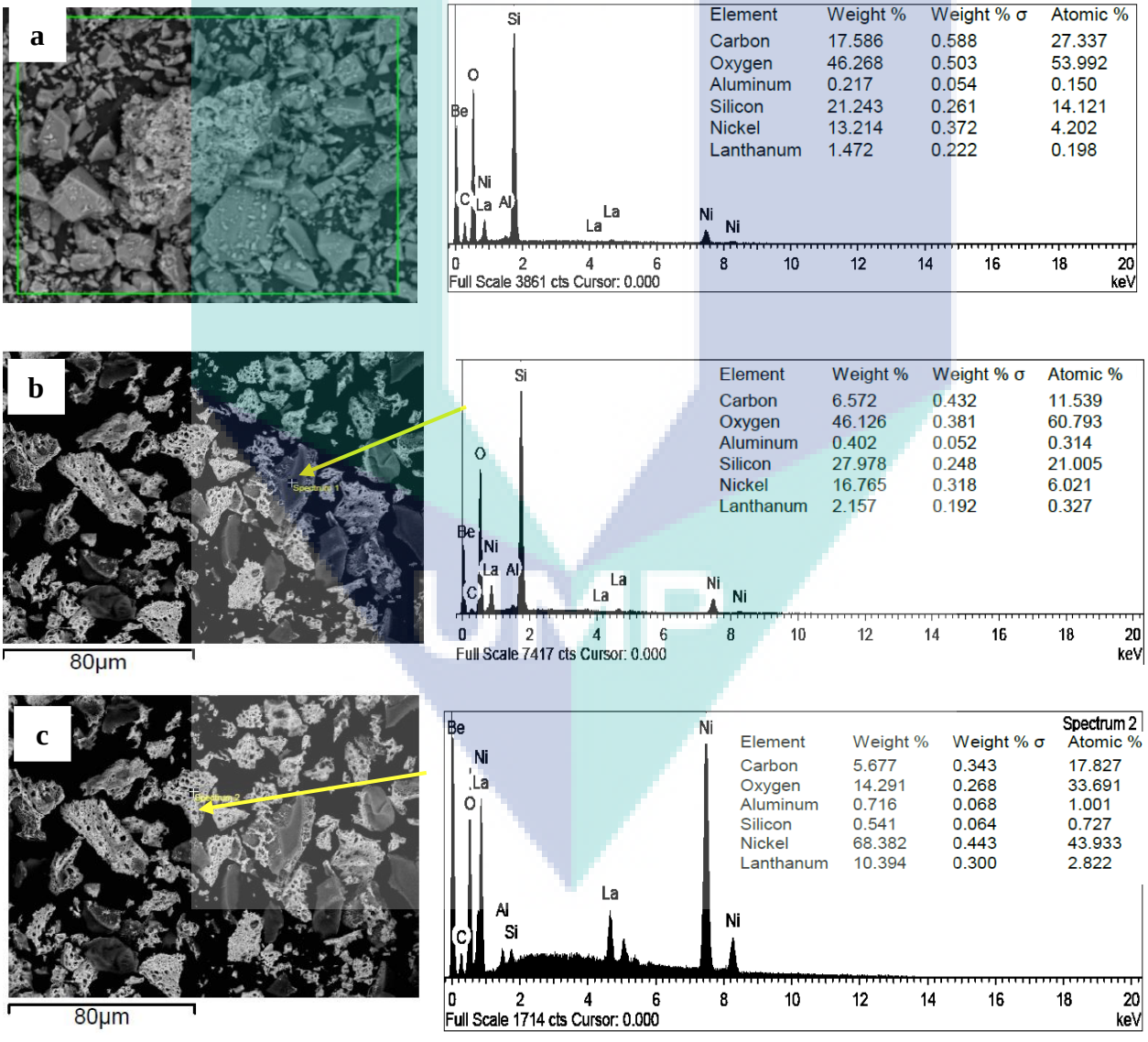

Figure 1. SEM-EDX images of Ni-La/SiO_2 catalyst after calcination at 800°C.

3.2 Effect of glycine-nitrate (G/N) ratio

Figure 2 shows the morphology of Ni-La/SiO_2 catalysts with different glycine-nitrate (G/N) ratios which are 0.5:1, 1:1 and 1.5:1. From the SEM micrographs, the variation of G/N does not show much significant different in the morphology. All Ni-La/SiO_2 catalysts produced from different G/N ratios of are highly porous and exhibited a good metal dispersion on the surface of the SiO_2 support. Ni-La catalyst is deposited well over the surface of support on the support surface. Among these catalysts, Ni/SiO_2 catalyst with G/N ratio of 0.5:1 (Figure 2a) seems to have a slight porous structure as compared to the other two (Figures 2b-c).

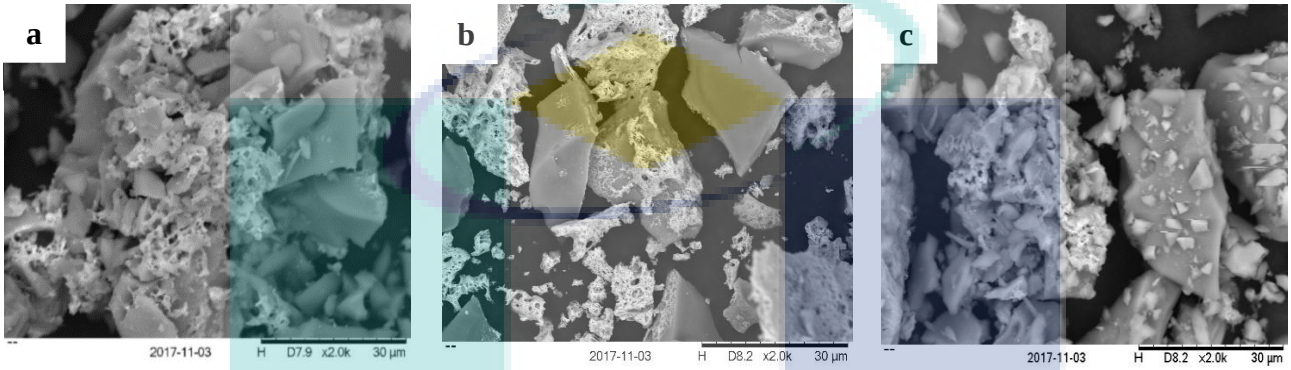

Figure 2. SEM images of Ni-La/ SiO_2 catalysts with glycine-nitrate (G/N) ratios of (a) 0.5:1 (b) 1:1 and (c) 1.5:1 at ×2,000 magnification

The effect of glycine-nitrate ratio was further evaluated using thermal gravimetric analysis (TGA). The TGA was performed on uncalcined Ni-La/SiO_2 catalysts to determine the relationship between the catalyst weight losses as a function of temperature. Figure 3 and Figure 4 show the TGA curve and differential thermal analysis (DTA) curve, respectively for Ni-La/SiO_2 catalyst prepared at different glycine-nitrate (G/N) ratios. The temperature was ramped from ambient temperature to 1000°C. In all catalysts, two major weight loss occur within in the temperature ranges between 25–200°C and above 250°C (Figures 3a-c). The first weight loss at temperature 25- 200ºC is caused by the evaporation of the physically adsorbed water on the surface of the Ni-La/SiO_2 catalyst (Bangale et al., 2013). This weight loss is proved by the DTA curve where the endothermic peaks are observed at temperature around 25–200°C (Figures 4a-c). The second weight loss at temperature above 250°C is probably due to the decomposition of the nitrates present in the catalysts (Afzall et al., 1993).

The weight loss for fuel-lean condition (G/N=0.5:1) is obvious (Figure 3a). At fuel-lean condition (G/N=0.5:1), it is suggested that there are available nitrates present in the catalyst due to an incomplete combustion during the in-situ combustion process. Thus, at temperature above 250°C, Ni nitrate available in sample is further decomposed to NiO, as reveals by the endothermic peak at temperature ~250ºC in the DTA curve (Figure 4a). On the other hand, a moderate weight loss is observed at fuel-rich condition (G/N=1.5:1), suggesting that the fuel (glycine) is sufficient for oxidation by the nitrates during the in-situ combustion process as shown in Figure 3c (Bansal, 2010). Therefore, it is concluded that, the catalyst weight loss decreases with the increase of glycine-nitrate (G/N) ratios from 0.5:1 to 1.5:1. However, weight gain is observed for Ni-La/SiO_2 prepared at glycine-nitrate (G/N) ratios of 1:1 (Figure 3b) at temperature higher than 400°C. This accompanied with a broad exothermic peak at 400ºC, given by the DTA curve (Figure 4b). The phenomena are probably due to due the oxidation of catalytic nickel particles during the thermal heating of the catalyst (Patil et al., 2015).

At the temperature up to 800 °C, the weight loss in all catalysts is about to plateau. According to Małecka et al. (2015), this probably due to an insignificant desorption of gaseous product from the catalyst surface at temperatures of 800°C and higher (Figures 3a-c). There is also no prominent change in the DTA curve as the temperature increases above 800°C. Therefore, 800°C can be considered as an optimum calcination temperature for Ni-La/SiO_2 catalyst. At this temperature, the catalyst is relatively stable and no longer has significant when further heated. The TGA results also

suggest that Ni-La/SiO_2 catalyst with high G/N ratio is able to reach a complete combustion during the in-situ self-combustion. As a conclusion, G/N ratio has a significant effect on the formation of stable structure of the catalyst.

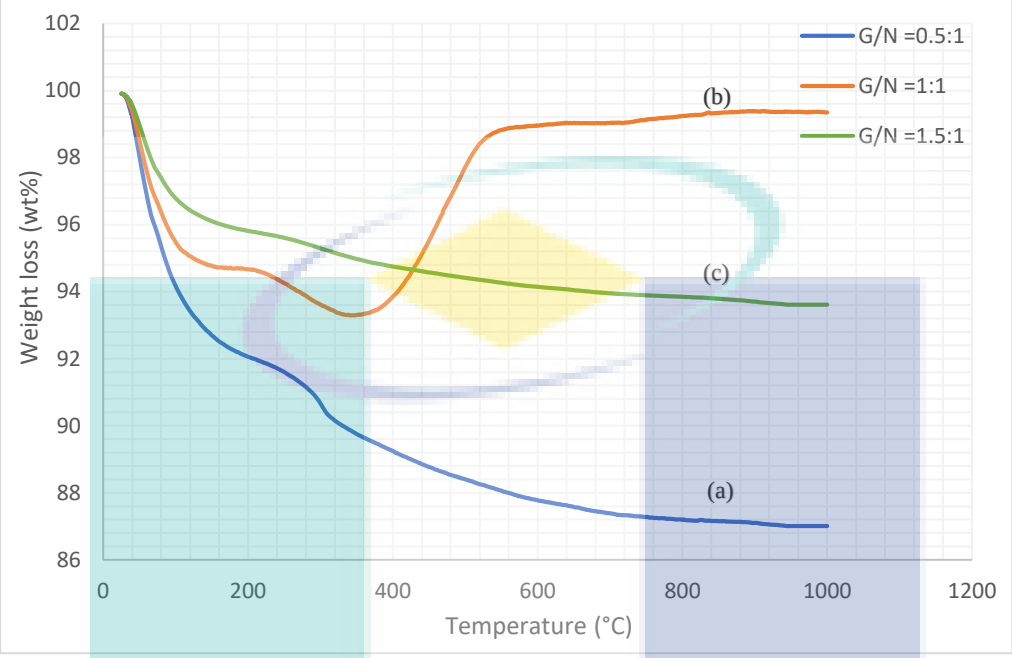

Figure 3. TGA curves of nickel-lanthanum supported on silica, Ni-La/SiO_2 catalyst at various glycine-nitrate (G/N) ratios

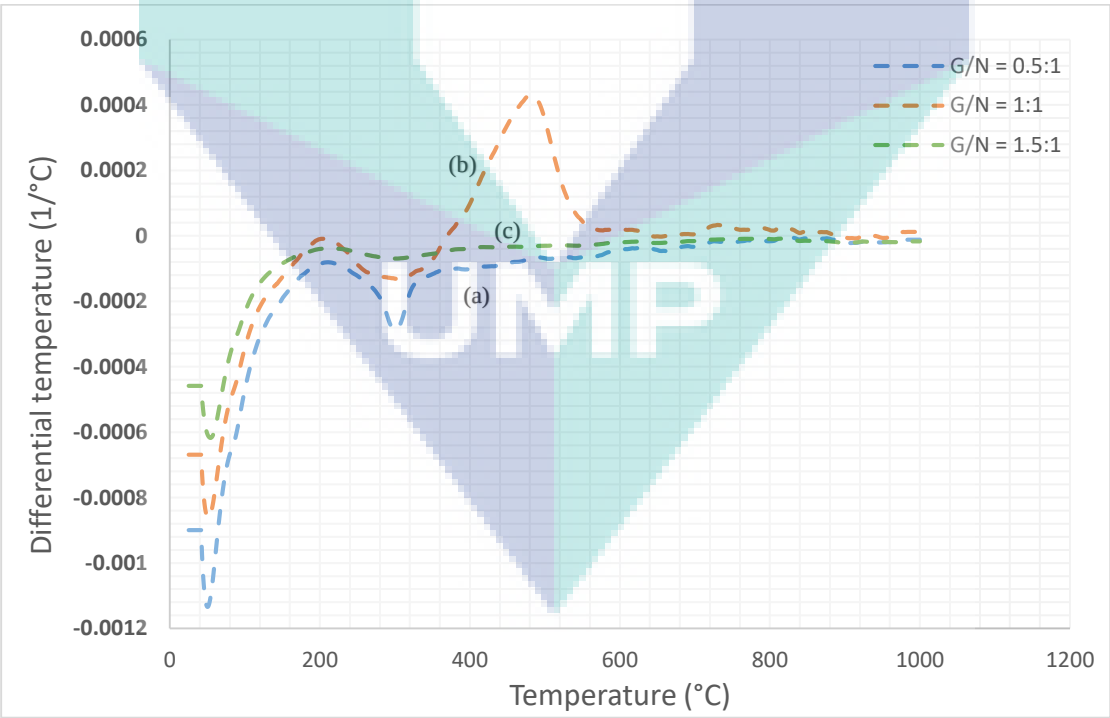

Figure 4. DTA curves of nickel-lanthanum supported on silica, Ni-La/SiO_2 catalyst at various glycine-nitrate (G/N) ratios

Figure 5 shows the XRD patterns of Ni-La/SiO_2 catalyst with different glycine-nitrate (G/N) ratios after 2 hours calcination at 800°C. From Figures 5 a-c, the peaks appear at 2θ =37.2, 43.3, and 62.9 which is belongs to NiO phase are observed in all Ni-La/SiO_2 catalysts with different G/N ratios of 0.5:1, 1:1 and 1.5:1. In previous study by Manukyan et al. (2013), nickel catalyst synthesized using G/N ratio of lower than 1.25:1 formed NiO when nickel nitrate−glycine mixture was combusted in air. Meanwhile, Ni can be formed when Nickel catalysts is synthesized using with G/N ratio of higher than 1.25:1.Similar mechanism is expected during the combustion reaction for the reaction media containing nickel-lanthanum nitrates−glycine on the porous silica in this work. However, no Ni phase is observed and only NiO phase is detected as one of the combustion products, regardless of any G/N ratios used in the range of 0.5- 1.5 for Ni-La/SiO_2 catalyst in this work. On the other hand, $LaNiO_3$ phase is only appeared at the Ni-La/SiO_2 catalyst with G/N ratios of 1:1. Except by this catalyst, Ni-La/SiO_2 catalysts prepared using glycine-nitrate (G/N) ratios of 0.5:1 and 1.5:1 are slightly amorphous. Besides, it can be seen that the most intense and sharpest peak is observed for Ni-La/SiO2 catalysts with G/N ratio of 1:1 (Figure 5b) which indicates that Ni-La/SiO2 catalyst with G/N ratio of 1:1 has the highest crystallinity. As a conclusion, glycine-nitrate (G/N) ratios will affect the presence of NiO, SiO_2 and lanthanum in Ni-La/SiO_2 catalyst.

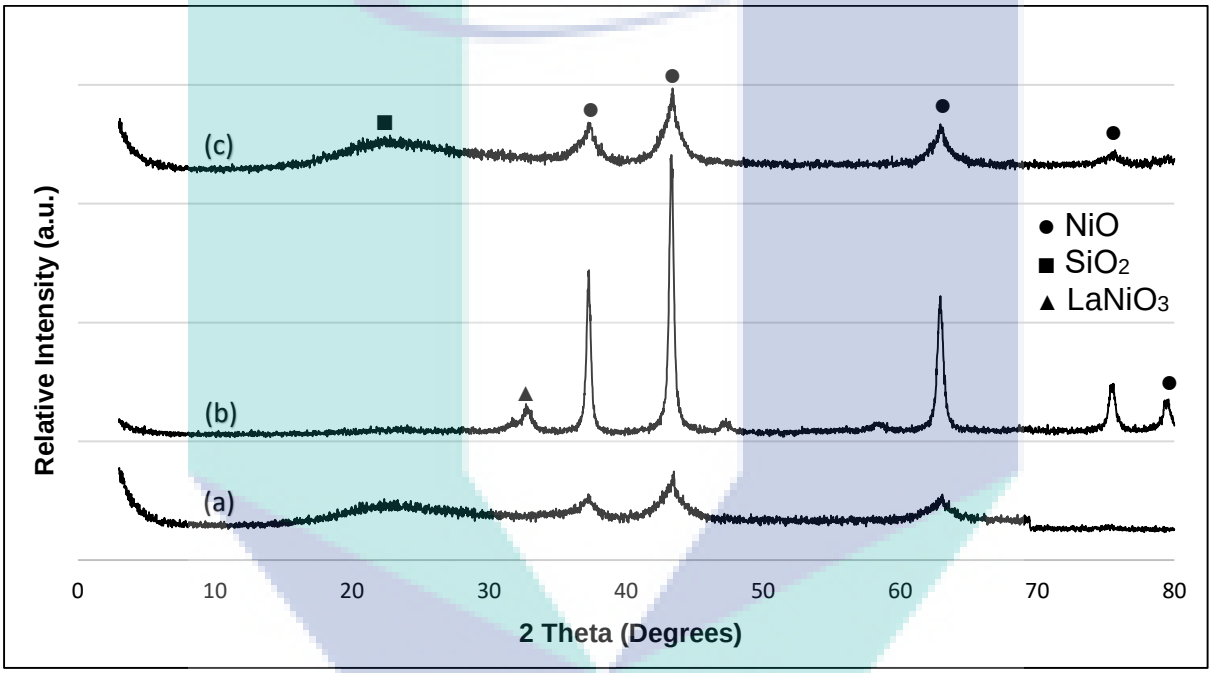

Figure 5: XRD patterns of Ni-La/SiO_2 catalysts with glycine-nitrate (G/N) ratios of (a) 0.5:1 (b) 1:1 (c) 1.5:1.

3.3 Effect of Ni-La catalyst to support ratio

Figure 6 shows the XRD patterns of Ni-La/SiO_2 catalysts at various Ni-La catalyst to support ratios. From Figures 6(a-c), the peaks of NiO were indicated by the phase angle at 2θ = 37.2, 43.3, and 62.9. Silica peaks exist as amorphous structure at 2θ = 23.04 (Figures 6a and c). Ni-La/SiO_2 for Ni-La to support ratio of 1:3 shows a weak crystallinity structure compared to the others two. From Figures 6(a-c), the diffraction peaks were more intense for low Ni-La catalyst to support ratio (1:3 and 1:5) when compared to high Ni-La catalyst to support ratio (1:8). The crystallinities of catalyst with Ni-La catalyst to support ratio of 1:5 is highest among all. Besides, $LaNiO_3$ phase was observed in the catalyst with Ni-La to support ratio of 1:5 at 2θ = 32.76 (Figure 6b). On the other hand, no diffraction peaks for $LaNiO_3$ phase was detected in both Ni-La to support ratios of 1:3 and 1:8 (Figures 6a and c). The absence of $LaNiO_3$ in peak suggested that lanthanum component is present either as amorphous phase or exist in small amount and unable to be detected by this technique. In addition, the absence of diffraction peaks for silica in Figure 6b suggests that the silica which is amorphous and below the XRD detection limit. In short, different Ni-La to support ratio will also affect the crystallinity as well as the presence of NiO, SiO_2 and lanthanum in Ni-La/SiO_2 catalyst.

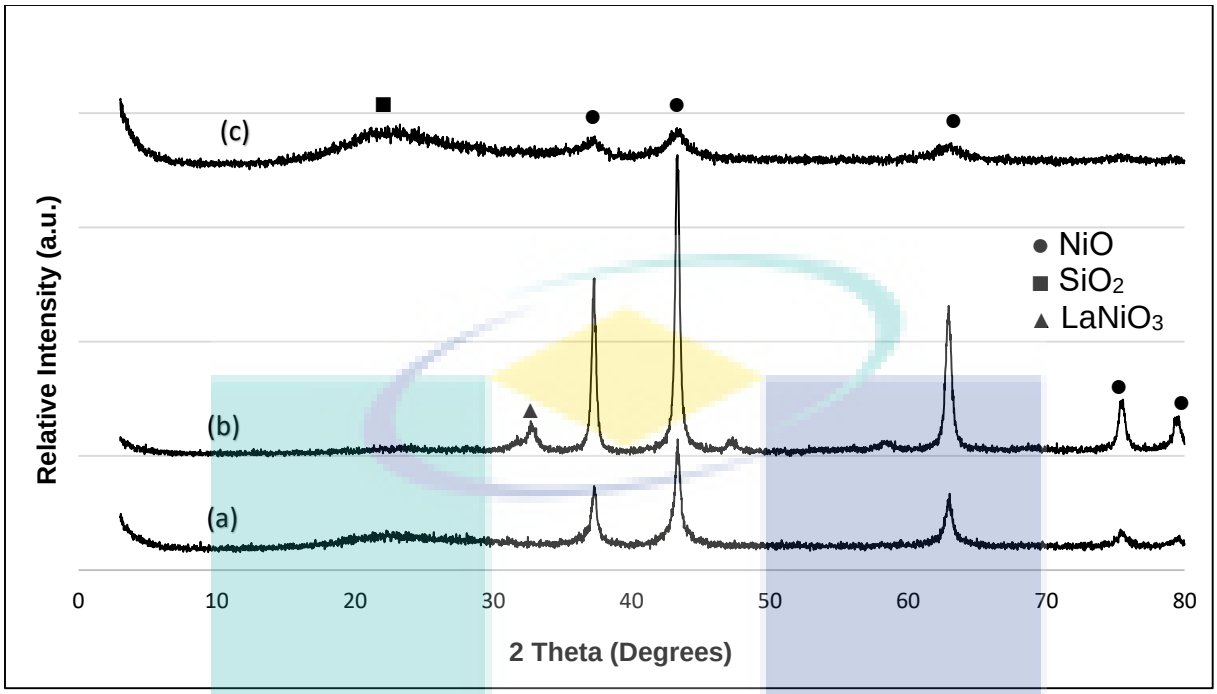

Figure 6: XRD patterns of Ni-La/SiO_2 catalysts with Ni-La to support ratios of a) 1:3 (b) 1:5 (c) 1:8

3.4 Effect of La loading

Figure 7 gives the XRD patterns of Ni-La/SiO_2 catalysts at different La loadings. From Figure 7a, it is observed that when a small quantity of lanthanum (3%wt) was used as a promoter, La phase was not observed in the catalyst. The phenomena is found as well in the catalyst with the highest La loading (10%wt) (Figure 7a). Therefore, the optimum lanthanum loading is at 5 wt% given by Figure 7a as it gives the intense and obvious peak for La phase. In overall, it is concluded that La loading of 5% is a suitable loading for promoter in the Ni-La/SiO_2 catalyst. In addition, La loading in Ni-La/SiO_2 catalysts will affect the crystallinity together with the presence of NiO, SiO_2 and lanthanum in the catalyst.

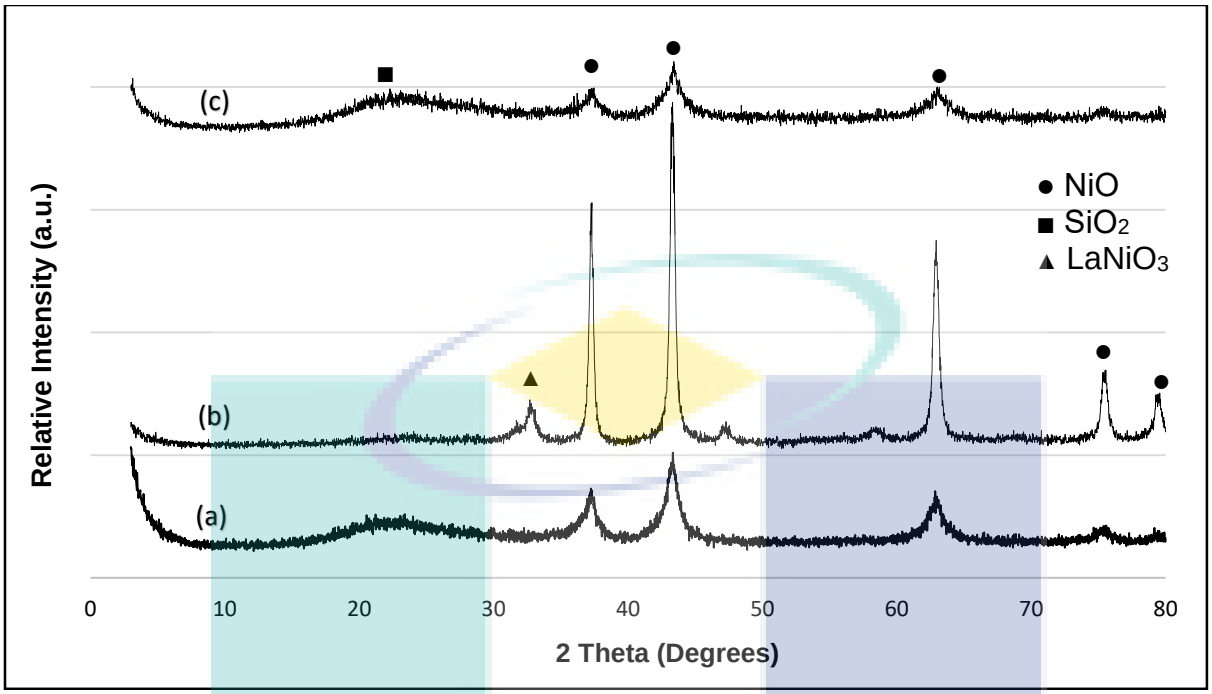

Figure 7: XRD patterns of Ni-La/SiO_2 catalysts with La loadings of (a) 3 wt% (b) 5 wt% (c) 10 wt%

The estimated average crystallite sizes of Ni-La/SiO_2 catalyst for various Ni-La to support ratio have calculated using Scherrer equation (Eq. 1) and tabulated in Table 1. The crystallite size of metallic Ni is a key factor for the formation of carbon. Small Ni crystallites are highly desirable in order to avoid the formation of carbon (Argyle & Bartholomew, 2015). The table shows that the crystallite size of Ni-La/SiO_2 reduces with the increase Ni-La to support ratio.

$$D = \frac{0.9\lambda}{\beta(cos\theta)} \qquad \text{(Equation 1)}$$

Where D is the average crystallite size, λ is wavelength of X-ray in the radiation, θ is diffraction angle, β is FWHMs full width at half maximum.

Table 1: The crystallite size of Ni-La/SiO_2 catalysts with different Ni-La to support ratio

Ni-La to support ratio	Crystallite average size (nm)
1:3	18.8750
1:5	18.4429
1:8	4.6750

4.0 Conclusion

In this work, Ni-La/SiO_2 has been successfully synthesized using in-situ self-combustion by incorporating inert silica support in the glycine-nitrate reaction media. The catalytic characteristics were studied at different glycine-to-nitrate (G/N) ratio (G/N= 0.5:1, 1:1, 1.5:1), Ni-La catalyst to support ratios (1:3, 1:5 and 1:8) lanthanum loadings (3 wt%, 5 wt% and 10 wt %). The SEM results show that varying the glycine to nitrate (G/N) ratios do not show significant difference in the morphology of catalyst. However, TGA analysis show the catalyst weight loss decreases with high glycine to nitrate (G/N) ratio. From XRD analysis, the optimum conditions for the Ni-La/SiO_2 are glycine-to-nitrate (G/N) ratio of 1:1 and Ni-La catalyst to support ratio of 1:5. Besides, La loadings of 5 wt% was found to be the optimum promoter for Ni-La/SiO_2. On the other hand, the crystallite size of Ni-La/SiO_2 is decreased with the increase

of Ni-La to support ratio, which is a desirable factor in order to reduce carbon formation. Therefore, glycine-to-nitrate (G/N) ratios, Ni-La to support ratio and lanthanum loading affect the crystallinity as well as the presence of NiO, SiO2 and lanthanum in Ni-La/SiO2 catalyst. As a conclusion, in-situ self-combustion method has a potential to produce a pure Ni-La/SiO_2 catalyst with porous structure and high crystallinity.

References

Afzall, M., Theocharis, C. R., Karim, S., & Afzal, M. (1993). Temperature programmed reduction of silica supported nickel catalysts. Colloid and Polymer Science, 1105(11), 1100–1105. https://doi.org/10.1007/BF00659300

Amin, A. M., Croiset, E., & Epling, W. (2011). Review of methane catalytic cracking for hydrogen production. International Journal of Hydrogen Energy, 36(4), 2904–2935. https://doi.org/10.1016/j.ijhydene.2010.11.035

Bangale, S. V, Patil, D. R., & Bamane, S. R. (2013). Preparation and electrical properties of nanocrystalline MgFe 2 O 4 oxide by combustion route. Archives of Applied Science Research, 3(5), 506–513.

Cross, A., Kumar, A., Wolf, E. E., & Mukasyan, A. S. (2012). Combustion Synthesis of a Nickel Supported Catalyst: Effect of Metal Distribution on the Activity during Ethanol Decomposition. Industrial & Engineering Chemistry Research, 51(37), 12004–12008. https://doi.org/10.1021/ie301478n

Cross, A., Roslyakov, S., Manukyan, K. V., Rouvimov, S., Rogachev, A. S., Kovalev, D., Mukasyan, A. S. (2014). In Situ Preparation of Highly Stable Ni-Based Supported Catalysts by Solution Combustion Synthesis. The Journal of Physical Chemistry C, 118(45), 26191–26198. https://doi.org/10.1021/jp508546n

Du, Y.-L., Wu, X., Cheng, Q., Huang, Y.-L., & Huang, W. (2017). Development of Ni-Based Catalysts Derived from Hydrotalcite-Like Compounds Precursors for Synthesis Gas Production via Methane or Ethanol Reforming. Catalysts, 7(2), 70. https://doi.org/10.3390/catal7020070

Małecka, B., Łącz, A., Drozdz, E., & Małecki, A. (2015). Thermal decomposition of d-metal nitrates supported on alumina. Journal of Thermal Analysis and Calorimetry, 119(2), 1053–1061. https://doi.org/10.1007/s10973-014-4262-9

Mukasyan, a. S., & Dinka, P. (2007). Novel approaches to solution-combustion synthesis of nanomaterials. International Journal of Self-Propagating High-Temperature Synthesis, 16(1), 23–35. https://doi.org/10.3103/S1061386207010049

Manukyan, K. V., Cross, A., Roslyakov, S., Rouvimov, S., Rogachev, A. S., Wolf, E. E., & Mukasyan, A. S. (2013). Solution Combustion Synthesis of Nano-Crystalline Metallic Materials: Mechanistic Studies. The Journal of Physical Chemistry C, 117(46), 24417–24427. https://doi.org/10.1021/JP408260M

Narottam P. Bansal, P. S. (2010). Advances in Solid Oxide Fuel Cells V. Canada: Wiley.

Sarika P.Patil, S.P. Patil, S.T.Jadhav, V.R.Puri, L. D. J. (2015). Synthesis and Characterization of α - Fe2O3/C Composite Anode for Lithium Ion, 41(73), 3–4.

Tanggarnjanavalukul, C., Donphai, W., Witoon, T., Chareonpanich, M., & Limtrakul, J. (2015). Deactivation of nickel catalysts in methane cracking reaction: Effect of bimodal meso-macropore structure of silica support. Chemical Engineering Journal, 262, 364–371. https://doi.org/10.1016/j.cej.2014.09.112

APPENDIX

(URP TECHNICAL PAPER 6)

IN-SITU PREPARATION OF NI-BASED CATALYST SUPPORTED ON AL_2O_3 USING SELF-COMBUSTION PROCESS

Teo Jet Yee and Asmida Ideris
Faculty of Chemical & Natural Resources Engineering,
Universiti Malaysia Pahang, 26300 Gambang, Pahang, MALAYSIA.
Tel: +60167503243.

ABSTRACT

Methane cracking is a promising technique to synthesis CO_X-free H_2. However, the main disadvantage of methane cracking is the formation of carbon on Ni catalyst surface which deactivates the Ni catalyst. Previously, various conventional methods have been developed to synthesis Ni-supported catalyst. However, the drawbacks of those methods are producing Ni-supported catalyst with relatively poor Ni dispersion. This morphology is favoured for carbon deposition. Therefore, the aim of this work is to synthesis Ni-supported catalyst with relatively high Ni dispersion. In-situ self-combustion synthesis has been employed as it is a low-cost and a simple synthesis process. The experiment has been conducted by mixing an oxidizer (nitrate), a fuel (glycine) and an inert porous support (alumina) to form a support-solution media. The support-solution media was heated and stirred overnight to form a viscous gel. Finally, the viscous gel was subjected to heat treatment until it self-ignited, producing catalyst ash powder. The experiment has been varied upon types of alumina support, glycine to nitrate (G/N) ratios and Ni:Al_2O_3 molar ratios. The Ni-supported on Al_2O_3 catalyst has been characterized using SEM and XRD. Based on the XRD results, a crystalline and pure of NiO/α-Al_2O_3 metal-supported catalyst is successfully obtained through in-situ self-combustion process. However, γ-Al_2O_3 is not a suitable support as there is an absence of crystalline Ni species on the NiO/γ-Al_2O_3 metal-supported catalyst, overlapped by the amorphous structure of the γ-Al_2O_3 support. NiO dispersion on alumina support increases as the Ni: alumina molar ratios increase from 1:1 to 1:5. It is found that Ni: alumina molar with the ratio of 1:5 has the highest NiO dispersion on the α-alumina support (40.7%). SEM images show that NiO/α-Al_2O_3 catalyst synthesized using in-situ self-combustion is found to be porous in structure. Additionally, the morphology of the supported catalyst appears to be the same and was not varied with the variation of glycine-nitrate (G/N) ratio from 0.5:1 to 1.5:1.

Keywords: Ni-supported Al_2O_3; In-situ self-combustion; Ni:Al_2O_3 molar ratio; glycine-nitrate (G/N) ratio

1. Introduction

Nickel (Ni) has been recognized as a low-cost and efficient catalyst for hydrogen production from methane cracking (Zhang et al, 1998). Nevertheless, methane reaction is still hindered by accumulation of carbon on Ni catalyst, which is produced during the reaction. Carbon deposition rate is influenced by the type of catalyst support and the morphology of catalyst surface (Morris et al, 2015). Catalyst morphology such as dispersion of metallic nickel on catalyst support and surface area of supported catalyst may affect the nature of carbon and the resistance of catalyst towards carbon. Supported catalyst with relatively large surface area and highly catalyst dispersion for example is essential to develop carbon-resistance Ni-based catalysts. Yang et al. (2004) has reported that Ni-Al_2O_3 with relatively high specific surface area and high metal dispersion will retard the formation of filamentous carbon. In addition, the catalytic activity is enhanced by the improvement of Ni surface area (Gao et al, 2015). Thus, Ni-based supported catalyst with high specific surface area and high Ni particles dispersion is crucial for methane cracking process.

Impregnation, co-precipitation and sol-gel are the common methods to synthesis Ni-based supported catalyst. Nevertheless, Ni-supported catalysts produce using these methods have relatively low specific surface area (Cross et al, 2012) or poor dispersion of Ni-particles (Barros et al., 2015). Under hydrocarbon atmosphere, low dispersed catalyst is more likely to form more carbon on catalyst surface (Adelino et al., 2009). Hence, a highly dispersed Ni-based supported catalyst is essential to provide carbon-resistance catalysts, thus catalyst preparation method which produces as such catalyst morphology should be employed.

Self-combustion technique is well-known for preparation of metal and perovskite catalysts. The technique also has been employed for the synthesis of metal-supported catalyst where catalyst metal is distributed over a bulk of inert support. The process which is also known as in-situ self-combustion has been reported to further increase active phase surface area, and improve the structural and thermal stability of catalyst (Cross et al, 2012). Ni-supported catalyst with improved surface area and Ni dispersion is expected to minimize carbon deposition and reduce the risk of sintering, and ultimately enhances the catalyst stability for methane cracking.

In the previous study, Cross et al. (2014) synthesize Ni-Al_2O_3 by combining addition of inert porous support during self-combustion catalyst synthesis allows the formation catalyst with dispersed particles. Sergio et al. (2013) stated that unsupported active catalyst alone does not allow for a high thermal stability and high activity in hydrocarbon processing at high temperature. Therefore, the use of supported catalyst is essential as the addition of support can further improve the dispersion of active catalyst phase and enhance the thermal stability of the catalyst. Based on in-situ self-combustion process carried out by Cross (2012) to synthesis Ni-Al_2O_3, they found that the distribution/dispersion of Ni particles on alumina support can be modified by controlling the contacting time between reaction-media and porous support (alumina).

In present work, Ni supported catalyst on Al_2O_3 is prepared using in-situ self-combustion process. Al_2O_3 is chosen as the support due to its thermal stability (Akande et al., 2005). It is reported that the nickel can be highly dispersed and maintain the dispersion on the alumina surface due to the strong interaction between Ni^{2+} and Al_2O_3 as support (Li et al., 2006). Since it is expected that the morphology (specific surface area, Ni dispersion on support and Ni crystalline size) of supported catalyst can be improved by various glycine to nitrate (G/N) ratios, types of alumina and Ni to support ratios, the effects will be further explored in this work.

2. Experimental

2.1 Materials and methods

The chemicals employed for this experiment is nickel (II) nitrate hexahydrate ($Ni(NO_3)_2{\cdot}6H_2O$), glycine ($C_2H_5NO_2$), γ-alumina (γ-Al_2O_3) and α-alumina (α-Al_2O_3) which are purchase from Merck (US). Nickel (II) nitrate hexahydrate, $Ni(NO_3)_2{\cdot}6H_2O$ is the main precursor for Ni catalyst and glycine, $C_2H_5NO_2$ will act as a fuel for combustion reaction. Type of supports is between γ-alumina, γ-Al_2O_3 and α-alumina, α-Al_2O_3.

2.2 In-situ self-combustion synthesis

The experiment is started with preparation of $Ni(NO_3)_2{\cdot}6H_2O$ solution. Glycine was added as a fuel at a specific glycine-nitrate (G/N) ratio with a different Glycine/Nitrate ratio (0.5, 1.0 and 1.5). Then, support was added to the solution mixture. Next, the solution-support media was heated at 90°C and stir for overnight. The mixture formed a viscous gel and was transformed to a ceramic evaporating dish. The viscous gel was heated to 180°C at which self-ignited combustion begins turning the gel solution into catalyst ash powder. The catalyst ash formed was then calcined in a furnace at 800°C with 2 hours. The experiment was varied upon various glycine-nitrate (G/N) ratio (G/N = 0.5, 1.0 and 1.5), types of alumina support (γ-Al_2O_3 and α-Al_2O_3) and Ni:Al_2O_3 molar ratio (1:1, 1:3 and 1:5). The morphology of the metal-supported catalyst produced was characterized using scanning electron microscopy (SEM) and X-ray diffraction (XRD) analysis.

2.3 Ni dispersion

Ni dispersion on the alumina support was calculated using data obtained from XRD analysis. The average crystal diameter of Ni was estimated by using Scherrer equation. Then, the average crystal diameter of Ni was employed to undergo a series of calculations to obtain dispersion of Ni particles on Al_2O_3.

$$D = \frac{K \cdot \lambda}{FWHM \cdot Cos\ \theta} \qquad \text{Equation 1}$$

Where D = Ni crystalline size/diameter (m)
λ = Wavelength of radiation (nm)
FWHM = Width of diffraction line at half of its maximum intensity (rad)
θ = Angle at the maximum intensity (rad)

$$N_i = \frac{M_{Ni}}{\frac{2}{3}\pi\left(\frac{D}{2}\right)^3 (p_{Ni})}$$ Equation 2

Where N_i = Number of Ni particles
M_{Ni} = Molecular weight of Ni (g/mol)
p_{Ni} = Density of Nickel (g/m^3)
D = Ni crystalline size/diameter (m)

$$S = 2\pi \left(\frac{D}{2}\right)^2 N_i$$ Equation 3

Where S = Overall surface area of Ni particles (m^2/g)
N_i = Number of Ni particles
D = Ni crystalline size/diameter (m)

$$d = \frac{Sk}{nN_A}$$ Equation 4

Where d = Dispersion of Ni particles on Al_2O_3
S = Overall surface area of Ni particles (m^2/g)
k = Value of constant
N_A = Avogadro constant

3. Result and discussion

3.1 Effect of type of alumina support

Figure 1 shows the XRD patterns of NiO, α-alumina, γ-alumina and Ni catalysts supported on α-alumina and γ-alumina. In the diffraction peaks for Figures 1c-e, the phase angle 2θ = 37.4, 43.5, 63, 75.6 and 79.6° are related to NiO phase. Zhao et al. (2012) has reported that the diffraction peaks at 37.4, 43.5, 63, 75.6 and 79.6° are attributed to the distinct peaks of cubic NiO. Accordingly, El-Kemary et al. (2013) also reported that the (111), (200), (220), (311) and (222) peaks at 2θ = 37.4, 43.5, 63, 75.6 and 79.6°, respectively are belongs to the crystal plane of bulk NiO. Meanwhile, the diffraction peaks at 2θ = 25.6, 35.1, 37.7, 43.3, 52.5, 57.5, 61.3, 66.5, 68.2 and 76.8° are related to α-alumina phase (Figure 4.1a). Feret et al. (2000) has referred the peaks at 2θ = 25.6, 35.1, 37.7, 43.3, 52.5, 57.5, 61.3, 66.5, 68.2 and 76.8° are attributed to Al_2O_3 structure. It is reported that the presence of peaks at (012), (104), (110), (113), (024), (116), (122), (214), (300) and (119) are corresponding to the crystal plane of α-alumina phase (Bourbia, 2012). Figure 1a shows the diffraction peaks at 2θ = 32.6, 37.2, 45.5 and 67.0° which are belonging to γ-alumina phase. Asencios et al. (2012) and Piriyawong et al. (2012) have described that the peaks for γ-alumina phase at 2θ = 32.6, 37.2, 45.5 and 67.0° with the crystal planes of (220), (311), (400) and (440), respectively are attributed to a poor crystalline chi-alumina structure. Additionally, the diffraction peaks of NiO/α-Al_2O_3 and NiO/γ-Al_2O_3 only indicate the presence of NiO, α-Al_2O_3 and γ-Al_2O_3 species. No other species are found during the catalyst preparation during in-situ self-combustion process.

The diffraction peaks of NiO, α-Al_2O_3 and NiO/α-Al_2O_3 show intense and sharp peaks which indicate the substances are in crystalline structure (Figures b, c, e). In contrast, the diffraction peaks of γ-Al_2O_3 (Figure 1a) and NiO/γ-Al_2O_3 (Figure 1d) indicate that both substances are amorphous in structure. NiO/γ-Al_2O_3 has much similar diffraction peaks as compared to that of γ-Al_2O_3 where the NiO peak in the diffraction pattern of NiO/γ-Al_2O_3 is not obvious. This indicates that the γ-Al_2O_3 is not a suitable support for Ni catalyst as there is no obvious presence of crystalline Ni species on the NiO/γ-Al_2O_3 metal-supported catalyst, overlapped by the amorphous structure of γ-Al_2O_3 support. Meanwhile, Ni species in the NiO/α-Al_2O_3 maintains its crystalline structure yet with a smaller size. NiO peaks at 63 and 75.6° related to (220) and (311) plane of bulk NiO appear in the NiO/α-Al_2O_3 diffraction pattern but at a smaller size. Meanwhile, NiO peaks at 37.4 and 43.5° which are related to (111) and (200) of NiO plane appear at the same phase with the α-Al_2O_3 peaks. From the XRD diffraction patterns, it is concluded that it is able to obtain a crystalline and pure of NiO/α-Al_2O_3 metal-supported catalyst using in-situ self-combustion process.

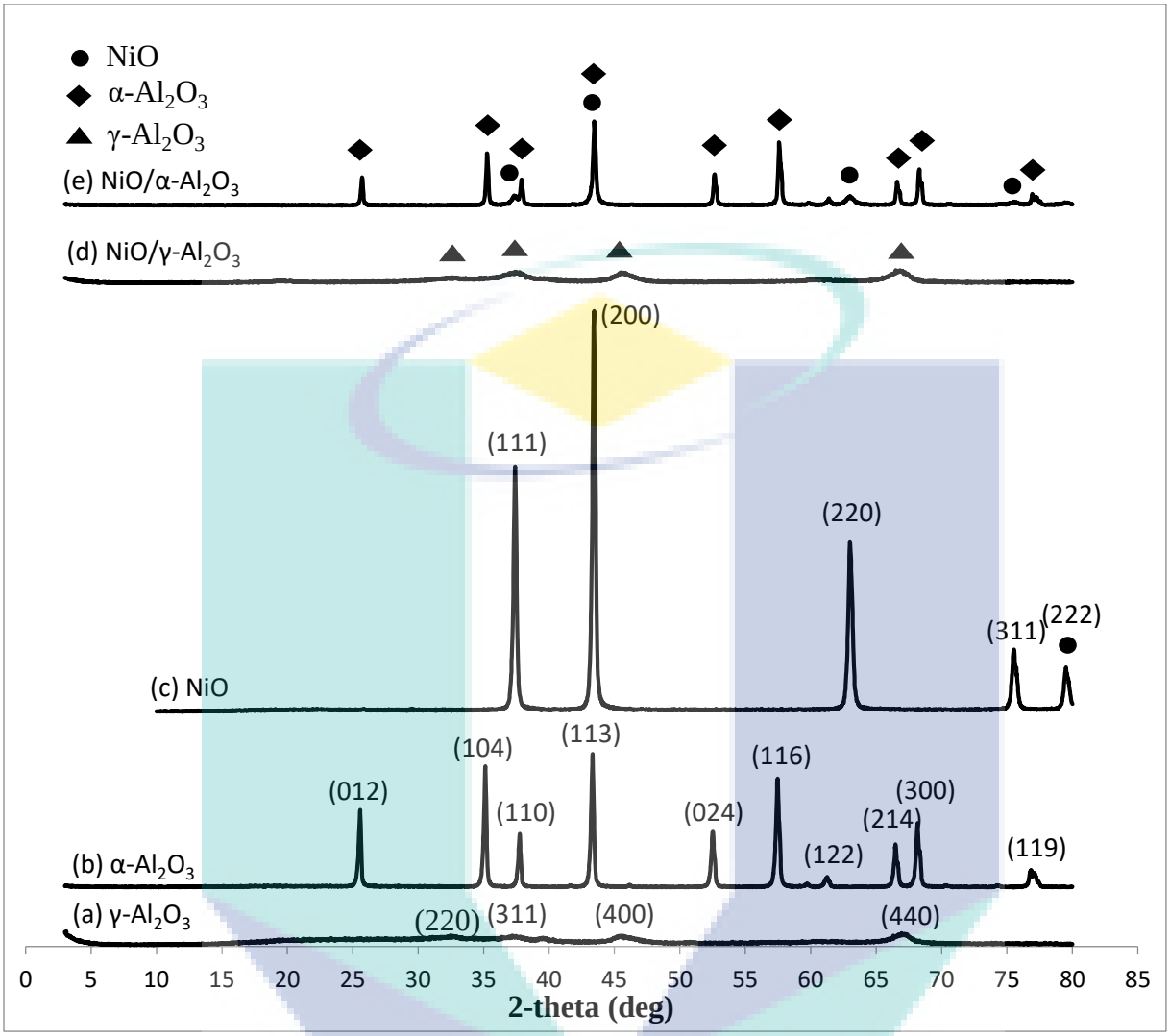

Figure 1 XRD patterns of catalysts after 2 hours of calcination at 800°C: (a) γ-alumina (b) α-alumina (c) NiO (d) NiO/ γ-Al_2O_3 and (e) NiO/α-Al_2O_3. Ni: alumina molar ratio =1:5 and glycine-nitrate (G/N) ratio =1:1.

3.2 Effect of Ni: Alumina Molar Ratio

XRD patterns of NiO/α-Al_2O_3 at various Ni: alumina molar ratios are shown in Figure 2. In overall, the NiO/α-Al_2O_3 catalysts produced from in-situ self-combustion synthesis have almost similar diffraction peaks at different Ni: alumina molar ratios. The diffraction peaks are more intense and sharper as the Ni: alumina molar ratio is reduced from 1:5 to 1:1. The NiO planes at (220) and (311) on NiO/α-Al_2O_3 become more obvious as the Ni: alumina molar ratios decreases from 1:5 to 1:1. This shows that NiO in the NiO/α-Al_2O_3 catalyst become more crystalline as the Ni: alumina molar ratios decreases. NiO/α-Al_2O_3 catalyst with the Ni: alumina molar ratio of 1:1 has the most crystalline structure.

The NiO crystalline size, surface area and dispersion of NiO on alumina support at various Ni: alumina molar ratios are tabulated in Table 1. The calculation of NiO dispersion on the alumina support is performed based on (220) NiO plane using Scherer equation. The crystalline size of NiO (nm) increases with the increases of Ni: alumina molar ratios from 1:1 to 1:5. Accordingly, the NiO surface area and NiO dispersion on alumina support increase as the Ni: alumina molar ratios increase from 1:1 to 1:5 which is in the same trend observed by Liu et al. (2013). A small outlier is observed at Ni: alumina molar ratio = 1:3. As a result, Ni: alumina molar ratio of 1:5 has the highest NiO dispersion on α-alumina support.

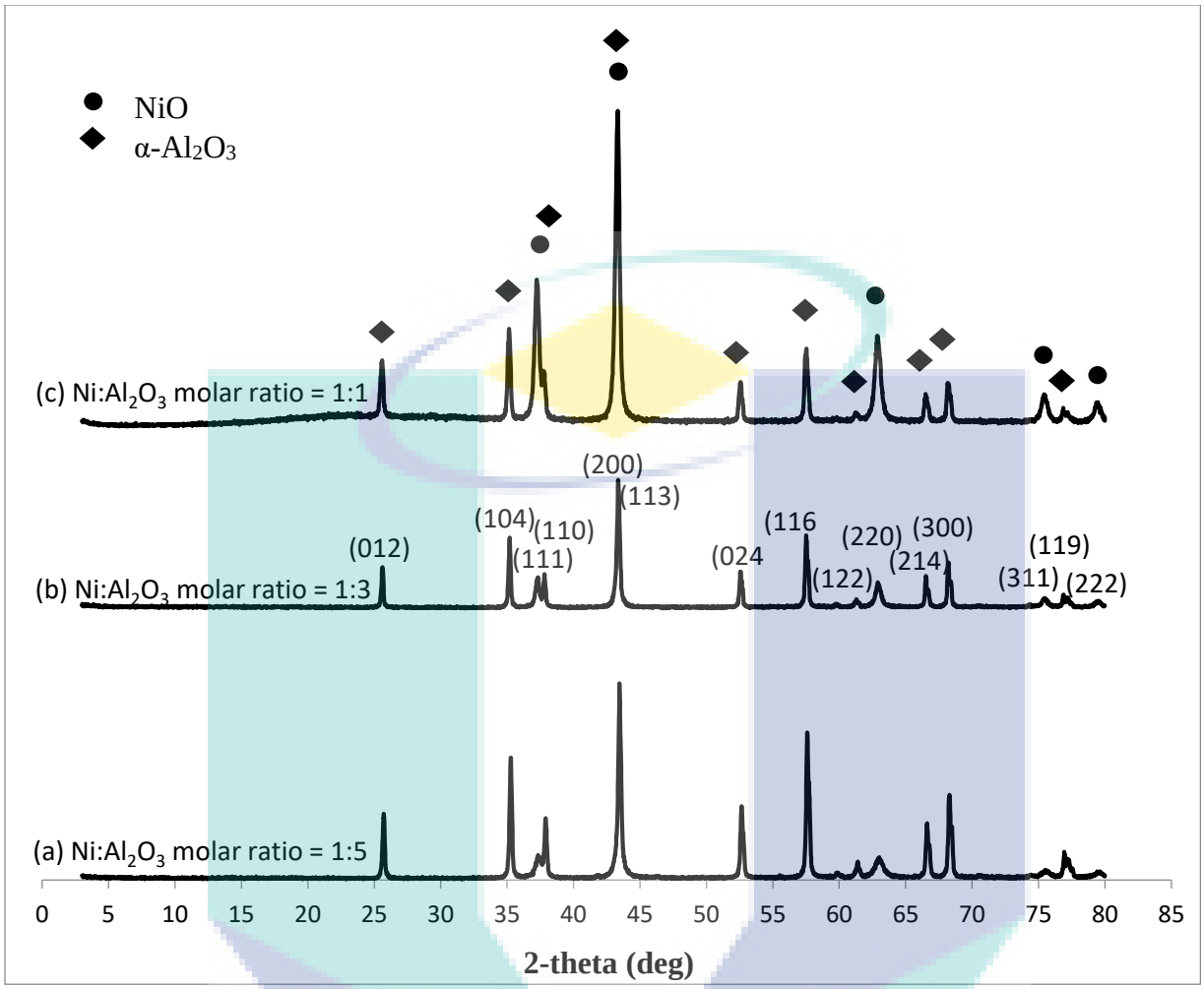

Figure 2 XRD patterns of catalysts after 2 hours of calcination at 800°C: (a) Ni:Al_2O_3 molar ratio = 1:5 (b) Ni:Al_2O_3 molar ratio = 1:3, and (c) Ni:Al_2O_3 molar ratio = 1:1. Glycine-nitrate (G/N) ratio =1:1.

Table 1 Crystalline size, surface area and NiO dispersion on alumina support at Ni: alumina molar ratios

Nickel : Alumina Molar ratio	Crystalline Size of NiO [a] (nm)	Surface area of NiO [a] (m^2g^{-1})	NiO dispersion on alumina support [a](%)
1:1	20.1	196	26.3
1:3	23.9	165	22.1
1:5	13.0	304	40.7

[a] Calculated from NiO (220) plane using Scherrer eqution from XRD.

The effect of at Ni: alumina molar ratios are also analyzed using SEM-EDX. Figure 3 shows the SEM-EDX analysis on NiO/α-Al_2O_3 catalyst with Ni: alumina molar ratios of 1:1, 1:3, and 1:5. EDX mapping was performed on the surface of NiO/α-Al_2O_3 catalyst. Ni composition decreases as the as Ni: alumina molar ratios increase from 1:1 to 1:5. This shows that the in-situ self-combustion synthesis is able to synthesize NiO supported on alumina catalyst with a controlled amount of elemental composition.

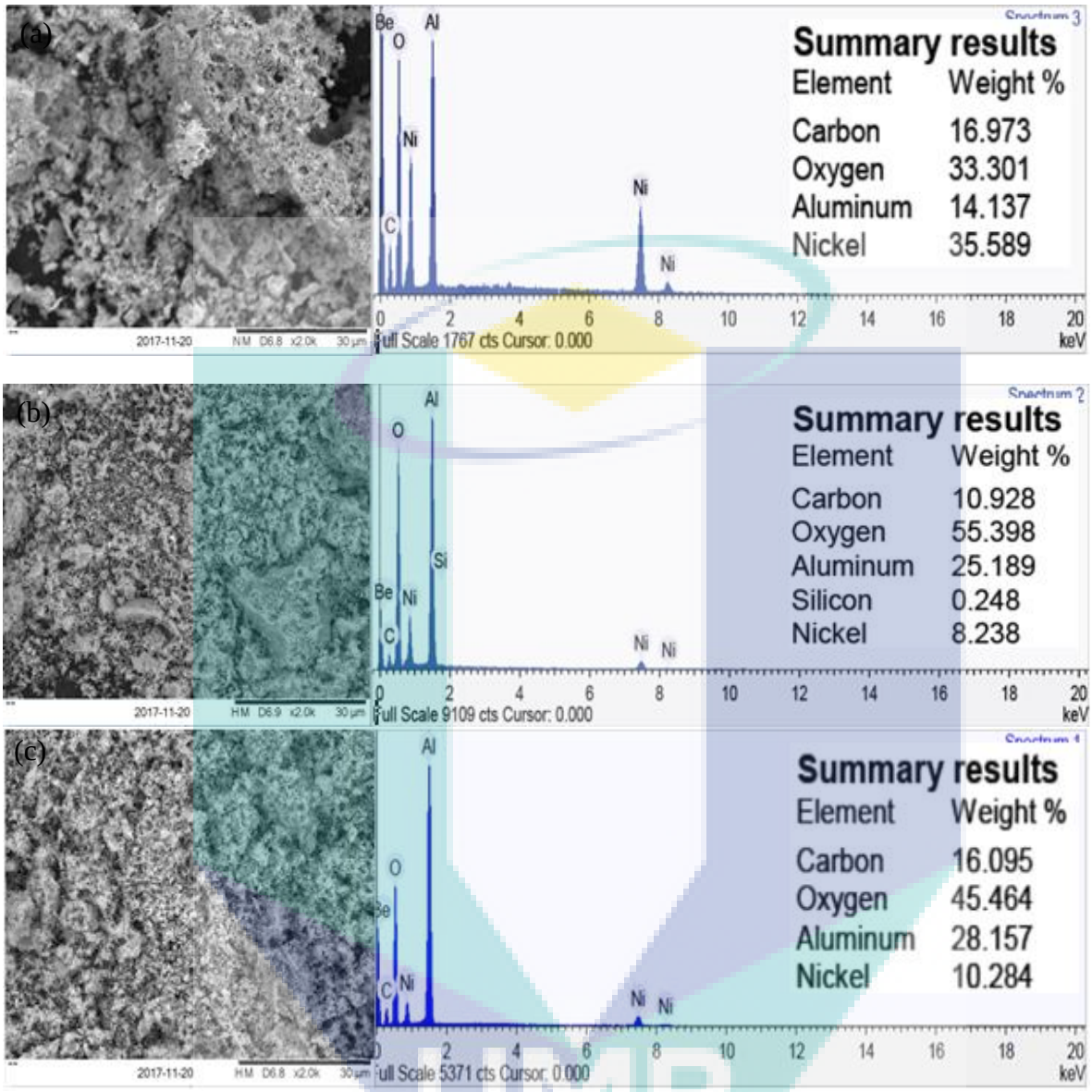

Figure 3 SEM-EDX analysis of NiO/α-Al_2O_3 at (a) Ni:Al_2O_3 molar ratio = 1:1 (b) Ni:Al_2O_3 molar ratio = 1:3 and (c) Ni:Al_2O_3 molar ratio = 1:5

3.3 Effect of glycine-nitrate (G/N) ratio

Figure 4 shows the SEM-EDX micrographs of NiO/α-Al_2O_3 metal supported catalysts at different glycine-nitrate (G/N) ratios. NiO/α-Al_2O_3 catalysts synthesized using in-situ self-combustion are found to be porous in structure. Catalyst porosity could help to increase the reaction contact area thus making it efficient for catalyst activity (Guo et al., 2010). However, the supported catalysts appear to be the same with each other and there is no different on the catalyst morphology due to the variation of glycine-nitrate (G/N) ratios from 0.5:1 to 1.5:1. Using the backscatter element (BSE), the distributions of NiO and α-Al_2O_3 support on the NiO/α-Al_2O_3 metal supported catalysts the can be distinguished according to atomic number. The light spot (Spot 1) of the catalyst surface is belong to α-Al_2O_3 while the dark sport (Spot 2) represents NiO.

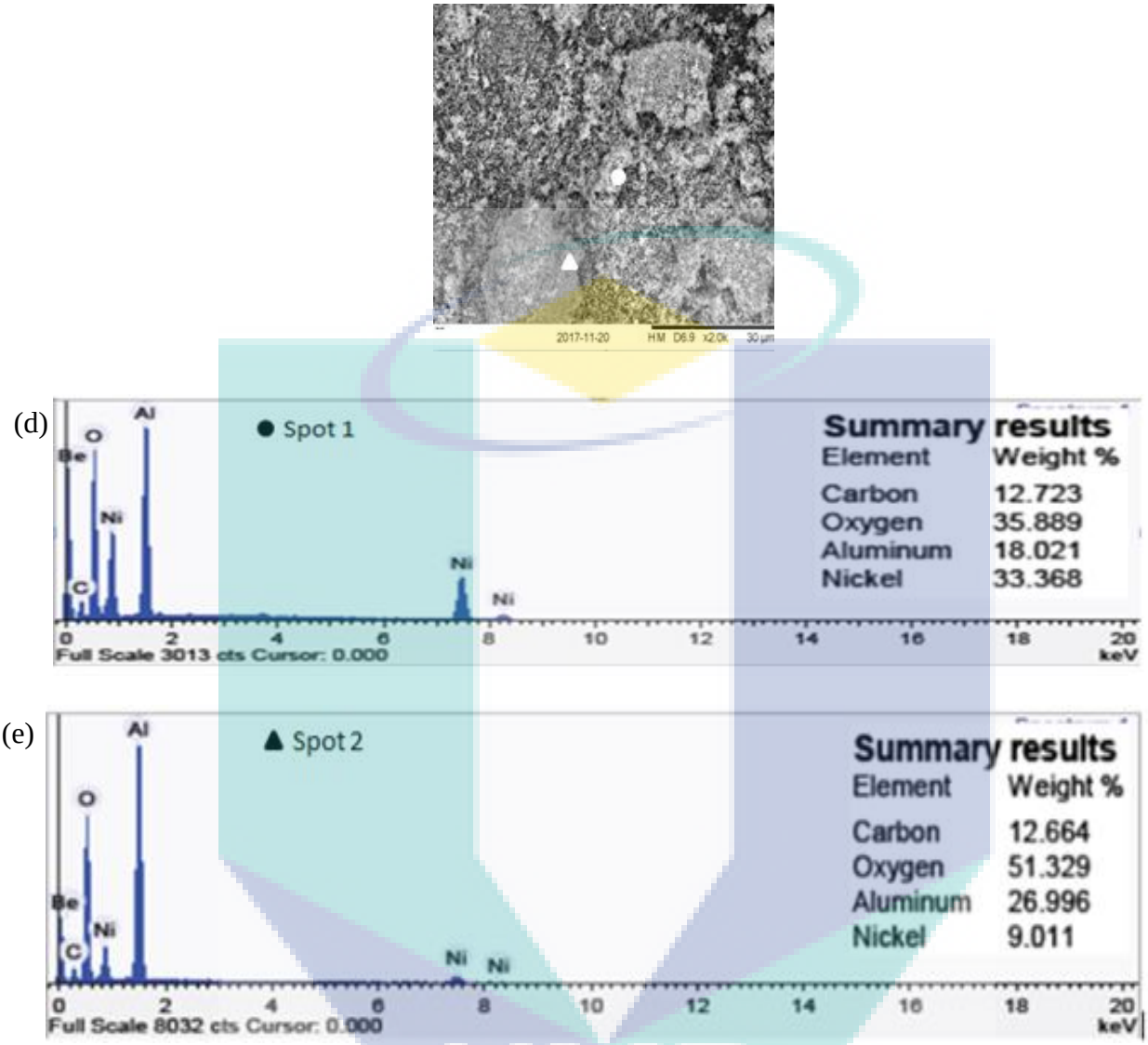

Figure 4 SEM images of NiO/α-Al_2O_3 catalyst (20,000x) and EDX results of NiO and α-Al_2O_3: (a) Glycine: nitrate ratio = 0.5:1, (b) Glycine: nitrate ratio = 1:1, (c) Glycine: nitrate ratio = 1.5:1, (d) EDX result of NiO and (e) EDX results of α-Al_2O_3

4.0 Conclusion

Nickel catalyst supported on alumina has been successfully synthesized using in-situ self-combustion synthesis. The effects of type of alumina, nickel to alumina molar ratio (Ni:Al_2O_3 = 1:1, 1:3 and 1:5) and different glycine-nitrate (G/N) ratios which are G/N = 0.5, 1.0 and 1.5 have been investigated and the prepared supported catalyst was characterized using scanning electron microscopy (SEM) and X-ray dispersion (XRD) analysis. Based on XRD results, it is able to obtain a crystalline and pure of NiO/α-Al_2O_3 metal-supported catalyst using in-situ self-combustion process. Moreover, it also indicated that the γ-Al_2O_3 is not a suitable support for Ni catalyst as there is no obvious presence of crystalline Ni species on the NiO/γ-Al_2O_3 metal-supported catalyst. NiO dispersion on alumina support increases as the Ni: alumina molar ratios from 1:1 to 1:5. As a result, Ni: alumina molar ratio of 1:5 has the highest NiO dispersion on α-alumina support with 40.7% Ni dispersion. Based on the SEM images, NiO/α-Al_2O_3 catalysts synthesized using in-situ self-combustion is found to be porous in structure. This could help to increase the reaction contact area. Finally, this work also shows that there is no different on the catalyst morphology due to the variation of glycine-nitrate (G/N) ratios from 0.5:1 to 1.5:1.

References

Adelino, F.C.C., & Figueiredo, J.L.C.C. (2009). *Hydrogen Production By Catalytic Decomposition Of Methane*. Porto: Department of Chemical Engineering Faculty of Engineering University of Porto. Print. A Thesis Submitted For The Degree Of Doctor Of Philosophy (Ph.D).

Akande, A., Idem, R., & Dalai, A. (2005). Synthesis, characterization and performance evaluation of Ni/Al2O3 catalysts for reforming of crude ethanol for hydrogen production. *Applied Catalysis A: General,287*, 159-175. doi:10.1016/j.apcata.2005.03.046

Asencios, Y. J., & Sun-Ko, M. (2012). *Applied Surface Science 258*, 10002– 10011.

Barros, B. S., Kulesz, J., Melo, D. M. de A., & Kienneman, A. (2015). Nickel-based Catalyst Precursor Prepared Via Microwave-induced Combustion Method: Thermodynamics of Synthesis and Performance in Dry Reforming of CH4. *material research*, *18*(4), 732–739. doi:http://dx.doi.org/10.1590/1516-1439.018115

Cross, A., Kumar, A., Wolf, E. E., & Mukasyan, A. S. (2012). Combustion Synthesis of a Nickel Supported Catalyst: Effect of Metal Distribution on the Activity during Ethanol Decomposition. *Industrial & Engineering Chemistry Research,51*(37), 12004-12008. doi:10.1021/ie301478n

Cross, A., Roslyakov, S., Manukyan, K. V., Rouvimov, S., Rogachev, A. S., Kovalev, D. Wolf, E E., & Mukasyan, A. S. (2014). In Situ Preparation of Highly Stable Ni-Based Supported Catalysts by Solution Combustion Synthesis. *The Journal of Physical Chemistry C,118*(45), 26191-26198. doi:10.1021/jp508546n

El-Kemary, M., N.Nagy, & I.El-Mehasseb. (2013). Nickel oxide nanoparticles: Synthesis and spectral studies of interactions with glucose. *Materials Sciencein Semiconductor Processing*, 1747-1750.

Gao, Y., Fanhui, M., Keming, J., Yan, S., & Zhong, L. (2015). Slurry phase methanation of carbon monoxide over nanosizedNi–Al2O3catalysts prepared by microwave-assisted

Guo, X., Mao, D., Lu, G., Wang, S., & Wu, G. (2010). Glycine–nitrate combustion synthesis of CuO–ZnO–ZrO2 catalysts for methanol synthesis from CO2 hydrogenation. *Journal of Catalysis,271*(2), 178-185. doi:10.1016/j.jcat.2010.01.009

Jamal, Y., & Wyszynski, M.-L. (1994). On-board generation of hydrogen-rich gaseous fuels*a review. *International Journal of Hydrogennergy*, *19*(7), 557-572

Li, G., Hu, L., & Hill, J. (2006). Comparison of reducibility and stability of alumina-supported Ni catalysts prepared by impregnation and co-precipitation. *Applied Catalysis A: General,301*(1), 16-24. Retrieved from http://doi.org/10.1016/j.apcata.2005.11.013

Liu, J., Li, C., Wang, F., He, S., Chen, H., Zhao, Y.. Duan, X. (2013). Enhanced low-temperature activity of CO2 methanation over highly-dispersed Ni/TiO2 catalyst†. *The Royal Society of Chemistry*. doi:10.1039/c3cy00355h
Morris D., A., & Calvin H., B. (2015). Heterogeneous Catalyst Deactivation and Regeneration: A Review. *catalysts*, *5*(2073-4344), 145–269. doi:10.3390/catal5010145

Piriyawong, V., Thongpool, V., Asanithi, P., & Limsuwan, P. (2012). Preparation and Characterization of Alumina Nanoparticles in DeionizedWater Using Laser Ablation Technique. *Journal of Nanomaterials*.

Satterfield, C. N. (1996). *Heterogeneous catalysis in industrial practice* (2nd ed.). Malabar, FL: Krieger Pub.

Sergio, L., González-Cortés, & Imbert, F. E. (2013). Fundamentals, properties and applications of solid catalysts prepared by solution combustion synthesis (SCS). *Applied Catalysis A: General,452*, 117-131. doi:10.1016/j.apcata.2012.11.024

Tomishige, K. (2007). Oxidative Steam Reforming of Methane over Ni Catalysts Modified with Noble Metals. *Journal of the Japan Petroleum Institute,50*(6), 287-298. doi:10.1627/jpi.50.287

Yang, Y.L. , Xu, H.Y., & Li,W.Z. (2004). Influence of the Nanoscale Support on Carbon Deposition and Carbon Elimination Over Ni/γ-Al_2O_3Catalyst for CH_4Conversion. *Journal of Nanoscience and Nanotechnology,4*(7), 891-895. doi:10.1166/jnn.2004.118

Zhang, T., & Amiridis, M.-D. (1998). Hydrogen production via the direct cracking over silica-supported nickel catalysts. *Applied Catalysis,167*, 161-172, and references within.

Zhao, A., Ying, W., Zhang, H., Ma, H., & Fang, D. (2012). Ni–Al2O3 catalysts prepared by solution combustion method for syngas methanation. *Catalysis Communications,17*, 34-38. doi:10.1016/j.catcom.2011.10.010